

**INVESTIGATION OF THE DETERIORATION
PROBLEMS OF EXCAVATED ANDESITE
MONUMENTS IN ARCHAEOLOGICAL SITES FOR
THE PURPOSE OF CONSERVATION**

**A Thesis Submitted to the
the Graduate School of Engineering and Sciences of
İzmir Institute of Technology
in Partial Fulfillment of the Requirements for the Degree of**

DOCTOR OF PHILOSOPHY

in Architecture

**by
Çağlayan Deniz KAPLAN**

**July 2015
İZMİR**

We approve the thesis of **Çağlayan Deniz KAPLAN**

Examining Committee Members:

Prof.Dr. Hasan BÖKE

Department of Architectural Restoration, İzmir Institute of Technology

Prof.Dr. Başak İPEKOĞLU

Department of Architectural Restoration, İzmir Institute of Technology

Assoc.Prof.Dr. Fehmi DOĞAN

Department of Architecture, İzmir Institute of Technology

Assoc.Prof.Dr. Şebnem YÜCEL

Department of Architecture, Yaşar University

Assist.Prof.Dr. Hülya YÜCEER

Department of Architecture, Adana Science and Technology University

02 July 2015

Prof.Dr. Hasan BÖKE

Supervisor,

Department of Architectural Restoration

İzmir Institute of Technology

Assoc.Prof.Dr. Şeniz ÇIKIŞ

Head of the Department of Architecture

Prof.Dr. Bilge KARAÇALI

Dean of the Graduate School of

Engineering and Sciences

ACKNOWLEDGMENTS

Foremost, I would like to express my deepest gratitude to my advisor, Prof.Dr. Hasan Bke, for his concern, guidance and patience throughout this research. I hope that one day I will become as good a researcher as he is. I have always admired his endless willingness to learn new things.

I gratefully acknowledge Prof.Dr. Bařak İpekođlu, head of the Department of Architectural Restoration, for guiding my research for the past several years and helping me to develop my background in both theory and practice in architectural restoration.

Special thanks to Assoc.Prof.Dr. Fehmi Dođan, for his valuable contributions in the progress of this thesis.

I would also like to thank Assoc.Prof.Dr. řebnem Ycel and Assist.Prof.Dr. Hlya Yceer for their attendance to my final defense jury and their valuable suggestions to this study.

I am also grateful to Prof.Dr. Nihayet Bizsel, for helping me to know the general aspects of the complex world of freshwater diatoms and for sharing her valuable source materials with me.

Fulya Murtezaođlu, Kerem řerifaki and Dr. Elif Uđurlu Sađın; I can not express the value of the years we spent together in our laboratory in a few words. Being a member of a crew known as "Restorasyoncular" by rest of the İYTE have always been an honor for me. Thank you all for your friendship and support.

My thanks to Kerem řerifaki once again, for his kind help and technical support in the SEM/EDS analyzes of this study.

I also owe my very special thanks to my beloved parents Hatice Kaplan, İbrahim Kaplan and my brother Mehmet Kaplan for their endless love, support and encouragement.

Finally, and most importantly, I wish to express my deepest gratitude to my dear wife Handan Kaplan for her love, support, encouragement and great patience. Nothing could be more precious than her great contribution to my life. This thesis is dedicated to her.

ABSTRACT

INVESTIGATION OF THE DETERIORATION PROBLEMS OF EXCAVATED ANDESITE MONUMENTS IN ARCHAEOLOGICAL SITES FOR THE PURPOSE OF CONSERVATION

Archaeological sites have to be preserved as the witnesses of the earliest human activities. Determination of deterioration processes of stone monuments in archaeological sites is one of the fundamental phases for their preservation. In this study, deterioration problems of excavated andesites from Aigai and Assos archaeological sites were investigated for the purpose of conservation. Within this intent, visual analysis of the andesite deteriorations was carried out with site surveys in four years intervals and basic physical, petrographic and microstructural properties, mineralogical, elemental and chemical compositions of interior parts and exterior surfaces of the andesites were determined and compared.

Visual analyses at the sites show that the progress of andesite deterioration after excavation is insignificant during the four years. The experimental results indicated the slight chemical deterioration of the silica and ferromagnesian minerals and calcium-feldspars through the action of carbon dioxide and water during burial resulted in the formation of clay minerals and calcium carbonate and hematite patinas on the andesite surfaces respectively. Presence of clay minerals promotes physical, chemical and biological deterioration. The experimental results indicated that excavations can be carried out by preventive conservation measures to prevent further andesite deteriorations in open air conditions.

As for the preventive conservation measures, the study suggests that the controlled drying of the andesites during excavations has to be supplied, clays on the stone surfaces have to be cleaned but but calcium carbonate layer have to be protected and biocides have to be implemented to prevent the biological formations. Site planning such as drainage to keep the water away from the monuments have to be supplied after their excavations.

ÖZET

ARKEOLOJİK ALANLARDAKİ ANDEZİT ANITLARIN KAZI SONRASI BOZULMA PROBLEMLERİNİN KORUMA AMAÇLI İNCELENMESİ

İnsanoğlunun en eski faaliyetlerinin tanığı olan arkeolojik alanlar korunmalıdır. Arkeolojik alanlardaki taş anıtların bozulma süreçlerinin belirlenmesi, onların korunması için temel aşamalardan biridir. Bu çalışmada, Aigai ve Assos arkeolojik alanlarında kazı sonrası ortaya çıkarılan andezitlerin bozulma sorunları koruma amaçlı incelenmiştir. Bu amaçla, alan çalışmalarıyla andezitlerdeki bozulmaların dört yıllık süreçteki görsel analizi yapılmış ve andezitlerin iç kısımları ile dış yüzeylerinin temel fiziksel, petrografik, mikroyapısal özellikleri, mineralojik, elemental ve kimyasal kompozisyonları belirlenmiş ve karşılaştırılmıştır.

Alanlardaki görsel analizler, andezitlerdeki kazı sonrası bozulmaların dört yıllık süreçte az olduğunu göstermektedir. Deneysel sonuçlar, silika ve ferromagnezyen mineraller ile kalsiyum-feldspatların toprak altında karbodiksioksit ve suyun etkisiyle az oranda kimyasal bozulmaya uğramasıyla, sırasıyla kil mineralleri ve andezit yüzeylerinde kalsiyum karbonat ve hematit patinalarının oluştuğunu göstermektedir. Kil minerallerinin varlığı, fiziksel, kimyasal ve biyolojik bozulmayı desteklemektedir. Deneysel sonuçlar, açık hava koşullarındaki taş bozulmalarının ilerleyişini engellemek için önleyici koruma müdahaleleri alınarak kazıların devam edebileceğini göstermektedir.

Önleyici koruma müdahaleleri olarak, bu çalışma, andezitlerin kazı sırasında kontrollü kurumaları sağlanmasını, taş yüzeylerindeki killerin temizlenmesini ancak kalsiyum karbonat tabakasının korunmasını ve biyolojik oluşumların engellenmesi için biyositlerin uygulanmasını önermektedir. Kazılardan sonra ise anıtlardan suyun uzak tutulması için drenaj gibi çevresel düzenlemeler sağlanmalıdır.

TABLE OF CONTENTS

LIST OF FIGURES	ix
LIST OF TABLES	xii
CHAPTER 1. INTRODUCTION	1
1.1. Problem Definition.....	4
1.2. Aim of the Study	4
1.3. Scope of the Study	5
1.4. Characteristics of Andesite	5
1.4.1 Physical and Mechanical Characteristics	6
1.4.2. Chemical Characteristics.....	8
1.4.3. Mineralogical and Petrographic Characteristics	14
1.5. Deterioration of Exposed Standing Andesites	15
1.6. Deterioration of Excavated Andesites	20
1.6.1. Characteristics of Subsoil Environment.....	23
1.6.2. Characteristics of the Materials.....	29
1.6.3. External Factors	31
1.7. Preventive and Active Conservation Measures in Archaeological Sites	32
CHAPTER 2. METHOD	34
2.1. Study Areas	35
2.1.1. Aigai	36
2.1.2. Assos	41
2.2. Visual Analysis of Stone Deteriorations Observed on the Andesites	47
2.3. Sampling	48
2.4. Experimental Studies	56
2.4.1. Determination of Basic Physical Properties of Interior and Exterior Parts of the Stones.....	63

2.4.2. Determination of Soluble Salt Contents in Soils and Andesites	64
2.4.3. Thermal Analysis of Soil and Stone Samples	64
2.4.4. Separation of Clay Fraction from Soil Samples.....	65
2.4.5. Determination of Mineralogical Characteristics	66
2.4.6. Determination of Chemical Compositions of Interior and Exterior Parts of the Stones.....	66
2.4.7. Petrographic and Microstructural Analysis.....	67
2.4.8. Calculation of Chemical Weathering Indices.....	68
CHAPTER 3. RESULTS AND DISCUSSIONS	70
3.1. Visual Analysis of Stone Deteriorations Observed on the Andesites...	70
3.2. Subsoil Characteristics of Aigai and Assos	90
3.2.1. Mineralogical Characteristics.....	91
3.2.2. Organic Material and Carbonate Contents	93
3.2.3. Soluble Salt Contents	95
3.3. Characteristics of Interior and Exterior Parts of the Andesites.....	96
3.3.1. Basic Physical Characteristics.....	96
3.3.2. Microstructural and Petrographic Characteristics	99
3.3.3. Mineralogical Characteristics.....	107
3.3.4. Chemical Characteristics.....	114
3.3.4.1. SEM/EDS and XRF Analysis	114
3.3.4.2. Chemical Weathering Indices	123
3.3.4.3. TGA Analyses	127
3.3.5. Soluble Salt Contents	131
3.4. Characteristics of Deposits Observed on the Andesites	133
3.4.1. Characteristics of White Deposits.....	133
3.4.1.1. Mineralogical Characteristics	133
3.4.1.2. Microstructural Characteristics	136
3.4.1.3. Chemical Characteristics.....	138
3.4.1.4. Presence of Freshwater Diatoms	142
3.4.2. Characteristics of Orange-Brown Deposits.....	146
3.4.2.1. Mineralogical and Chemical Characteristics	146

CHAPTER 4. CONCLUSIONS	149
REFERENCES	152
APPENDICES	
APPENDIX A. SOLUBLE SALT CONTENTS OF SOILS.....	165
APPENDIX B. BASIC PHYSICAL PROPERTIES OF INTERIOR AND EXTERIOR PARTS OF ANDESITES.....	166
APPENDIX C. TGA RESULTS OF INTERIOR AND EXTERIOR PARTS, CLAY FRACTIONS AND WHITE DEPOSITS OF ANDESITES AND CLAY FRACTIONS OF SOILS	167
APPENDIX D. SOLUBLE SALT CONTENTS OF ANDESITES	169

LIST OF FIGURES

<u>Figure</u>	<u>Page</u>
Figure 1.1. Geological map of Yuntdağ (a) and Behram (b) volcanic units.....	12
Figure 1.2. The components of subsoil environment.....	24
Figure 2.1. Map showing location of Aigai and Assos.....	35
Figure 2.2. Topographic Map of Aigai	38
Figure 2.3. Agora building in Aigai.....	39
Figure 2.8. Map of Assos.....	43
Figure 2.9. Temple of Athena in Assos	44
Figure 2.10. Temple of Athena in Assos	44
Figure 2.11. Northern Stoa of Assos.....	45
Figure 2.12. Bouleuterion of Assos	45
Figure 2.13. Theatre of Assos.....	46
Figure 2.14. Fortification walls and Necropolis of Assos	46
Figure 3.1. FT-IR spectrum of clay fraction of AiSo3 and AsSo4.....	92
Figure 3.2. XRD spectrums of clay fractions of AiSo1, AiSo2, AiSo3 and AiSo4	92
Figure 3.3. XRD spectrum of clay fraction of AiSo4.....	93
Figure 3.4. % Organic material and carbonate contents of soil samples of.....	94
Figure 3.5. SEM images of organic materials in AiSo1 (a) (b) and AsSo1 (c)	95
Figure 3.6. % Soluble salt contents of the soil samples.....	96
Figure 3.7. Density (g/cm^3) (a) and porosity (%) (b) values of Aigai Andesites	97
Figure 3.8. Density (g/cm^3) (a) and porosity (%) (b) values of Assos Andesites.....	98
Figure 3.9. BSE images of the minerals in the interior parts of Aigai andesites	100
Figure 3.10. Photomicrograph of interior parts of Ai2 and Ai5	101
Figure 3.11. BSE images of the minerals in the interior parts of Assos andesites	101
Figure 3.12. Photomicrograph of As8	101
Figure 3.13. BSE images of the single mineral grain observed in Ai2, twinning minerals in Ai9 and oscillatory zoning observed in As1	102
Figure 3.14. BSE images of the corona mineral texture of As2 and Ai6	102
Figure 3.15. SEM images of pore formation and micro-cracks of exterior parts of Ai1 (a), Ai2 (b) (c), Ai6 (d), Ai8 (e) and Ai9 (f)	103

Figure 3.16. SEM images of pore formation and micro-cracks of exterior parts of As1 (a) (b), As2 (c) (d), As5 (d) and As7 (f)	103
Figure 3.17. BSE images with the dimensions of the cracks observed on Ai1 (a) and As4 (b)	104
Figure 3.18. BSE images with the dimensions of the pores observed on Ai11 (a), As5 (b) and As7 (c)	104
Figure 3.19. BSE images of the cracks observed on Ai2 (a), As3 (b) and As6 (c)	105
Figure 3.20. BSE images of Aigai andesites from surfaces to the inner cores	106
Figure 3.21. BSE images of Assos andesites from surfaces to the inner cores	106
Figure 3.22. XRD patterns of interior parts of andesite samples of Aigai (Aix_I).....	107
Figure 3.23. XRD patterns of interior parts of andesite samples of Assos (Asx_I)	108
Figure 3.24. FT-IR spectrum of surface crack of Ai2 - Ai11 (a) and As2 - As5 (b).....	109
Figure 3.25. SEM images of hyphae observed on Ai2 (a), Ai3(b), As5 (c) and As8 (d).....	113
Figure 3.26. Biological forms observed on the walls of bouleuterion of Aigai (a) and stoa Assos (b).....	113
Figure 3.27. XRF results showing the elemental composition of Aigai andesites	115
Figure 3.28. XRF results showing the elemental composition of Assos andesites	115
Figure 3.29. Total alkali-silica diagram of the stone samples	116
Figure 3.30. Total alkali-silica diagram of the stone samples	118
Figure 3.31. SiO ₂ - FeO*/MgO diagram of the stone samples	119
Figure 3.32. TGA results of interior parts of the andesite samples	128
Figure 3.33. TGA results of exterior parts and clay fractions of the andesite samples.....	128
Figure 3.34. % Organic material and carbonate contents of andesite samples of Aigai and Assos	129
Figure 3.35. TGA graphs of exterior surfaces of Ai5 (a), Ai8 (b) and Ai10.....	129
Figure 3.36. TGA graphs of exterior surfaces of As2 (a), As3 (b) and As4 (c)	130
Figure 3.37. SEM images of organic materials on the surface of Ai2 (a) and Ai5 (b) (c)	130

Figure 3.38. SEM images of organic materials on the surface of As7 (a) and As8 (b) (c)	131
Figure 3.39. % Soluble salt contents of the andesite samples	132
Figure 3.40. XRD pattern of white deposits of Aigai	134
Figure 3.41. XRD pattern of white deposits of Assos	134
Figure 3.42. FT-IR spectra of white deposits of Aigai: 1 (a), 2 (b), 7 (c) and 11 (d)	135
Figure 3.43. FT-IR spectra of white deposits of Assos: 1 (a), 2(b) and 7 (c)	135
Figure 3.44. SEM images of white deposits of stone sections: Ai2 (a), Ai11 (b) and As1 (c)	136
Figure 3.45. SEM images of white deposits of Ai2 (a), Ai9 (b) and Ai 11(c)	137
Figure 3.46. SEM images of white deposits of As1 (a), As2 (b) and As7 (c)	137
Figure 3.47. SEM images of organic materials and calcite crystals on the surface of Ai9	137
Figure 3.48. Mapping of Ai2 based on chemical composition	138
Figure 3.49. Mapping of Ai9 based on chemical composition	139
Figure 3.50. Mapping of As2 based on chemical composition	139
Figure 3.51. TGA graphs of white deposits of Ai1, Ai2 (b), Ai9 (c) and As11 (d)	140
Figure 3.52. TGA graphs of white deposits of As1 and As2 (b)	140
Figure 3.53. Diatom specie observed in Ai11 (a) and mapping of the diatom based on chemical composition (b)	144
Figure 3.54. Diatom specie observed in Ai2 (a) and mapping of the diatom based on chemical composition (b)	144
Figure 3.55. Orange-brown depositions on Ai1 (a) and Ai6 (b)	146
Figure 3.56. XRD pattern of surface of Ai1	147
Figure 3.57. Mapping of Ai6 based on chemical composition	147

LIST OF TABLES

<u>Table</u>	<u>Page</u>
Table 1.1. Density (g/cm ³) and porosity (%) values and compression strength (MPa) of Ankara, Niğde, Konya, Afyon, İzmir and Manisa andesites	7
Table 1.2. Major element contents of Yuntdağ (Manisa), Buca (İzmir), Yamanlar (İzmir), Dikili (İzmir), Behram (Çanakkale), Ankara, Niğde, Şarkışla (Sivas), Afyon, and Isparta andesites.....	10
Table 1.3. Chemical Diagrams of Yuntdağ volcanics, Behram volcanics	13
Table 1.4. Summary of weathering indices of WIP and CIA	19
Table 1.5. Andesite-forming minerals, their average amounts in andesite structure, their resistance to chemical deterioration and the abrasion pH values for these minerals.....	30
Table 2.1. Labels and definitions of the samples collected from Aigai.....	49
Table 2.2. Labels and definitions of the samples collected from Assos	53
Table 2.3. Laboratory analyses applied to the samples taken from Aigai	58
Table 2.4. Laboratory analyses applied to the samples taken from Assos	61
Table 3.1. Visual analysis of exposed standing and excavated parts of the partially excavated andesites in Aigai archaeological site.....	73
Table 3.2. Visual analysis of exposed standing and excavated parts of the partially excavated andesites in Assos archaeological site	76
Table 3.3. Comparison of deterioration progresses observed on the andesites in Aigai archaeological site between the years 2010 and 2014	77
Table 3.4. Comparison of deterioration progresses observed on the andesites in Assos archaeological site between the years 2010 and 2014	85
Table 3.5. Mineralogical Characteristics of Interior Parts and Exterior Surfaces of Aigai Andesites	109
Table 3.6. Mineralogical Characteristics of Sound Interior Parts and Deteriorated Exterior Surfaces of Assos Andesites	110
Table 3.7. SEM/EDS and XRF Results (Elemental Compositions) of Interior Parts of Aigai and Assos Andesites	117

Table 3.8. Major element contents of Yuntdağ, Behram, Aigai and Assos andesites.....	121
Table 3.9. Chemical Diagrams of Yuntdağ volcanics, Behram volcanics and Aigai and Assos andesites.....	122
Table 3.10. SEM/EDS and <i>XRF</i> Results (Elemental Compositions) of Exterior Parts of Aigai and Assos Andesites.....	125
Table 3.11. CIA and WIP Results for Aigai and Assos Andesites based on <i>XRF</i> Results.....	126
Table 3.12. Classification of freshwater diatom species observed on andesite samples	143

CHAPTER 1

INTRODUCTION

Archaeological sites are the existing witnesses of the ancient traditions. Providing physical relationship between past and present, archaeological sites and findings represent non-renewable cultural resources. Thus, preservation of all archaeological information gathered from archaeological sites and findings is not only preservation of the past, but also preservation of cultural identity and all traditional, historical, scientific and aesthetic values associated with human being.

The need for the preservation of archaeological monuments was declared for the first time in Madrid Conference held in 1904 (KUMID 2015). However, first sophisticated and coordinated attempt for the conservation of archaeological sites is the Athens Charter for the Restoration of Historic Monuments (1931) (ICOMOS 1931). In the Athens Charter, the preservation of the archaeological monuments and findings was first declared as an interdisciplinary problem. The protective measures of accurate documentation and reburial of archaeological findings were also articulated for the first time in the Athens Charter. In 1956, the Recommendation on International Principles Applicable to Archaeological Excavations (UNESCO), the importance of both excavated and unexcavated archaeological sites were emphasized and leaving these sites partially or totally unexcavated in case of not maintaining the sufficient excavation methods, maintenance and conservation methods was recommended (UNESCO 1956). These charters and recommendations were extended by many other charters and policies such as Venice Charter (1964) through the threats of unscientific excavations which result in further deterioration of excavated archaeological materials and the importance of interdisciplinary collaboration and using distinguishable modern techniques and advanced technologies in conservation works (ICOMOS 1964). The definition of archaeological site was expanded with the declaration of Burra Charter in 1979. Instead of monuments and findings, with a holistic context, landscapes, spaces and views were included as the components of the places (Australia ICOMOS 1979). Finally, the European Convention on the Protection of the Archaeological Heritage held in 1990 and revised in 1992 emphasized threats of unscientific excavations again and recommended

the proper provision of sufficient archaeological management and the collaboration of professional people before excavating the sites (ICOMOS 1990, Council of Europe 1992). Indeed, it recommends non-destructive techniques, aerial and ground survey, and sampling wherever possible, in preference to total excavation except on sites and monuments threatened by development, land-use change, looting, or natural deterioration. It also recommends partial excavations, leaving a portion undisturbed for future research (Council of Europe 1992).

The concept of cultural heritage gained a broader understanding with the declaration of the Nara Document on Authenticity, which had been declared as a result of the conference held by ICOMOS in 1994 (ICOMOS 1994). According to the Nara document, the importance and the necessity of preserving the historic monuments for future generations are related to their “authenticity”. The authenticity of a monument was linked to the worth of a great variety of sources of information (form and design, materials and substance, use and function, traditions and techniques, location and setting, and sprits and feelings) that the monument involves and the building materials are the part of this integrity (ICOMOS 1994).

One of the common arguments in the charters and policies concerning conservation of archaeological sites is increasing rate of deterioration caused by many reasons, especially lack of site conservation before excavation works and scientific conservation approaches to the archaeological sites and findings. In the light of charters and policies, modern conservation theory emphasizes the importance of scientific conservation as a fundamental need to preserve the integrity of the buildings and objects (Viñas 2005). In the modern theory, conservation should attempt to preserve the *true nature* of the historic objects, which relies mainly upon their material constituents, after their exposure to atmospheric conditions. Thus, determination of the characteristics and deterioration processes of historic building materials is one of the fundamental phases for the conservation of monuments (Viñas 2005).

One of the most important materials traditionally used for structural and ornamental purposes was natural stones (Siegesmund et al. 2002, Miller et al 2012). The deterioration and conservation of these stones is a problem identified since antiquity. Both Strabon and Herodotus recognized the deterioration of building stones and recommended preventive actions (Camuffo 1992, Pope et al. 2002). Since antiquity, the investigation of the factors that promote this process and the conservation of these stones are still very important research topics (Siegesmund et al. 2002).

Among various types of natural stones, one of the most commonly used in the construction of ancient buildings is andesite. The use of andesite was preferred by ancient civilizations to construct the buildings because it is easily pliable material and the next most abundant volcanic rock after basalt (Naumann 2007, Hamblin and Christiansen 2003). As used in most of the worldwide cultural heritage monuments, andesites were used as main building material by many ancient civilizations in Anatolia (Naumann 2007). Especially in Western Anatolia, the use of andesites can be seen in many ancient cities such as Assos (Çanakkale), Gülpınar (Çanakkale), Aigai (Manisa), Kyme (İzmir), Daskyleion (İzmir), Pergamon (İzmir), Erythrai (İzmir) and Smyrna (İzmir). The use of andesite was not only common in ancient periods. Both Seljuk and Ottoman builders used andesites extensively as a building and ornamentation material (Ergun 2009). In İzmir, the use of andesites can be seen in many historical monuments and houses either. In the construction of the arches of ancient Agora of Smyrna, many Ottoman mosques such as Salepçioğlu Mosque and in many historical dwellings, builders preferred to use red-gray and green andesites as a building material. The Historical Elevator (Asansör) Building, which is one of the symbols of İzmir city, was first a stone quarry constructed to get andesite in 1800s (Türkmen and Kun 2001, Ergun 2009). Considering the most use of andesite, determination of its characteristics and deterioration processes is essential for the conservation of all these historical buildings.

1.1. Problem Definition

Andesites are one of the most common natural stones used since time immemorial by the civilizations for both structural and ornamental purposes in worldwide and Turkey. For the conservation of the andesite monuments and findings, their characteristics and deterioration processes must be evaluated properly.

There are many buried archaeological monuments and findings in the subsoil environments. Excavation of these monuments and findings has been one of the main problems of conservation works. In this context, many factors, such as composition of the buried materials (organic or inorganic), the characteristics of the soil and time of burial, are related to the problems of conservation works.

In Turkey, there are many buried andesite monuments and findings in archaeological sites. Determination of the deterioration problems of these monuments and findings after their excavations affects the excavation decisions in terms of their conservation. Thus, determination of the deterioration problems of excavated andesites is important. In this study, these problems are investigated.

1.2. Aim of the Study

The aim of this study is the investigation of the deterioration problems of buried and excavated andesites for the purpose of conservation. In this context, investigation of the deterioration problems of buried and excavated andesites also forms a basis for the excavation decisions and necessary preservation measures after the excavations. Besides forming a basis for the conservation of excavated andesites, this dissertation also aims to fill the gap in the literature about the deterioration processes of buried and excavated andesites.

1.3. Scope of the Study

In the scope of this study, Aigai (Manisa) and Assos (Çanakkale) archaeological sites were selected. All the monuments in the sites were constructed with andesites in the same period and the excavation works in the sites are still ongoing. Aigai archaeological site was selected as an inland site and Assos was selected as a coastal archaeological site to find out the possible effects of being near the seashore in the deterioration processes of both buried and excavated andesites.

The study was carried out with the excavated monuments in Aigai and Assos archaeological sites as it focuses on the deterioration of excavated andesites. In other words, all the studied monuments were in subsoil environments before their excavations. Thus, the factors which may affect the deterioration of the buried and exposed standing andesites were also evaluated as their importance in the excavated deterioration process.

1.4. Characteristics of Andesite

Andesite is an igneous rock and the next most abundant stone type after basalt in worldwide (Fichter and Farmer 1975). They are composed of plagioclase feldspars (such as albite, andesine, labradorite and anorthite), mafic minerals (such as amphibole, biotite, and pyroxene) with little or no quartz (Fichter and Farmer 1975).

According to differences in the cooling processes and cooling places of the andesites during their formation, they have specific chemical, mineralogical and physical characteristics although there are general properties (Spock 1953). In the following parts, physical and mechanical, chemical, mineralogical and petrographic characteristics of the sound andesites and recent studies on these characteristics in Turkey will be explained.

1.4.1 Physical and Mechanical Characteristics

Physical and mechanical properties of andesites were generally described according to their density and porosity percentage values and compressive strengths respectively. In the literature, the average density and porosity values of the sound andesites range between 2.50-2.80 g/cm³ and 0.2-8.0 % respectively (Jaeger and Cook 1979, Howe 2001, Brady and Brown 2004).

The most important andesite quarries in Turkey are in Manisa, Çanakkale and İzmir in Western Anatolia and in Ankara, Afyonkarahisar and Çankırı in Central Anatolia (Türkmen and Kun 2001, Ergun 2009). Their average porosity values for sound ones were found between 3.48 and 12.23 % and density values were determined as ranging between 2.06 and 3.03 g/cm³ (Table 1.1) (Taqieddin 1972, Karpuz 1982, Tokmak 2005, Yavuz 2006, Kaplan 2009, Murtezaoğlu 2009, Koca et al. 2011, Sarıışık et al. 2011, Kaplan et al. 2013, Kaputoğlu 2013, Korkanç 2013, Tufan and Kun 2014).

The compressive strength of the andesites determined between 23.05 and 140.33 MPa (Table 1.1) (Taqieddin 1972, Karpuz 1982, Yavuz 2006, Koca et al. 2011, Sarıışık et al. 2011, Kaputoğlu 2013).

Table 1.1. Density (g/cm³) and porosity (%) values and compression strength (MPa) of Ankara, Niğde, Konya, Afyon, İzmir and Manisa andesites

City	Reference	Location	Density (g/cm ³)	Porosity (%)	Compression Strength (MPa)
Ankara	Taqieddin (1972)	Y.mahalle	–	10.26	48.94
		Çubuk	–	10.26	140.33
		H.Gazi	–	11.14	48.54
		Keçiören	–	11.14	48.50
	Karpuz (1982)	Y.mahalle	2.42	5.71	34.62
		Esentepe	2.37	7.42	40.40
		Gölbaşı	2.25	7.84	33.34
	Tokmak (2005)	Castle	2.31	7.30	–
		Castle	2.22	7.70	–
		Castle	2.23	10.47	–
		Gölbaşı	3.03	10.95	–
		Gölbaşı	2.06	9.56	–
Yavuz (2006)	Gölbaşı	–	6.99	119.8	
	Gölbaşı	–	12.23	70.55	
Niğde	Korkanç (2013)	Castle	–	5.39	31.66
		Hasköy	–	5.81	49.60
Konya	Zedef et al. 2011	Gölcük	–	–	90.7
Afyon	Sarışık et al. (2011)	Iscehisar	2.61	15.75	40.7
İzmir	Koca et al. (2011)	Karatepe	–	4.54	23.05
		Karatepe	–	4.69	34.48
		Karatepe	–	3.48	39.68
	Kaputoğlu (2013)	Buca	2.40	5.80	–
		Buca	2.30	4.90	–
Tufan and Kun (2014)	Menemen	–	4.17	–	
Manisa	Murtezaoğlu (2009)	Yuntdağ	2.4	8.0	–
	Kaplan (2009)	Yuntdağ	2.4	8.4	–

1.4.2. Chemical Characteristics

Chemical compositions of the rocks are one of the most important features in their classification and also determination of the geological setting of the rocks.

Andesites are dominated by the elements of SiO₂, Al₂O₃, Fe₂O₃, TiO₂, P₂O₅, CaO, MgO, Na₂O and K₂O (Spock 1953, Press and Siever 2002). In the general classification of the rocks based on their chemical characteristics, andesites are classified as an intermediate igneous rock with their 53-65 % SiO₂ (silica) content, which change according to their formation process (Spock 1953).

Recent studies show that the elements in the andesites in different parts of Turkey varied between 54.2-68.6% for SiO₂, 14.2-19.4% for Al₂O₃, 4.0-10.7% for Fe₂O₃, 0.1-1.1% for TiO₂, 0.1-0.8% for P₂O₅, 1.6-7.2% for CaO, 1.0-4.8% for MgO, 0.9-5.8% for Na₂O and 1.7-6.0% for K₂O (Table 1.2) (Tankut 1985, Gökten and Floyd 1987, Ercan et al. 1995, Akay and Erdoğan 2004, Karacık et al. 2007, Kaplan 2009, Murtezaoğlu 2009, Koralay 2010, Sarıışık et al. 2011, Uzun and Terzi 2012, Kaplan et al. 2013, Kaputoğlu 2013, Korkanç 2013, Seghedi et al. 2015).

Chemical compositions of the rocks used to find out the geological setting of the different areas in Anatolia. In the literature, geological setting of the western Anatolia is divided as Çanakkale-Balıkesir, Balıkesir-İzmir and İzmir-Manisa regions and the geological maps based on different geological periods were prepared and different rock formations including andesites were stated with their petrographic and chemical characteristics in these studies (Borsi et al. 1972, Öngür 1973, Akyürek ve Sosyal 1983, Ercan et al. 1995).

Geological age of western Anatolia was first studied by Borsi et al. 1972 by radiometric (radioactive) age dating analyses, which is based on the comparison of the amounts of a natural radioactive isotope and its decay products, by using decay rates. The study shows that the formation age of western Anatolia was between 21.5 and 16.8 million years (Early-Middle Miocene) (Ercan et al. 1995). Öngür (1973) was focused on the Çanakkale region and divided to three sub-regions (units) as Ayvacık, Babakale and Behram (Assos) based on their volcanic activity. Öngür (1973) also determined that the Behram (Assos) volcanic unit was the volcanic center of the region which had the most explosion capacity. Having two periods of activity, first period of activity resulted in the formation of quartzlallite, lallite, dacite and rhyolite and second period resulted in the

formation of ignimbrite and andesite (Öngür 1973). Based on previous studies and chemical analysis of the stone samples collected from different places, which was mentioned before, Ercan et al. 1995 prepared the geological map of Biga peninsula, Gökçeada, Bozcaada and Tavşan Island (Figure 1.1). Akyürek and Sosyal (1983) were focused on the geological characteristics of the southern part of Biga peninsula and titled the southern part of the Bergama as Yuntdağ volcanics for the first time. The study of Akyürek and Sosyal (1983) also shows that the Yuntdağ volcanics are composed of andesite, tufa and lahar. In the regional scale, the geological map of İzmir-Balıkesir volcanic region, including Yuntdağ and Yamanlar volcanic units was studied extensively by Seghedi et al. (2015) based on chemical and petrographic analyses (Figure 1.1).

In these studies, elemental compositions of the rocks also used in further chemical classifications as the same type of rocks in the same region may have different chemical characteristics (Spock 1953). Chemical diagrams based on elemental compositions ($\text{Na}_2\text{O}+\text{K}_2\text{O}$ vs SiO_2 and SiO_2 vs FeO/MgO diagrams) of the rocks in Yuntdağ and Behram volcanics, in which the study areas of this study are included, show that all the volcanics are composed of andesites (Table 1.3). The diagrams show that the andesites are generally subalkaline and composed of both tholeiite (iron rich) and calc-alkaline (calcium rich) stones (Table 1.3) (Miyashiro 1974, Peccerillo and Taylor 1976, LeMaitre 1989, Ercan et al. 1995, Akay and Erdoğan 2004, Seghedi et al. 2015).

Table 1.2. Major element contents of Yuntdağ (Manisa), Buca (İzmir), Yamanlar (İzmir), Dikili (İzmir), Behram (Çanakale), Ankara, Niğde, Şarkışla (Sivas), Afyon, and Isparta andesites

Samples	Reference	Elemental Composition								
		SiO ₂	Na ₂ O	MgO	Al ₂ O ₃	K ₂ O	CaO	TiO ₂	FeO	P ₂ O ₅
Yuntdağ Andesites (Manisa)	Akay and Erdoğan (2004)	63.4	3.5	2.4	15.9	3.0	4.8	0.6	4.5	0.1
		59.7	3.4	2.8	16.8	2.7	5.8	0.8	5.3	0.2
		62.7	3.7	1.0	17.4	2.5	5.2	0.6	4.3	0.2
		62.2	3.3	2.7	15.5	2.8	4.9	0.7	4.1	0.2
		63.4	3.1	2.4	16.0	3.6	3.7	0.6	4.0	0.2
		63.4	3.1	2.9	15.2	2.8	5.2	0.6	4.3	0.1
		60.4	3.3	3.2	16.6	2.2	6.3	0.6	4.8	0.1
		60.3	3.5	2.3	18.1	2.4	6.0	0.7	4.7	0.2
		61.2	3.1	4.0	15.0	2.6	5.8	0.5	5.4	0.2
		60.3	2.8	4.8	14.3	2.8	6.0	0.6	5.7	0.2
		61.6	3.2	2.4	16.0	3.1	4.1	0.6	4.1	0.2
		59.7	3.3	2.9	16.8	3.2	5.0	0.6	5.3	0.2
		61.6	3.3	2.4	16.4	3.2	5.0	0.6	5.0	0.2
		60.0	3.4	3.1	16.6	3.1	5.4	0.7	5.5	0.2
	59.7	2.9	3.1	14.9	4.0	5.3	0.7	6.0	0.4	
		Murtezaoğlu (2009)	58.5	3.4	2.3	19.4	3.9	2.9	–	9.8
	Kaplan (2009)	58.0	3.5	2.0	18.7	3.7	3.0	–	10.7	0.7
		59.5	3.0	2.0	18.1	4.4	3.0	–	9.3	0.7
	Seghedi et al. (2015)	60.0	3.4	3.1	16.6	3.1	5.4	0.7	5.5	0.2
		68.6	3.4	0.3	15.0	5.3	1.6	0.1	3.1	0.1
		54.7	2.9	2.5	17.3	3.5	7.2	0.9	5.8	0.5
Buca (İzmir)	Kaputoğlu (2013)	60.6	2.6	1.8	14.2	4.1	5.5	0.6	5.5	0.4
Yamanlar (İzmir)	Seghedi et al. (2015)	55.4	2.7	2.8	15.5	3.7	6.5	0.7	6.1	0.3
		61.4	2.7	2.1	15.5	3.4	3.8	0.5	4.8	0.2
Dikili (İzmir)	Karacık et al. (2007)	60.8	3.0	4.5	14.6	2.5	6.4	0.6	5.8	0.2
		61.8	2.9	2.6	15.9	3.3	4.7	0.5	4.2	0.1
		64.2	3.0	2.2	14.4	3.4	4.6	0.6	4.4	0.2

(cont. on next page)

Table 1.2 (cont.).

Behram Andesites (Çanakkale)	Ercan et al. (1995)	56.0	2.8	3.0	16.0	3.3	6.6	1.1	7.7	0.3
		56.5	3.4	2.2	17.2	3.3	6.3	1.0	7.3	0.3
		58.1	3.0	1.8	17.1	3.4	6.0	1.1	7.9	0.4
Ankara	Tankut (1985)	60.0	3.6	5.5	15.5	1.9	6.8	0.3	6.2	–
		61.44	3.7	3.1	17.7	2.7	5.9	0.5	4.8	–
		61.49	3.6	4.7	16.3	2.0	6.3	0.2	5.1	–
Niğde	Korkaç (2013)	59.6	3.2	3.2	16.4	2.5	6.6	0.2	5.3	0.1
Şarkışla (Sivas)	Gökten and Floyd (1987)	62.0	5.1	0.9	16.5	2.6	3.9	0.6	5.3	0.2
		58.3	5.5	2.8	17.2	0.4	5.6	0.5	4.6	0.2
		63.7	8.7	0.9	17.5	2.1	3.1	0.5	3.7	0.1
Afyon	Sarıışık et al. (2011)	62.3	2.9	2.8	14.7	6.0	4.2	0.1	4.0	0.8
Isparta	Koralay (2010)	61.6	3.4	1.5	17.2	2.3	5.6	0.5	5.5	0.2
		59.1	3.7	2.1	17.4	1.7	6.5	0.7	6.7	0.2
	Uzun and Terzi (2012)	54.2	5.8	1.4	17.6	5.6	4.1	0.6	7.9	0.1

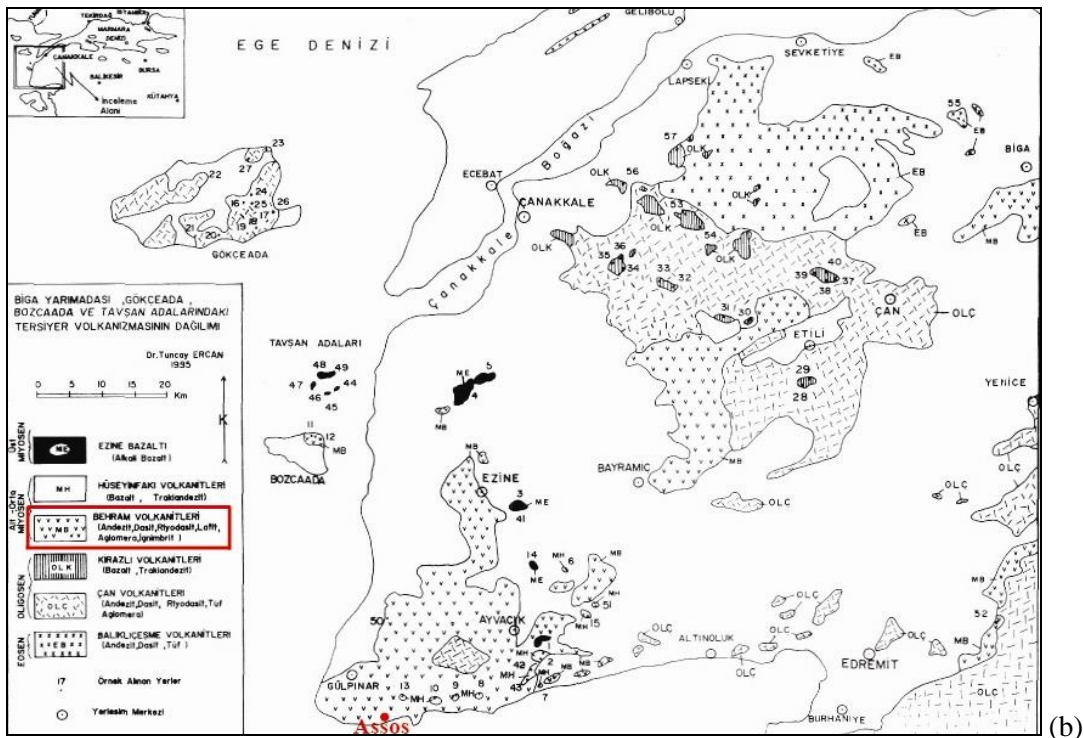
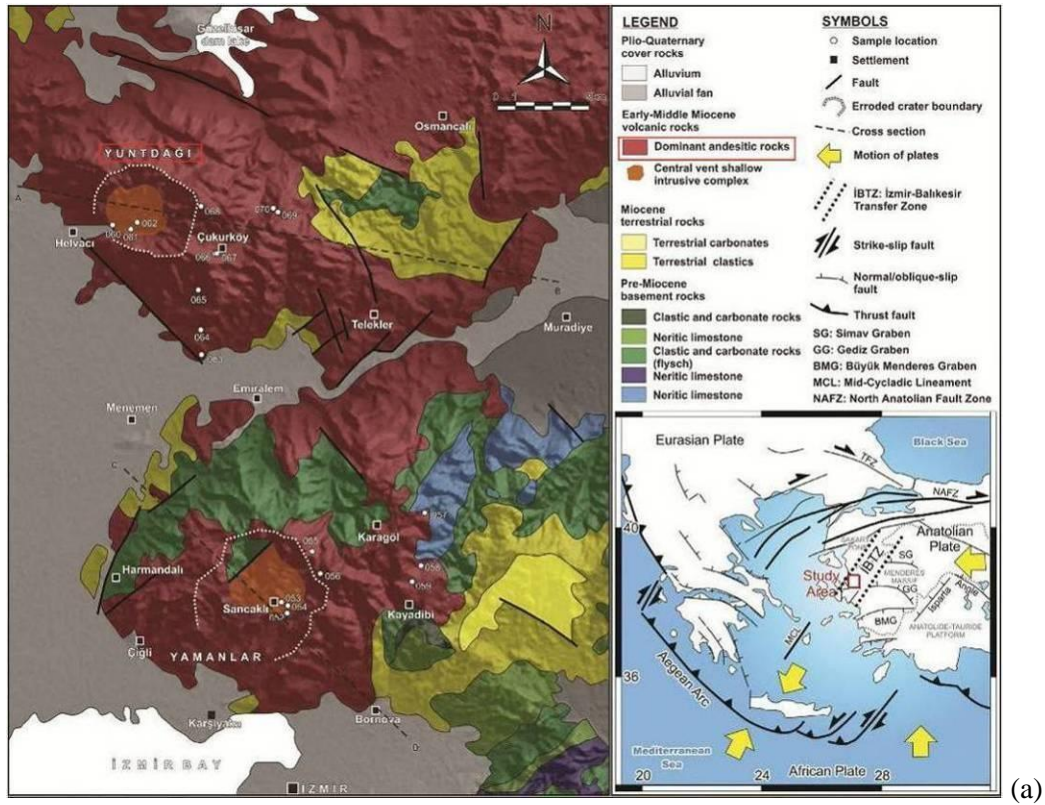
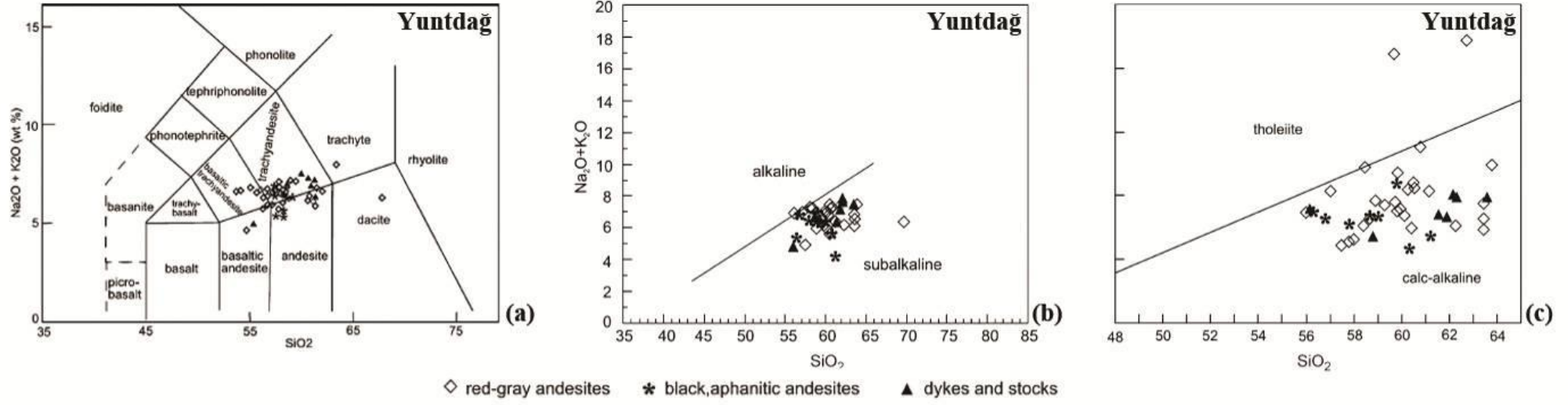
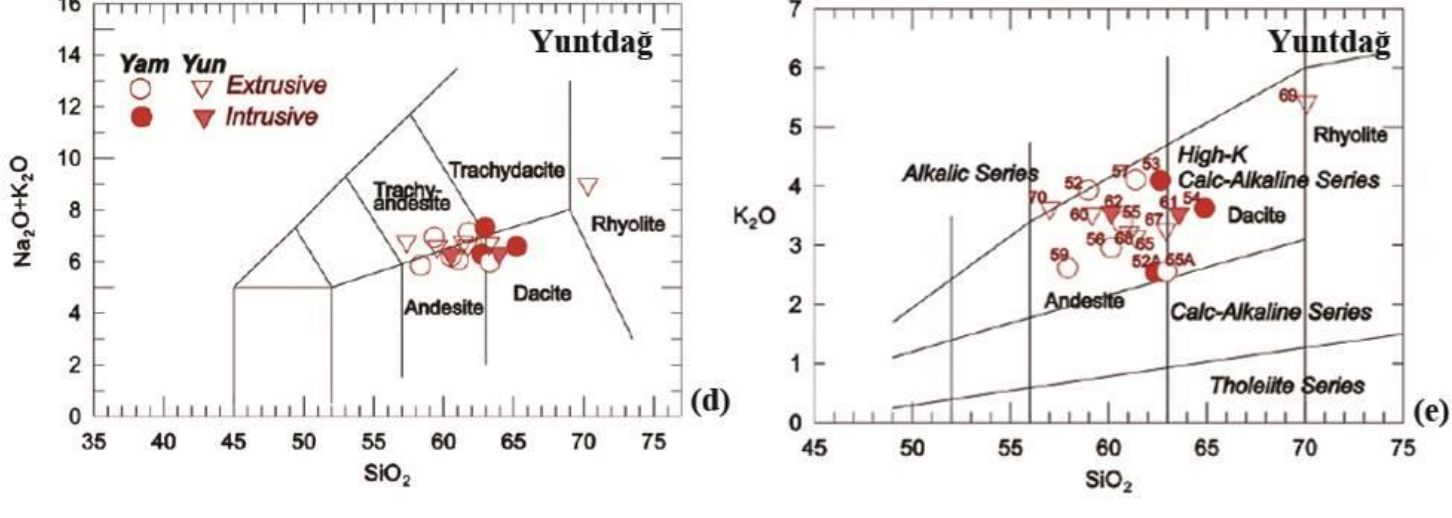
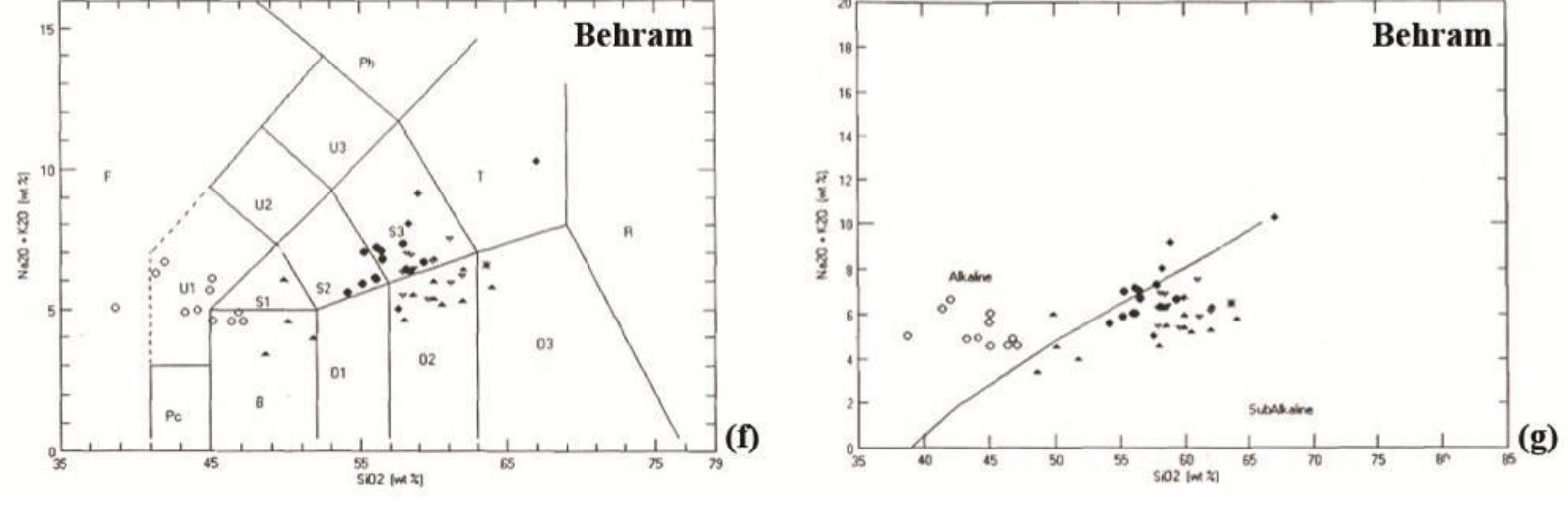


Figure 1.1. Geological map of Yunt dağ (a) (Source: Seghedi et al. 2015) and Behram (b) (Source: Ercan et al. 1995) volcanic units

Table 1.3. Chemical Diagrams of Yuntdağ volcanics (Source: Akay and Erdoğan 2004, Seghedi et al. 2015), Behram volcanics (Source: Ercan et al. 1995)

<p>Akay and Erdoğan 2004</p>	 <p>(a) $(\text{Na}_2\text{O}+\text{K}_2\text{O})$ vs SiO_2 diagram of LeMaitre (1989) showing the distribution of different phases of the Yuntdağ volcanics. (b) $\text{Na}_2\text{O}+\text{K}_2\text{O}$ vs SiO_2 diagram of Yuntdağ volcanics. (Source: Miashiro 1974) (c) SiO_2 vs FeO/MgO diagram of Yuntdağ volcanics. (Source: Miashiro 1974)</p>	<p>(a) $(\text{Na}_2\text{O}+\text{K}_2\text{O})$ vs SiO_2 diagram of LeMaitre (1989) showing the distribution of different phases of the Yuntdağ volcanics. (b) $\text{Na}_2\text{O}+\text{K}_2\text{O}$ vs SiO_2 diagram of Yuntdağ volcanics. (Source: Miashiro 1974) (c) SiO_2 vs FeO/MgO diagram of Yuntdağ volcanics. (Source: Miashiro 1974)</p>
<p>Seghedi et al. 2015</p>	 <p>(d) $(\text{Na}_2\text{O}+\text{K}_2\text{O})$ vs SiO_2 diagram of LeMaitre (1989) showing the distribution of different phases of the Yuntdağ and Yamanlar volcanics. (e) K_2O vs SiO_2 diagram of Yuntdağ and Yamanlar volcanics. (Source: Peccerillo and Taylor 1976)</p>	<p>(d) $(\text{Na}_2\text{O}+\text{K}_2\text{O})$ vs SiO_2 diagram of LeMaitre (1989) showing the distribution of different phases of the Yuntdağ and Yamanlar volcanics. (e) K_2O vs SiO_2 diagram of Yuntdağ and Yamanlar volcanics. (Source: Peccerillo and Taylor 1976)</p>
<p>Ercan et al. 1995</p>	 <p>(f) $(\text{Na}_2\text{O}+\text{K}_2\text{O})$ vs SiO_2 diagram of LeMaitre (1989) showing the distribution of different phases of the Behram volcanics. (g) $\text{Na}_2\text{O}+\text{K}_2\text{O}$ vs SiO_2 diagram of Behram volcanics (Source: Miashiro 1974)</p>	<p>(f) $(\text{Na}_2\text{O}+\text{K}_2\text{O})$ vs SiO_2 diagram of LeMaitre (1989) showing the distribution of different phases of the Behram volcanics. (g) $\text{Na}_2\text{O}+\text{K}_2\text{O}$ vs SiO_2 diagram of Behram volcanics (Source: Miashiro 1974)</p>

1.4.3. Mineralogical and Petrographic Characteristics

Andesites are composed of plagioclase feldspars, mafic with little or no quartz as mentioned before (Fichter and Farmer 1975). As for the other characteristics, amount of the minerals in the andesites differ according to their formation process (Spock 1953).

Mineralogical and petrographic analyses of the andesites in Turkey show that they are mostly composed of plagioclase feldspars, alkali feldspars, pyroxene, biotite, hornblende, mica, quartz and volcanic glass as matrix (Akyürek ve Sosyal 1983, Tankut 1985, Gökten and Floyd 1987, Ercan et al. 1995, Zedef and Ünal 2003, Akay and Erdoğan 2004, Tokmak 2005, Orhan et. al 2006, Yavuz 2006 and 2011, Murtezaoğlu 2009, Kaplan 2009, Koralay 2010, Zedef et al. 2011, Korkanç 2013 and Seghedi et al. 2015).

The texture of andesite is generally aphanitic (fine grained) and based on its mineralogical characteristics, its color is variable as the shades of grey, purple, brown, green and almost black (Spock 1953). The studies on the petrographic characteristics of the andesites also show that they are generally aphanitic (Fichter and Farmer 1975, Tokmak 2005, Yavuz 2006, Orhan et al. 2006, Murtezaoğlu 2009, Kaplan 2009, Koralay 2010, Sak et al. 2010, Korkanç 2013 and Seghedi et al. 2015). Except the aphanitic ones, Zedef and Ünal (2003) and Yavuz (2011) determined the porphyritic texture of Niğde and Isparta andesites respectively.

As the characterization of the andesites of different regions, their deterioration problems were also studied by many researchers. In the following parts, the processes of the deterioration of exposed standing andesites, buried materials including stones and excavated andesites and the recent studies on these subjects will be introduced.

1.5. Deterioration of Exposed Standing Andesites

Deterioration and conservation of stones most comprehensively discussed in the book of Doehne and Price (2010). The review study briefly explains the deterioration factors and conservation methods for each stone. For the causes of deterioration for exposed standing stones including andesites, the study underlines the effects of freeze-thaw and wetting-drying cycles, biological growth, relative humidity, soluble salts, clays, wind, rain, air pollution, human interventions and natural disasters.

Experimental studies on the deterioration of the exposed standing andesites are mainly based on the comparison of physical, chemical and mineralogical characteristics of interior cores and deteriorated surfaces. In this context, *physical deterioration* of the andesites is generally studied with the changes in density and porosity values of interior parts and exterior surfaces. The studies show increase in the porosity and decrease in the density values in the deteriorated parts of the andesites (Oguchi and Matsukura 1999, Tokmak 2005, Yavuz 2006, Sak et al. 2010, Korkanç 2013). Physical deterioration of the andesites was also explained by the determination of pore volumes and weight losses in deteriorated parts. As an increase in pore volumes, the comparison of the pore volumes in the sound and deteriorated parts of the andesites show that the pores are less than 10 mm in diameter in the sound parts whereas it is more than 100 mm in the weathering rinds of the andesites in the study of Jamtveit et al. (2011). Increase in the porosity and decrease in the density in the deteriorated parts of the andesites also cause weight losses. As a result of the the physical deterioration of the andesites in five year period on a saturated soil environment, $0.002\% \text{ year}^{-1}$ weight loss was determined by Matsukura and Hirose (1999).

Generation of living organisms such as lichens and algae on the andesite surfaces cause *biological deterioration* of the stones and determined by mineralogical and microstructural analyses. Effects of the lichens to the andesites were studied by Ascaso et al. (1990). The study indicates that andesite surfaces with the presence of water are suitable environment for the generation of lichens. Several types of lichens were determined on andesite surfaces. Besides soiling of the stone surfaces, chemical action of lichens to the stone minerals by the excretion of organic acids was underlined and chemical changes in biotite as transforming to phyllosilicates was determined (Ascaso et al. 1990).

Chemical deterioration of the exposed standing andesites was formed as a result of hydrolysis, dissolution and oxidation processes of the minerals and resulted in the formation of secondary minerals (deterioration products) (Press and Siever 2002). As a result of chemical deterioration of andesite forming minerals, formation of clay minerals (kaolinite, halloysite and smectite etc.), hematite and gibbsite was determined by Reiche (1943), Colman (1982), Mulyanto et al. (1999), Mulyanto and Stoops (2003), Tokmak (2005), Orhan et al. (2006), Lee and Yi (2007), Murtezaoglu (2009), Orhan et al. (2006) and Sak et al. (2010). Formation of the clay minerals in andesites is described as a result of dissolution of volcanic glass and plagioclase feldspars. Presence of hematite and goethite in the deteriorated parts are described as a result of dissolution and subsequent oxidation of iron-feldspars such as pyroxene and amphibole (Colman 1982, Mulyanto et al. 1999, Oguchi 2000, Mulyanto and Stoops 2003, Tokmak 2005, Orhan et al. 2006, Murtezaoglu 2009, Sak et al. 2010). Apart from the presence clay minerals, hematite and gibbsite, formation of gypsum and apatite, resulted from deterioration of Ca-feldspars in SO₂-polluted atmosphere, on the andesite surfaces was determined by Moropoulou et al. (2003).

Chemical deterioration of the andesites also resulted from the dissolution of the minerals. In the studies, it is explained by the comparison of the elemental characteristics, which means types and/or amounts of the elements, of sound and deteriorated parts of the stones (Reiche 1943). Change amounts of the elements, which is also called mobility of the elements, is also resulted from the formation of secondary minerals (Reiche 1943).

Elemental characteristics of sound and deteriorated parts of the andesites were compared by Mulyanto et al. (1999) and decrease in SiO₂ (from 61.1 to 56.6) and increase in Al₂O₃ (from 16.8 to 27.5), resulted from the formation of clay minerals in the deteriorated parts were determined. The same comparison by Oguchi (2000) revealed higher FeO+Fe₂O₃ content and lower amounts of CaO, MgO, Na₂O and K₂O content in the deteriorated parts as a result of dissolution of alkali/alkaline earth metals with the presence of water. In SO₂-polluted atmospheric conditions, characteristics of gypsum layer formed on the andesite surfaces studied by Moropoulou et al. (2003) show lower concentrations of Si and Al and slightly higher concentration of Ca, which is resulted from the dissolution of calcium feldspars.

Elemental changes resulted from the chemical deterioration of the stones are used in the weathering indices, for the evaluation of the chemical deterioration of the stones. Chemical weathering indices generally used by the geologists and they are mainly proposed for felsic and/or intermediate stones such as andesites (Düzgören-Aydın et al. 2002, Ceryan Ş. 2008). These indices are based on the calculation of the changes in the amounts of the elements or element oxides (mobility of major cations) after chemical deterioration (Ceryan Ş. 2008, Bahlburg and Dobrzinski 2009).

Chemical weathering indices were proposed for the first time by Reiche (1943) as the weathering potential index (WPI) and the product index (PI) with the formulas of:

$$\text{WPI} = (\text{K}_2\text{O} + \text{Na}_2\text{O} + \text{CaO} + \text{MgO} - \text{H}_2\text{O}) \times 100 / (\text{SiO}_2 + \text{Al}_2\text{O}_3 + \text{Fe}_2\text{O}_3 + \text{FeO} + \text{TiO}_2 + \text{CaO} + \text{MgO} + \text{Na}_2\text{O} + \text{K}_2\text{O})$$

$$\text{PI} = (\text{SiO}_2 \times 100) / (\text{SiO}_2 + \text{Al}_2\text{O}_3 + \text{Fe}_2\text{O}_3 + \text{FeO} + \text{TiO}_2)$$

where decreasing WPI means decreasing mobile cations and increasing clay content and decreasing PI means decreasing silica content with the deterioration process of the stones (Gupta and Rao 2001). Ruxton (1986) developed a weathering index by taking silica loss as a total element loss and assuming alumina remains constant during deterioration with the formula (Gupta and Rao 2001):

$$\text{Ratio} = \text{Silica (SiO}_2\text{)} / \text{Alumina (Al}_2\text{O}_3\text{)}$$

However, this formula has not been found suitable for basic and ultrabasic rocks. It has been found more suitable for the acidic rocks in draining and humid climates (Irfan 1996). Parker (1970) proposed an index, which is called the Weathering Index of Parker (WIP), applicable to acidic, intermediate and basic rocks in all conditions where hydrolysis is the main agent of silicate deterioration. WIP considers mirroring the changes in Mg^{2+} , Ca^{2+} , K^+ and Na^+ as a major process of chemical deterioration with the formula of (Parker 1970, Hamdan and Burnham 1996):

$$\text{WIP} = [(\text{Na}^* / 0.35) + (\text{Mg}^* / 0.9) + (\text{K}^* / 0.25) + (\text{Ca}^* / 0.7)] \times 100$$

or

$$\text{WIP} = [(2\text{Na}_2\text{O} / 0.35) + (\text{MgO} / 0.9) + (2\text{K}_2\text{O} / 0.25) + (\text{CaO} / 0.7)] \times 100$$

where the cations* represent the atomic percentage of an element divided atomic weight (Parker 1970, Bahlburg and Dobrzinski 2009).

Results of WIP are commonly between ≥ 100 and 0 and the smaller WIP values indicate stronger chemical deterioration (Table 1.4) (Parker 1970, Hamdan and Burnham 1996). However, WIP lacks of consideration of a relatively immobile Al_2O_3 in formula which would help to monitor the changes of composition of the relevant mineral components (Bahlburg and Dobrzinski 2009, Shao et al. 2012).

This disadvantage of WIP was overcome in the Chemical Index of Alteration (CIA) proposed by Nesbitt and Young (1982) to reconstruct the paleoclimate from Early Proterozoic sediments of the north of Lake Huron. CIA is based on monitoring the hydrolysis of feldspar and volcanic glass and their conversion to clays as a result of chemical deterioration (Shao et al. 2012). It represents a ratio of predominantly immobile Al_2O_3 to the mobile cations Ca^{2+} , K^+ and Na^+ as oxides. It defined as:

$$CIA = \left(\frac{Al_2O_3}{Al_2O_3 + Na_2O + K_2O + CaO} \right) \times 100$$

where the major element oxides are given in molecular proportions. Opposite to WIP values, highest degree of deterioration in CIA has a value of 100 and represents kaolinite. Illite is between 75 and 90, muscovite is 75, the feldspars are 50 and fresh igneous rocks have the values between 30 and 55 according to their chemical characteristics (Table 1.4) (Nesbitt and Young 1982, Fedo et al. 1995, Bahlburg and Dobrzinski 2009). Among many chemical weathering indices, the Weathering Index of Parker (WIP) (Parker 1970, Hamdan and Burnham 1996) and the Chemical Index of Alteration (CIA) (Nesbitt and Young 1982) are the two commonly applied indices (Shao et al. 2012).

Chemical weathering indices of CIA and WPI were studied to determine the weathering degrees of the andesitic and granitic stones by using polarizing microscope, SEM, XRD and XRF analyses by Lee and Yi (2007). The CIA result of basalt was 50.38; andesite 52.38; andesitic tuff 51.19; and micrographic granite 53.23. The amount of Al_2O_3 remains in the same samples increase CIA values. The WPI value of basalt was 8.28, andesite 8.14, andesitic tuff 5.35, rhyolite tuff 6.07, micrographic granite 4.06, and alkali granite was 5.57. The results showed the chemical deterioration of the stones.

Table 1.4. Summary of weathering indices of WIP (Source: Parker 1970) and CIA (Source: Nesbitt and Young 1982)

Stone Type	CIA			WIP		
	Optimum Fresh	Deteriorated	Optimum Deteriorated	Optimum Fresh	Deteriorated	Optimum Deteriorated
Granite	$45 < x < 55$	$55 \leq x < 75$	100	>100	$0 < x \leq 100$	0
Basalt	$30 < x < 45$	$45 \leq x < 75$	100			
Diorite	$45 < x < 55$	$55 \leq x < 75$	100			
Andesite	$45 < x < 55$	$55 \leq x < 75$	100			

The factors effective in the deterioration of exposed standing stones differ from the factors effective in the buried and excavated stones as the deterioration processes take place in different environments. Although there are many studies about the deterioration of exposed standing stones including andesites, the studies on the buried and excavated andesites are too scarce. In the following parts, the studies concerning the deterioration of excavated andesites with the burial processes will be explained. Deterioration of buried stones and the factors effective in this process will be explained including the other buried materials as the lack of studies on the deterioration of buried stones.

1.6. Deterioration of Excavated Andesites

Deterioration process of the excavated materials has two preliminary deterioration processes. As previously mentioned, first process starts with their exposure to atmospheric conditions as a building material and takes place during exposure. Second process is the burial process, which takes place in the subsoil environment. The last phase starts with the re-exposure of the materials to atmospheric conditions after their excavation.

For the deterioration of buried materials including stones, Cronyn (2002) is the most comprehensive work which explains the main factors effective in the deterioration of different materials during burial and after their excavation.

In the literature, determination of the deterioration process of the buried stones became an important subject at the end of the 1980s due to fast deterioration process of the excavated materials. Early works on the study of deterioration of buried stones were focused on the patinas on the stone surfaces.

Patinas on the ancient marble sculptures and other artifacts were studied by Margolis and Showers (1988) by stable isotope mass spectroscopy, scanning electron microscopy, electron microprobe and PIXE techniques. The analyses were applied to fresh interior marble to outer deteriorated surfaces and the results were compared. The comparison of the results indicates that the patinas are composed of calcium oxalate, clay minerals and iron oxides. Formation of calcium oxalate is resulted from the chemical deterioration of carbonate minerals effects of oxalic acid, produced by micro organisms.

The calcium oxalate patinas on the calcarenite stone surfaces buried for almost 6150 years with powdered samples and small single pieces were also determined by Garcia-Valles et al. (2010) by using polarizing light microscope, scanning electron microscope, X-ray diffraction analysis and a colorimetric analyzes. The results of the study also show that the patinas (25-100 μm thick) are related to a burial environment and formed as a result of chemical deterioration of the carbonate minerals in the stones by biological activity. Studied patinas have uniform color (beige-orange), texture (granular) and composition (main composition is calcite with between 60-90 %) and also have a protective role on the stone surfaces (Garcia-Valles et al. 2010).

The patinas on the marble surfaces were also studied by Polikreti (2007) and Polikreti and Christofides (2009) by using optical microscopy, ultraviolet-induced fluorescence, electron paramagnetic resonance (EPR) spectroscopy and laser ablation inductively coupled plasma mass spectrometry (LA-ICP-MS). Clay minerals and iron were determined in the patina on the marble surfaces buried for thousands of years by Polikreti (2007). Both clay minerals and iron were indicated to originate from the soil structure with the dissolution of the feldspars and iron oxides in soil structure and subsequent accumulation to the marble surfaces. The comparison of the patinas of ancient (about 1000 years) and recently (50 years) buried marble surfaces by Polikreti and Christofides (2009) show that the calcium ions originate from the weathered marble surface as a result of calcite dissolution. For burial periods in the scale of 1000 years, humates are always present on marble surfaces independently of the soil type and recently (time scale of 50 years) buried surfaces shows that the blue-green emission and consequently the presence of humates in marble patinas are not affected by the soil organic matter content.

Patinas on the buried sandstones was studied by Ilani et al (2002 and 2008) with the samples buried about 4600 years, by using SEM-EDS, XRD, radiocarbon dating and accelerator mass spectrometry (AMS) analyses. Two types of patinas determined on the sandstones. First is thin layers of a black to orange-brown, iron oxide-rich patina resulted from biological activity (mainly fungal activity) and second is light beige patina mainly composed of carbonates, quartz and feldspar grains which originated from the chemical deterioration of the stone forming minerals. AMS analyses of the carbon particles in the patina show the calibrated radiocarbon age of 2340-2150 Cal BP and a conventional radiocarbon age of 2250±40 years BP. The results of AMS analyses and the presence of microcolonial fungi and associated pitting indicate slow growth of the patinas over many years.

For the igneous rocks, deterioration of buried granites beneath acid peat within the Mourne Mountains of Northern Ireland for 20 months was studied by Power (1989) by scanning electron microscopy with small tablets. The study show that burial time for 20 months, even under very aggressive conditions, is not enough for the deterioration of the granites since significant deterioration of the granites could not determined.

Deterioration of granites with dolomite and limestone samples buried in shallow pits beneath a variety of vegetation cover types in Kärkevagge was studied by Thorn et al. (2006) by monitoring mass losses of the samples. Stone samples with ≈6.2 mm

diameter buried for ten years and then mass losses were determined. Total losses of the stones determined between 0.2 and 25.7% for dolomite, 0.07 and 0.57% for granite and 0.2 and 32.1% for limestone samples showing the deterioration rate order as limestone>dolomite>granite. Dolomite was indicated as the most useful material for monitoring mass loss with limestone deterioration is too rapid and granite deterioration during burial is too slow. As the critical factors influencing buried stone deterioration, the effects of climate and soil pH, vegetation cover and ground moisture are underlined.

Deterioration of buried and excavated igneous rocks of Bronze Age which were buried for up to 2500 years within a wet, acid environment and then exposed was studied by Curran et al. (2002) and Warke et al. (2010). The studies were carried on the recently and previously (sixteen years ago) excavated quartz porphyry and porphyritic andesite samples by using SEM and XRD analysis. Outer bleached margin was observed on both recently and previously excavated stone surfaces. Examination of the patinas indicates that the bleached appearance may be due to the degradation of ferromagnesian minerals (biotite, hornblende and pyroxene) during burial. The main difference of the patinas on recently and previously excavated andesites related to structural integrity. In the majority of previously exposed samples, the patina is friable and unstable whereas it is more stable in recently excavated ones. The unstable situation of the patinas on the previously stones may be due to the biological growth formed on the stone surfaces, after their excavation. The studies underline the rapid deterioration process of igneous rocks within a few months of exposure after the structural and mineralogical weaknesses occurred during burial (Curran 2002, Warke et al. 2010).

Apart from the characteristics of the patinas observed on the stone surfaces, the factors effective in the deterioration of buried and excavated stones are also stated in the previous studies. Based on these studies and the review study of Cronyn (2002), the factors effective in the deterioration of buried and excavated andesites can be stated as:

- Characteristics of subsoil environment: presence of water, micro-organisms, soil type, clay and soluble salt content, site topography, ground temperature, oxygen, soil pH and depth of burial;
- Characteristics of buried material: composition of the artifact and material size;
- External factors: vegetation cover, land use and environmental pollution.

In the following sections, these factors will be explained.

1.6.1. Characteristics of Subsoil Environment

Longevity of buried materials is related to many parameters of subsoil environment (Williams et al. 1986). As the number of the factors effective above the ground, there are also numerous factors effective in the intersection of the stone and the soil that covers it (Thorn et al. 2006). Thus, the characteristics of the subsoil environment are the most important parameters in the deterioration of buried materials.

In general, subsoil environment is divided into two parts as *shallow* and *deep burial* areas (Crow 2008, Velde and Meunier 2008). Shallow burial areas represent the top few meters of the soil section and deeper part of this parts are called deep burial areas. Shallow burial areas are subdivided in to two horizons (zones) as O and A horizons and deep burial areas are subdivided in to three horizons as E, B and C horizons (Figure 1.2) (Velde and Meunier 2008). Every horizon has its own set of characteristics.

The *O horizon* is a surface horizon which is made up mostly of decomposed organic matter and leaf litter. The *A horizon*, which is also called rhizosphere, is the surface layer composed of plant roots and sand, silt, and clay. With the presence of organic materials, clays, water and air coexist in this layer (Amundson 2003, Velde and Meunier 2008). Thus, the horizon creates appropriate environment for physical, chemical and biological deterioration of the buried materials (April and Keller 1990, Colin, et al. 1992, Velde and Meunier 2008). The *E horizon* (shown as B_h in the Figure 1.2) is light in color and mostly composed of sand and silt. It has been heavily leached in which soluble nutrients are lost from the soil due to precipitation or irrigation. The *B horizon* is a subsurface horizon which has accumulated from the layers above and contains clay and mineral deposits which it receives from layers above it when mineralized water drips from the soil above. The *C horizon*, which is also known as the saprolite, is the deteriorated rock zone. Plant roots do not penetrate into this layer and very little organic material is found. The most important process in this zone is that hydration and chemical dissolution of stone minerals. As a chemical deterioration, anhydrous and low hydration state rock minerals are transformed into hydrous (OH) forms in C horizon (Velde and Meunier 2008). The deepest layer of the subsoil environment is the fresh rock (bedrock).

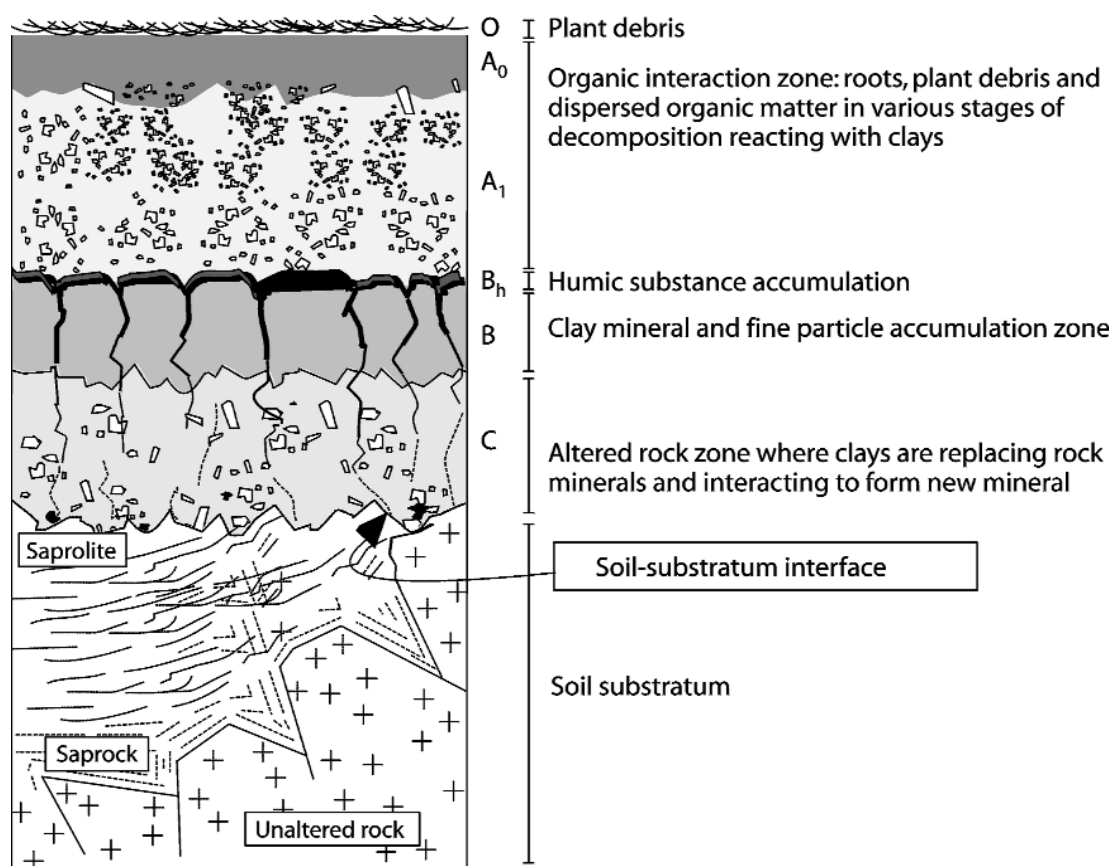


Figure 1.2. The components of subsoil environment
(Source: Velde and Meunier 2008)

Deterioration of the buried materials takes place in the layers mentioned above and the characteristics of these layers have direct effects on this process. One of the most important characteristics is site topography, which is directly related to four important parameters in the deterioration of buried artifacts: temperature, depth of burial, drainage and surface movement of geological materials (Curran et al. 2002). The temperature and moisture values of subsoil environments do not show as diverse varieties as in air (Spock 1953, Cronyn 2002). However, the surface layers may affect from the temperature changes of the atmosphere. Thus, freeze-thaw cycles in the atmosphere may cause frost damage as a physical deterioration and warm temperatures increase the rate of chemical deterioration and biological growth (Cronyn 2002). The stability of the burial environment increases through deeper parts of the subsoil through the deep burial areas. Hence, physical deterioration of stone proceeds in the soil slowly. Shallow burial environments are more porous than deep burial environments. It creates more dynamic environment for chemical changes and generation of biological forms (Cronyn 2002).

In other words, deterioration of the same buried materials in different horizons in shallow areas such as organic-interaction zone and clay mineral zone will be different (Velde and Meunier 2008). Depth of burial is also play a major role in the deterioration of buried materials. The weight of the soil over the materials may deform the soft materials, such as pottery, buried in it (Cronyn 2002, Crow 2008).

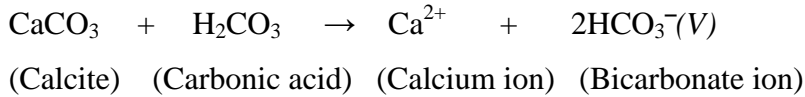
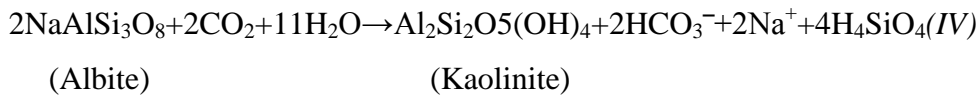
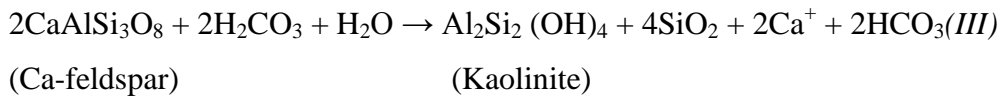
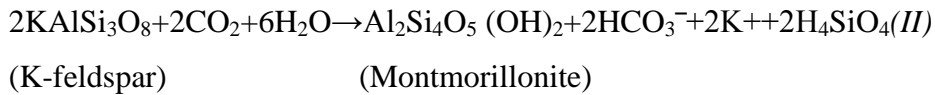
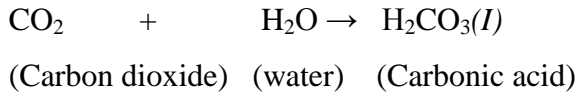
Topography of the site also has a direct effect on the drainage, which is directly specify the movement of water in subsoil environment and thus affect the chemical characteristics of the environment as it carries chemically active substances such as carbon dioxide (Spock 1953, Curran et al. 2002). In general, poor-drained sites exhibit higher deterioration rates of burial materials than well-drained sites (Curran et al. 2002, Velde and Meunier 2008). As in the movement of water, topographical features as slope also affect the movement of geological materials such as clays which have both chemical and biological effects on the buried materials (Velde and Meunier 2008).

The presence of water in the subsoil environment has chemical effects on buried materials (Cronyn 2002). The waterlogged areas provide an anaerobic burial environment and thus prevent the interaction of oxygen, which is one of the main destructive factors for organic materials. However, hydrolysis is prevalent because of the saturation of the materials and dissolution of the minerals inexorable. Thus, organic materials get weaker in the presence of water in the subsoil environment (Cronyn 2002).

The presence of water also effective in the deterioration of buried inorganic materials such as stones. The effects of water to the buried stones are also generally chemical. In the presence of water, stone minerals react with it and hydration occurs as deterioration. For the igneous rocks, feldspars in the stones turn into clay minerals and other secondary minerals as a result of this reaction (Press and Siever 2002).

In the burial environment, the reaction of water with carbon dioxide (CO_2) gas results in the formation of carbonic acid (H_2CO_3) (Reaction I). Formation of carbonic acid promotes the chemical deterioration of organic materials such as wood (Tjeerdsma and Militz 2005). As the most common natural acid, carbonic acid also causes dissolution of stone forming minerals in the igneous rocks and formation of clay minerals (Chen et al. 1999, Press and Siever 2002, Mortatti and Probst 2003) (Reaction II, III and IV). The presence of clay minerals in the stone structure cause further deterioration of stones which will be explained in more detail in following parts (3.3.3). Formation of carbonic acid in the subsoil environment also causes the deterioration of sedimentary and metamorphic rocks as the igneous rocks. The reaction of carbonic acid

with the calcite, which is the major mineral of the sedimentary and metamorphic rocks such as dolomite and limestone, causes dissolution of the mineral. When calcite dissolves, the calcium and bicarbonate ions are carried away in the solution (Reaction V) (Press and Siever 2002).



The presence of water in subsoil environment also promotes the formation of different organisms which have both physical and chemical effects on the materials (Cronyn 2002). Micro-organisms such as bacteria, algae, fungi and lichen are primitive and susceptible to changes in the environment. However, some of their species have adapted to live in extreme pH or oxygen necessity (Cronyn 2002). Their effects on the burial materials are both physical and chemical. During burial, the activities of organic materials in the soil structure by the excretion of various enzymes and acids, such as carbonic acid promote the dissolution of stone forming minerals as mentioned before (Chen et al. 1999, Mortatti and Probst 2003). Depending on mineral type, pH of the environment and organic acid type; organic acids are able to induce a 2-4 fold increase in mineral dissolution rate in comparison with the presence of water (Jones 1998). For the silicate minerals, the impact of organic acids on weathering rate by organic acids found in soil solutions is not too much significance (Drever and Stillings 1997, Jones 1998). The effects of these organisms on the materials are more obvious on organic

materials which are the food source of these organisms (Cronyn 2002). The physical effect of the micro-organisms on the materials is their hyphae penetration through the voids of the materials and swelling/shrinkage action of the hyphae in the voids cause new micro-cracks in the material structures (Chen et al. 1999).

The respiration of the microorganisms results in the formation of oxygen, which has a direct role in the deterioration of buried materials (Cronyn 2002). Inversely related to the amount of water, oxygen mainly occurs within the voids of the materials as a gas and it is an oxidizing agent and thus takes in part in many redox reactions. Its presence or absence in the subsoil environment has also the basic control of organism formation which has deteriorating effects on burial materials (Cronyn 2002).

The presence and activities of micro-organisms with the presence of water content govern the soil pH (chemical environment) in the subsoil environments (Nord et al. 2005). Soil pH is one of the most important factors determining artifact and mineral longevity and thus affecting the in situ preservation of materials (Matthiesen 2004, Crow 2008). The stability of buried materials, which is the measure of the tendency of a chemical substance to resist decomposition or change, is considerably affected by pH of the environment. Some materials are better preserved at acid or alkaline environments (such as bone) while some others stable at neutral pH (such as igneous rocks) (Cronyn 2002, Crow 2008). The stability of different minerals and their abrasive pH values will be explained in the following parts.

As mentioned before, deterioration process of buried materials is the result of interaction processes between artifact surfaces and soil (Crow 2008). Thus, soil type, which is the composition of the soil, is one of the most important parameter as it determines the extent of many other potential impacts to the buried materials (Crow 2008, Polikreti and Christofides 2009, Garcia-Valles et al. 2010). As different burial environments, different soil types favor the preservation of different types of materials. The compositional similarities of buried artifact and soil have preventive effects on burial artifacts as the dissolution of the artifact minerals in the subsoil environment continues until stabilization with the burial environment is gathered. For example, gypsum is more preserved in soils saturated with calcium (Crow 2008).

As the mineralogical characteristics, clay and soluble salt of contents of the subsoil environment are the important parameters determining the soil type. Clays are fine grained (size less than 2 μm) mineral components which have good capacity of hydration and which give plasticity to rocks and materials (Guggenheim and Martin

1995). Because of their huge outer and inner surfaces per unit, clays are very reactive minerals (Velde and Meunier 2008) and they can form and transform both at surface and subsurface of the Earth and also at deteriorated stones (Thorn et al. 2002).

The presence of the clay minerals and soluble salts in materials is supported by the surrounding soil. The soluble salts and clays in the soil structure fill the cracks of the materials burial (Cronyn 2002). While the penetration occur during burial, they do not have direct effects before excavation of these materials. As an indirect effect, water holding capacities of clays increase the rate of interaction between water and material minerals. In other words, the more soil contains clays, the more it increases water retention and thus chemical deterioration rate increase (Thorn et al. 2002).

Direct effects of the clay minerals and soluble salts are more likely to be after excavation of these materials when rapid and massive temperature and humidity changes start to occur more widely than usually occur in burial environment (Wüst and McLane 2000, Curran et al 2002, Warke et al 2010). As a result of these changes, deposited clay and soluble salts may lead to a rapid deterioration of stone which is faster than exposed standing stones (Power 1989, Thorn et al. 2002, Cronyn 2002, Warke et al 2010). The crystallization of soluble salts in the stone structure causes pressure on the walls of the cracks. The pressure widens these cracks and physical deterioration occurs (Cronyn 2002). Clay minerals in the cracks of the stones swell and shrink with wetting-drying processes. In the process of swelling and shrinkage, cracks further propagate in the pores of the stone (Press and Siever 2002, Scherer 2006). As far as promoting physical weathering, clay minerals also constitute appropriate environment for biological formations (Chen et al. 1999). After excavation of the stones, the presence of the clays in the stone structure and on the stone surfaces and atmospheric conditions create appropriate environment for the rapid formation of biological forms on the stones. The biological forms promote both physical and chemical deterioration of stones. Hyphae penetration of biological forms through the voids in the stone causes mechanical force as a physical deterioration which also promotes chemical deterioration in creating new places for clay and salt minerals and water, and also contributing to acid dissolution, oxidation and chelation (Chen et al. 1999, Pope et al. 2002).

As previously explained, materials are generally better preserved in burial conditions and excavation of these materials without conservation considerations causes faster deterioration. Without conservation measurements, archaeological excavations cause loss of information (Cronyn 2002).

1.6.2. Characteristics of the Materials

Buried materials are composed of many organic and inorganic components and every material has its own set of characteristics. The effects of same burial environment to different materials are certainly different based on composition of the artifacts (Kars 1997). As having different formation process, stones exhibit a wide range of mineral composition, texture and structure. Therefore, the physical and chemical properties of different types of stones are extremely variable, resulting in stones with widely different abilities to resist deterioration (Miller et al. 2012).

The resistance of the stone forming minerals (durability against chemical deterioration) from the most stable to the least stable can be stated as:

iron oxides (hematite) > aluminum hydroxides > quartz > clay minerals > muscovite mica > potassium feldspars > biotite mica > sodium-rich feldspars > amphiboles > pyroxene > calcium-rich feldspars > olivine > calcite > halite (Press and Siever 2002).

The sequence show that the stability of the rock-forming minerals ranges from iron oxides at the most stable end to salt and carbonate minerals at the least stable end (Press and Siever 2002). Although many of the minerals in the igneous rocks are chemically stable and chemical deterioration of igneous rocks is generally slow and being limited to dissolution (Cronyn 2002), the andesite-forming minerals can be stated from the most stable to the least stable as:

quartz > clay minerals > muscovite mica > potassium feldspars > biotite mica > sodium-rich feldspars > amphiboles (hornblende) > pyroxene > calcium-rich feldspars (Press and Siever 2002).

As can be seen from the sequence, stone-forming minerals differ in their relative resistance to chemical deterioration with calcium-rich feldspars having the less resistant while quartz is the most resistant mineral in the andesite structure. As mentioned before, different minerals have different abrasion pH values. Andesite-forming minerals, their average amounts in andesite structure, their resistance to chemical deterioration and the abrasion pH values for these minerals can be seen in Table 1.5 (Eggleton et al. 1986, Press and Siever 2002, Banstra and Brantley 2008). As seen in table, low pH values or acidic environments promote chemical deterioration of andesite-forming where the deterioration of calcium feldspars starts in basic environment (Banstra and Brantley 2008).

Many of the minerals in the igneous rocks are chemically stable. Thus, chemical deterioration of igneous rocks is generally slow and being limited to dissolution (Cronyn 2002). However, it is enhanced by acidic conditions. In other words, low pH values or acidic environments promote chemical deterioration of silicate minerals and the formation of clay minerals (Velde and Meunier 2008).

Table 1.5. Andesite-forming minerals, their average amounts in andesite structure (Source: Press and Siever 2002), their resistance to chemical deterioration (Source: Eggleton et al. 1986, Press and Siever 2002) and the abrasion pH values for these minerals (Source: Banstra and Brantley 2008)

Mineral group (related minerals)	Average amount (%)	Abrasion pH Values	Resistance
<i>Quartz (quartz, cristobalite)</i>	2	< 5	↑ Increase in the resistance ↓
<i>Muscovite mica (muscovite)</i>	2 (with biotite mica)	< 7	
<i>K-Feldspars (orthoclase, microcline)</i>	1	< 8	
<i>Biotite mica (biotite)</i>	2 (with muscovite mica)	< 7	
<i>Na-Feldspars (albite)</i>	61 (with Ca-feldspars)	< 7 10	
<i>Amphiboles (hornblende)</i>	17	< 6 10	
<i>Pyroxene (orthoferrosilite)</i>	18	< 7	
<i>Ca-Feldspars (anorthite, labradorite)</i>	61 (with Na-feldspars)	≤ 8	

As the mineralogical characteristics, the size of materials has a direct proportion with their deterioration as in atmospheric conditions. In other words, bigger sizes of materials provide greater surfaces for physical, chemical and biological deterioration (Thorn et al. 2002).

1.6.3. External Factors

External factors such as vegetation cover above the soil structure, land use and environmental pollution are the effective factors in the deterioration of buried materials. Vegetation cover on the burial materials has physical and chemical effects on the materials. Trees alter the site's moisture regime and the chemistry of wet atmospheric deposition that reaches the soil. In the root zones of subsoil environments (O and A horizons), vegetation roots bind the fine particles of soil such as clays and thus water retention capacity and chemical deterioration rate of buried materials increase. Vegetation cover also changes the soil chemistry. Trees such as conifers may produce more acidic soil than most broadleaves and they reduce the soil fauna population, thus decreasing bioturbation (Velde and Meunier 2008, Crow 2008). Effects of vegetation cover to buried materials may also be physical. Forces created by the roots of the plants in the soil cause cracks or disintegrations of the materials (Velde and Meunier 2008).

As the vegetation cover, use of the lands above the buried materials has many effects. Land use changes are generally caused by social, political and economic shifts and in some cases, can be a major threat for the preservation of buried materials. This is because they bring about some changes in site characters (Davidson and Wilson 2006). The threats to buried materials caused by the land use changes can be stated as (Davidson and Wilson 2006);

- Urban and rural development
- Mineral extraction
- Agricultural and forestry processes (drainage, harvesting, ploughing etc...)
- Changes in land use management, for example from grazing to arable area.

Environmental pollution in urban sites also creates a serious problem for buried, excavated and exposed standing artifacts as it results in the acidification of air and soil environment (Nord et al. 2005, Davidson and Wilson 2006). Sulfur and nitrogen species (under certain circumstances) are mainly formed by burning of fossil fuels and they can be transported long distances via atmosphere. As sulfur and nitrogen, ammonia from manure, which may locally induce nitrogen pollution, can contribute to soil acidification (Nord et al. 2005). In rural areas also, chemicals used for agricultural purposes may

cause the acidification of soil environment (Davidson and Wilson 2006). Recent studies show that burial materials rich in silicates such as stones and ceramics show comparatively good resistance although metals (except gold) more or less rapidly corrode in soil. The most serious effects of soil acidification is to iron, bronze, copper and lead artifacts. Organic materials are less affected from soil acidification than metals (Nord et al. 2005).

1.7. Preventive and Active Conservation Measures in Archaeological Sites

Conservation of the stones was subjected in numerous studies as their characteristics and deterioration processes. These studies were summarized in the review book of Doehne and Price (2010).

Doehne and Price (2010) describe stone conservation as, doing something to stone and/or its environment to prevent further deterioration of the materials. In general, stone conservation measures are divided in to two topics as preventive and active conservation measures. These topics are also consisted of many techniques which are used in stone conservation (Doehne and Price 2010). Although there are many techniques which are used for movable and immovable stones, ones for the immovable stones will be mentioned in the following parts. Because all the studied andesite monuments are immovable and located in-situ conditions.

Preventive conservation measures, which are based on the prevention of further deterioration of the stones, generally concerned with the control of water, relative humidity and drying (Doehne and Price 2010). General preventive conservation measures for the immovable stones on the sites embrace a wide range of topics as: legislation to protect individual buildings and monuments, pollution control, traffic control, control of groundwater, visitor management, disaster planning (Baer and Snickars 2001, Doehne and Price 2010), wind fences, reburial of the monuments (Demas 2004, Doehne and Price 2010), control of drying, ground water, moisture and biological growth (Doehne and Price 2010).

Active conservation measures are not only prevention of the further stone deteriorations, but also treatment of the current deteriorations. Thus, it is generally concerned with doing something to the stones instead of their environments (Doehne and Price 2010). In other words, active conservation treatments are used for the treatment of the stone deteriorations by targeting the deterioration type, and then to prevent further deteriorations. As the preventive conservation measures, active conservation measures also embrace a wide range of topics as: cleaning techniques such as laser leaning latex poultice method and biological cleaning; consolidation techniques such as lime, organic polymers, alkoxysilanes, epoxies, acrylics and emulsions; surface coating techniques such as water repellents, anti-graffiti coatings, colloidal silica, and crystal growth inhibitors (Doehne and Price 2010).

Selection of the appropriate interventions is very critical phase of stone conservation even for preventive or active conservation measures. Before the implementation of the interventions, conservation strategies for the stones must be designed. These strategies must be based on the characteristics of the stones and their deterioration processes which were evaluated by laboratory analyses. Because incompatible interventions to the stones cause further deterioration of the materials instead of their conservation. In the following parts, method of this study for the evaluation of the characteristics and deterioration processes of the andesites will be explained.

CHAPTER 2

METHOD

This study focuses on the investigation of the deterioration problems of buried and excavated andesites to form a basis for the excavation decisions and necessary conservation measures for the purpose of their conservation. In this part, brief information about the history and the characteristics of the studied archaeological sites are given and site survey and sampling phases of the study and the experimental processes to determine the stone deterioration are discussed in detail. The visual analysis of the stone deteriorations was carried out with the site surveys in October 2010 and October 2014. The experimental data was collected from several experiments in which standard test methods, X-ray Diffraction (XRD), Fourier transformed infrared spectroscopy (FT-IR), Scanning Electron Microscope (SEM) equipped with X-Ray Energy Dispersive System (EDS), X-ray fluorescence (XRF), thermo-gravimetric analysis (TGA), polarized microscope and IC chromatography were used.

The surfaces of the exposed standing and recently excavated andesites in studied sites were documented in 2010 and 2014 by site surveys for the visual analysis of the deterioration types observed on the andesites. The andesite surfaces were compared to find out the progresses of the exposed standing and recently excavated andesite deteriorations in four years. The results of the experimental studies for the interior parts and exterior surfaces of the andesites and soils were also compared to find out the deterioration types and processes of buried and excavated andesites. The comparison of the andesite surfaces and experimental studies revealed the deterioration of excavated andesites.

2.1. Study Areas

In this study, Aigai (Manisa) and Assos (Çanakkale) archaeological sites were selected to determine the deterioration problems of excavated andesites (Figure 2.1). All the monuments in the sites were constructed with andesites in the same period and the excavation works in the sites are still ongoing. Aigai archaeological site was selected as an inland site and Assos was selected as a coastal archaeological site to find out the possible effects of being near the seashore in the deterioration processes of both buried and excavated andesites.



Figure 2.1. Map showing location of Aigai and Assos
(Source: World Coin Catalog 2015)

2.1.1. Aigai

Aigai (Nemrutkale), which is situated almost on top of the Mount Gün (a part of the Yunt mountain chain), is an ancient inland site in the northwest part of Turkey, in Manisa central district. It is located 80 km from İzmir centre, 14 km from Aliğa Village of İzmir and 2 km from Köselier village of Manisa (Figure 2.1). The site is 360 meters from sea level and almost 15 km far from the sea.

According to the information gathered from the excavations, the history of the city goes back to seventh century BC (Doğer 2007). Beginning from this period, the city was settled and inhabited till the end of seventh century AD. Then it was resettled again in Byzantine time in twelfth and thirteenth centuries AD (Doğer 2004).

The oldest written documents about Aigai belong to ancient historian Herodotos. According to Herodotos, Aigai was a member of twelve Aeolian settlements, traditionally known as the Aeolian Dodecapolis (Aigai, Killa, Aigirossa, Elaia, Cyme, Larissa, Neoteichos, Temnos, Grynion, Myrina, Pitane and Smyrna) (Hanfmann 1948). The cities were constructed by Aiolians who emigrated from Greece in the 1100s B.C (Herodotos 1991). Although ten of these cities were built near the seashore, Aigai and Temnos were built among the mountains (Ramsay 1881).

For a few centuries, Aigai was a member of the independent Aiolian city groups with Cyme assuming the leadership. Because of its location, the city did not gain political and commercial importance. But its location provided an advantage to the city because it was not affected by Persian attacks to the Hellenic cities. Because of this reason, Aigai developed in Hellenistic period and constructed most of its monumental buildings in this period (Ramsay 1881, Umar 2002). Various wars occurred in Aigai in the third century BC. In this century, the city included in the dynasty of Kingdom of Pergamon and the Kingdom of Seleukos respectively and then Kingdom of Pergamon again in 218 BC (in the Hellenistic period). After then, the dynasty of Prusias II from Bithynia started (Bohn and Schuchhardt 1889). In the first century BC, the hegemony of the Romans started. The city suffered enormous damage as a result of an earthquake in 17 AD (Umar 2002). And then it was rebuilt along with the other Aiol cities by the Emperor Tiberius in 34-35 AD. Because of Arabic raids in seventh century AD, the city was abundant till twelfth century AD when the Byzantine settlement was started (Doğer 2007).

After Herodotos, the historians Plinius, Tacitus, Strabon, Scylax, Xenophon, Plutarch and Titnaios mentioned Aigai in their works (Ramsay 1881). Scientific survey at Aigai started by W. M. Ramsay in his work “Journal of Hellenic Studies” in 1881 after his visit to Aigai with S. Reniach. Following Ramsay, S. Reniach mentioned Aigai in his work “Bulletin Hellenique” in 1882. In 1889, Richard Bohn and Carl Schunchhardt, who were the members of Pergamon excavation, published their work “Altümer von Aegae” after their comprehensive research in the site. The first Turkish researcher who surveyed and photographed Aigai was Prof. Dr. Bilge Umar in 1980 (Tül 1995). First excavations started in Aigai by Prof. Dr. Ersin Doğer from Department of Classical Archaeology, Ege University in 2004. Since 2004, the ancient streets of the city and some ancient buildings such as Hellenistic bouleuterion and stoa buildings, macellum and Byzantine church were totally excavated. The excavations are still continuing with the supervision of Prof. Dr. Ersin Doğer at different parts of the site.

Necropolis of the ancient site lies on the north eastern part of the settlement. There are city gates called Iron Gate and Tiberius Gate, Byzantian chapel and building blocks at the northern part of the site. West of the site is Theatre and Temple of Agora. There is Stadium of the city on south and Bouleuterion, Stoa, Agora, Macellum and Shops at the southern part of the archaeological site (Figure 2.2).

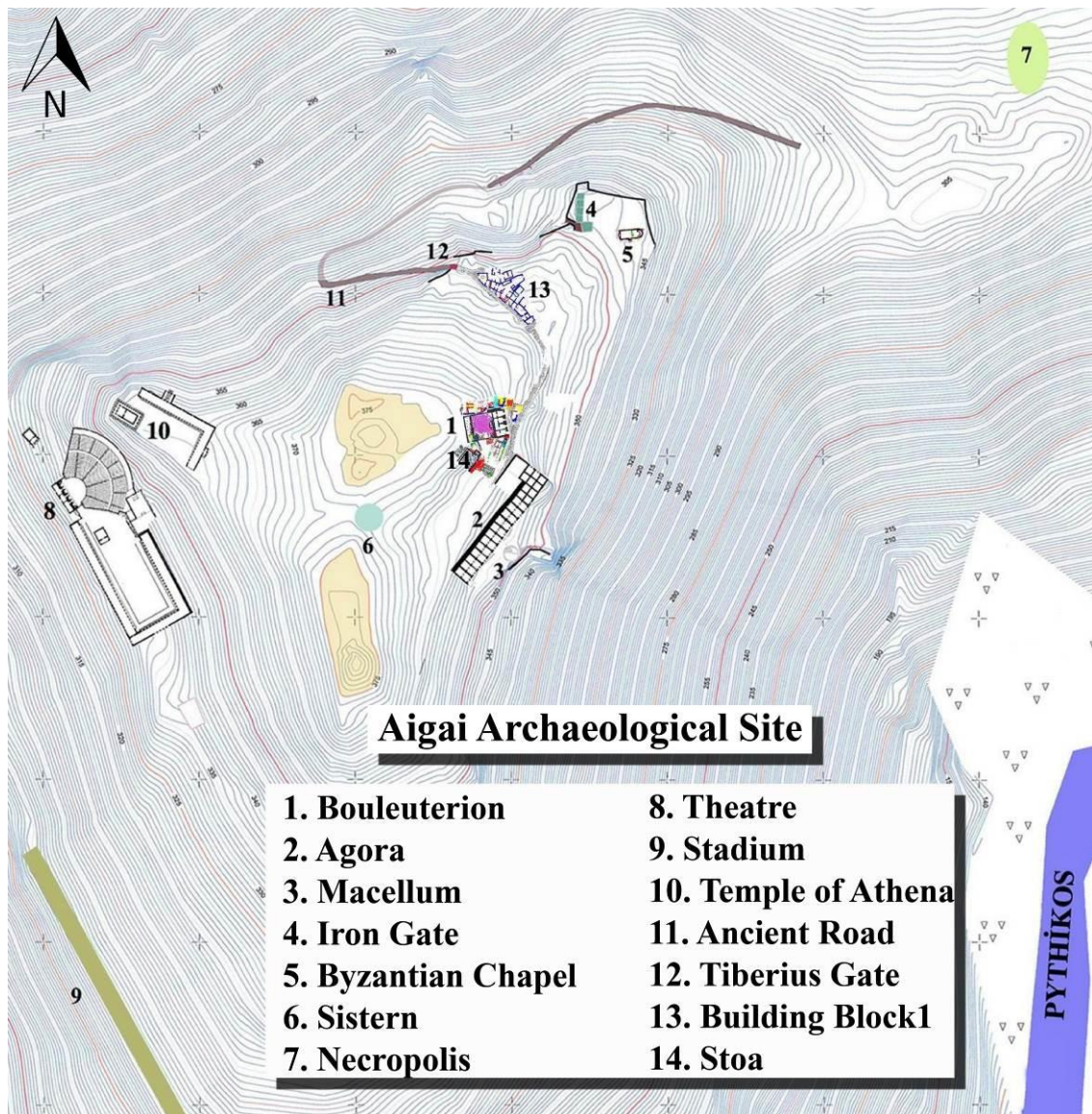


Figure 2.2. Topographic Map of Aigai
(Source: Aigai Kazısı Resmi Web Sitesi 2015)

The most important monuments in the site are three storey agora with stoas in the front (2nd century BC) (Figure 2.3, Figure 2.), bouleuterion (late 2nd and early 1st century BC) (Figure 2.), theatre (Figure 2.) and public baths (1st and 2nd centuries AD) (Figure 2.). All the monuments in the site were constructed and the roads were covered with andesite, which is also local stone of the area.



Figure 2.3. Agora building in Aigai
(Source: Panoramio 2015)



Figure 2.4. Stoa of Aigai



Figure 2.5. Bouleuterion building in Aigai



Figure 2.6. Theatre of Aigai



Figure 2.7. Northern (a) and Gymnasium (b) Baths of Aigai

2.1.2. Assos

Assos (Behramkale/Behramköy) is an ancient coastal site in the northwest part of Turkey, in Ayvacık district of Çanakkale. It is located 17 km from Ayvacık and 88.8 km from Çanakkale (Figure 2.1). The site is 234 meters from sea level and was constructed on a hilltop and foot slopes of mountain which is composed of andesites.

It is not known exactly who first settled in Assos but it is known that the city was settled and inhabited since Early Bronze Age till now, without interruption over the intervening centuries. From antiquity until the 1950s, the site was a small but busy commercial port. The present name of the site, Behramkale, is derived from name of Byzantine official who came to Assos on duty: Makhram (Serdaroğlu 1956).

The oldest information about Assos can be gathered from the historians Homeros and Strabon. Homeros wrote that the people who lived around the site were Lelegians (Homeros 1962). Strabon also confirmed this information and he claims that the name Assos was derived from Pedasos. According to Strabon, the Methymnian immigrants from Lesbos were settled in Assos (Strabon 1969, Serdaroğlu 1956).

Assos was the most powerful city of the Gulf of Edremit until it was captured by the Lydians in 560 BC. After 546 BC, the city was included in the Persian hegemony. The city, along with other cities such as Phokaea, Samos, Teos, Miletos and Lesbos, became a member of Delian confederacy in the Ionic-Aeolic region in 478 BC. After 407 BC, the Persian hegemony in the site started again. Following the King's Peace (Peace of Antalkidas) in 387 BC, first Eubolos and then Hermenias, who was a student

of Plato, and friend of Aristoteles, was became king. In the hegemony of Hermenias, ancient philosopher Aristoteles lived in Assos for three years and gave lectures at the gymnasium. Hermenias' independency finished until 345 BC and the city was governed by the Persians again. After then, the city was governed by Alexander the Great, Gallians, Pergamon and Romans. During Byzantine period, the city was connected to province of Asia. It was one of the first cities in Western Anatolia to accept Christianity and in fifth century AD, became a center of bishopric. In this period, many Roman buildings in the site were destroyed; marble building stones and sculptures were burnt to obtain lime and reused (Serdaroğlu 1956).

The city had several attacks during Seljukian and Ottoman period and thus the population of the city decreased gradually and it turned into small village. In 1204 AD, the region was captured by Francs and then by Turks in 1288. Since then, the region has been under the rule of Turks with no interruptions (Serdaroğlu 1956).

The first comprehensive publication about the city was written by Choiseul Gouffier in the second volume of his *Voyage Pittoresque dans l'Empire Ottoman* (1809). The book was based on his excursion to the area in 1785. After Gouffier, Assos was studied by Colonel Leake (1800), Dr. Hunt (1801), Richer (1816), Prokesch von Osten (1826), Charles Texier (1833) and many others (Arslan and Böhlendorf Arslan 2014).

Excavations in Assos started on 19th April of 1881 by Joseph T. Clarke and Francis H. Bacon (Archaeological Institute of America) and continued until 1883. The first excavations were focused on the Temple of Athena, necropolis, agora and theatre. The results of the excavation were published in 1921 (Serdaroğlu 1995). Hundred years after the beginning of first excavations, new excavations began in 1981 by Prof. Dr. Ümit Serdaroğlu and continued until 2005. In this time the excavation in Necropolis were expanded and the restoration of the Temple of Athena was started. Since 2006, the excavations have been conducted with the supervision of Prof. Dr. Nurettin Arslan (Çanakkale Onsekiz Mart University) at different parts of the site.

The ancient site has two gates one the eastern and western fortification walls (Figure 2.4). Acropolis of the city, where the Temple of Athena (540-530 BC) (Figure 2.5, Figure 2.6) is situated, was constructed on the hilltop of the mountain. With the Temple of Athena, there are also Hüdavendigâr Mosque (14th century AD) and a cistern on the hilltop. From hilltop through the foot slopes of the Assos, there are other monumental buildings such as Agora (2nd. century BC), Northern Stoa (2nd. century BC)

(Figure 2.7), Bouleuterion (4th. century BC) (Figure 2.8), Gymnasium (2nd. century BC) and Theatre (4th.and 3rd. centuries BC and some alterations during Roman Period) (Figure 2.9). The Necropolis is on the north western part, lies in front of the Western Gate of the city (Figure 2.10).

As in Aigai, all the buildings in the site were constructed and the roads were covered with andesite, which is also local stone of the area (Figure 2.10).

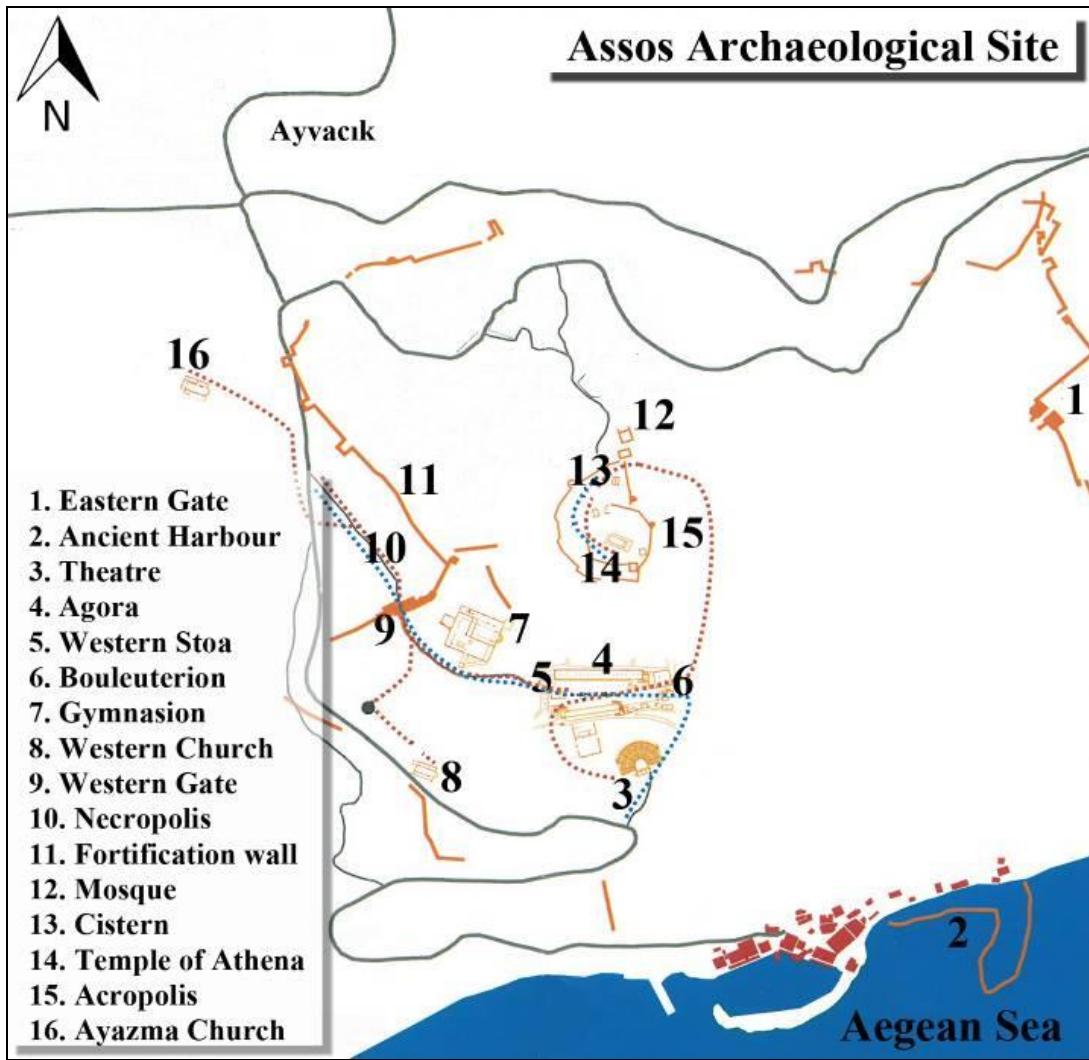


Figure 2.4. Map of Assos
(Source: Assos Kazısı Resmi Web Sitesi 2015)



Figure 2.5. Temple of Athena in Assos



Figure 2.6. Temple of Athena in Assos



Figure 2.7. Northern Stoa of Assos



Figure 2.8. Bouleuterion of Assos



Figure 2.9. Theatre of Assos



Figure 2.10. Fortification walls and Necropolis of Assos

2.2. Visual Analysis of Stone Deteriorations Observed on the Andesites

As mentioned before, Aigai and Assos archaeological sites were selected to determine the deterioration problems of excavated andesites. All the monuments in the sites were constructed with andesites in the same period and the excavation works in the sites are still ongoing.

Deterioration of the andesites used in Aigai and Assos archaeological sites was determined by in-situ visual observations and documented with the photos of the andesites taken in 2010 and 2014. The surfaces of the exposed standing andesites, which are approximately exposed to atmospheric conditions since 2500 years for both archaeological sites, and exposed standing parts and recently excavated parts of the partially excavated monuments were compared to each other. Comparison was carried out and in two phases:

- In the first phase, recently excavated and exposed standing parts of the partially excavated andesites were compared.
- Second phase of the comparison consisted of completely exposed standing and excavated andesites and partially excavated andesites between 2010 and 2014. Progresses of the andesite deteriorations in four years period were evaluated.

In the comparison, visible deterioration types such as crack formation, progress of the current cracks, spalling, pitting or loss of stone material, biological growth and colour changes (discoloration) were examined on the andesites.

The photos were taken from necropolis, agora, bouleuterion, stoa, shop and public bath buildings in Aigai and from necropolis, fortification walls, bouleuterion, stoa, theatre and gymnasium buildings in Assos archaeological site. Except agora building in Aigai and western fortification walls of Assos archaeological site, all the other monuments were partially or totally excavated.

All the photos, which were taken in 2010 and 2014, were taken in October to decrease the environmental effects of the different seasons. The photos also were tried to be taken from the same points of view in case current site conditions are appropriate. The comparison of the photos revealed the progress of stone deteriorations which is visible by naked eye.

2.3. Sampling

Experimental studies are carried out with the nineteen stone and nine soil samples collected from excavated sections of different buildings in Aigai and Assos archaeological sites. Because of the limited availability in the collection of the samples, which was resulted from the historical and cultural values of the materials, samples were collected in sufficient number for the experiments. During sampling, stones and soils were collected by hand and in different sizes suitable for the analyses and without harming the monuments. In the collection of the stone samples, detached stones were preferred. Soil samples were collected in order to find out the type of clay minerals and soluble salts in soil structure and to compare them with the stones.


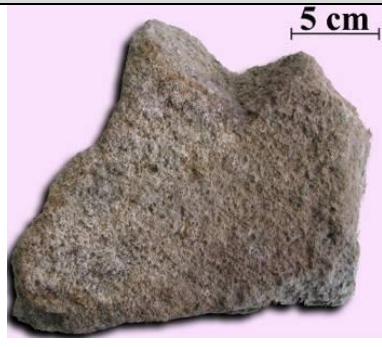
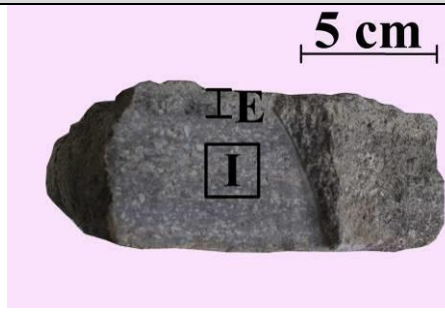








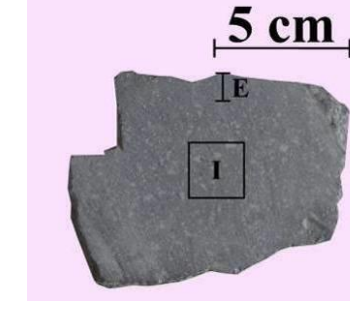
Stone samples were labeled with the letters showing the site they were collected from (Aigai: Ai and Assos: As) and soil samples were labeled with the letters showing the site they were collected from and their type of being soil (Aigai: AiSo and Assos: AsSo).

In this study, eleven stone and five soil samples were collected from excavated parts of Aigai in 2010. The samples were taken from bouleuterion, stoa, shop and public bath buildings. Soil samples were taken from the soil section in stoa building in 2010 (Table 2.1).

From excavated parts of Assos in 2010, eight stone and four soil samples were collected. The samples were taken from necropolis, bouleuterion, stoa, theatre and gymnasium buildings. Soil samples were taken from the stoa, theatre and gymnasium buildings (Table 2.2).


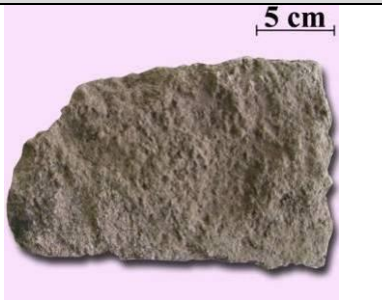
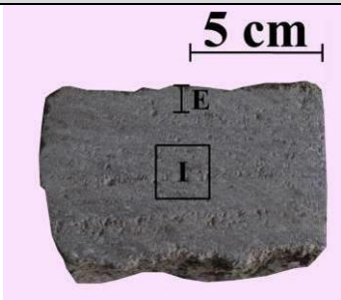


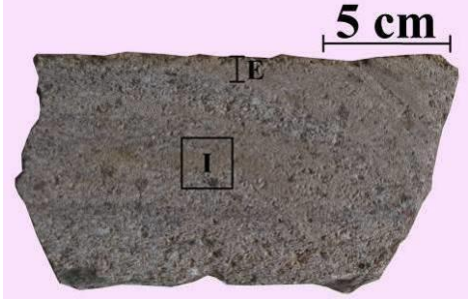


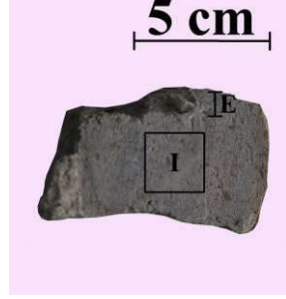



All the samples were collected from the regions which were in shallow burial parts of the subsoil environment before the excavations. The locations of the andesite and soil samples used to change between 10-200 cm before the excavations, during burial (Table 2.1, Table 2.2). In other words, samples were in O or A horizons, which composed of sand, organic materials, plant roots, silt and clay and also with the presence of water and air (Amundson 2003, Velde and Meunier 2008).

Table 2.1. Labels and definitions of the samples collected from Aigai

		Location	Sample	Definition	Label	Section	Definition
Stone Samples	Ai1			Northern cavea of Bouleuterion Excavation year: 2005 Sampling year: 2010 <u>Burial depth</u> Shallow burial ≈ 150 cm	Ai1_E		Exterior part of the sample approximately 1.5 cm from its surface to the interior part.
					Ai1_I		Core of the sample approximately 2x2 cm in dimensions.
					Ai1_Wd		White deposition on the stone surface.
					Ai1_Od		Orange deposition on the stone surface.
	Ai2			Southern cavea of Bouleuterion Excavation year: 2005 Sampling year: 2010 <u>Burial depth</u> Shallow burial ≈ 200 cm	Ai2_E		Exterior part of the sample approximately 1.5 cm from its surface to the interior part.
					Ai2_I		Core of the sample approximately 2x2 cm in dimensions.
					Ai2_Wd		White deposition on the stone surface.
					Ai2_Cr		Fine grained particles of the stone in the cracks close to the surface.
	Ai3			Northern backstage wall of Bouleuterion Excavation year: 2006 Sampling year: 2010 <u>Burial depth</u> Shallow burial ≈ 50 cm	Ai3_E		Exterior part of the sample approximately 1.5 cm from its surface to the interior part.
					Ai3_I		Core of the sample approximately 2x2 cm in dimensions.
	Ai4			Southern backstage wall of Bouleuterion Excavation year: 2009 Sampling year: 2010 <u>Burial depth</u> Shallow burial ≈ 120 cm	Ai4_E		Exterior part of the sample approximately 1.5 cm from its surface to the interior part.
					Ai4_I		Core of the sample approximately 2x2 cm in dimensions.

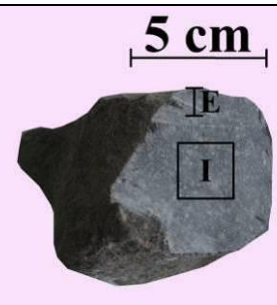
(cont. on next page)

Table 2.1 (cont.).

		Location	Sample	Definition	Label	Section	Definition
Stone Samples	Ai5			First Shop adjacent to southern wall of Bouleuterion Excavation year: 2006 Sampling year: 2010 <u>Burial depth</u> Shallow burial ≈ 100 cm	Ai5_E		Exterior part of the sample approximately 1.5 cm from its surface to the interior part.
					Ai5_I		Core of the sample approximately 2x2 cm in dimensions.
	Ai6			Southern wall of Stoa Excavation year: 2010 Sampling year: 2010 <u>Burial depth</u> Shallow burial ≈ 100 cm	Ai6_E		Exterior part of the sample approximately 1.5 cm from its surface to the interior part.
					Ai6_I		Core of the sample approximately 2x2 cm in dimensions.
	Ai7			Southern wall of Stoa Excavation year: 2010 Sampling year: 2010 <u>Burial depth</u> Shallow burial ≈ 150 cm	Ai7_E		Exterior part of the sample approximately 1.5 cm from its surface to the interior part.
					Ai7_I		Core of the sample approximately 2x2 cm in dimensions.
	Ai8			Southern wall of Stoa Excavation year: 2010 Sampling year: 2010 <u>Burial depth</u> Shallow burial ≈ 180 cm	Ai8_E		Exterior part of the sample approximately 1.0 cm from its surface to the interior part.
					Ai8_I		Core of the sample approximately 1x1 cm in dimensions.

(cont. on next page)

Table 2.1 (cont.).

		Location	Sample	Definition	Label	Section	Definition
Stone Samples	Ai9			Southern wall of Stoa Excavation year: 2010 Sampling year: 2010 <u>Burial depth</u> Shallow burial ≈ 150 cm	Ai9_E		Exterior part of the sample approximately 1.5 cm from its surface to the interior part.
					Ai9_I		Core of the sample approximately 2x2 cm in dimensions.
					Ai9_Wd		White deposition on the stone surface.
	Ai10			Northern wall of Stoa Excavation year: 2010 Sampling year: 2010 <u>Burial depth</u> Shallow burial ≈ 100 cm	Ai10_E		Exterior part of the sample approximately 1.5 cm from its surface to the interior part.
					Ai10_I		Core of the sample approximately 2x2 cm in dimensions.
	Ai11			Western wall of Public Bath Excavation year: 2006 Sampling year: 2010 <u>Burial depth</u> Shallow burial ≈ 100 cm	Ai11_E		Exterior part of the sample approximately 1.5 cm from its surface to the interior part.
Ai11_I					Core of the sample approximately 2x2 cm in dimensions.		
Ai11_Wd					White deposition on the stone surface.		
Ai11_Cr					Fine grained particles of the stone in the cracks close to the surface.		
Soil Samples	AiSo1		—	Northeast part of Stoa Excavation year: 2010 Sampling year: 2010 <u>Burial depth</u> Shallow burial ≈ 200 cm	AsSo1_Cl	—	Clay fraction of the soil sample.

(cont. on next page)

Table 2.1 (cont.).







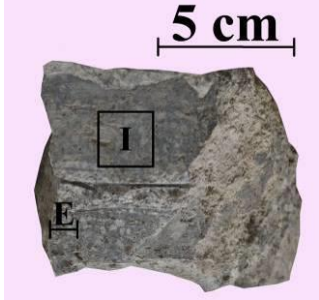


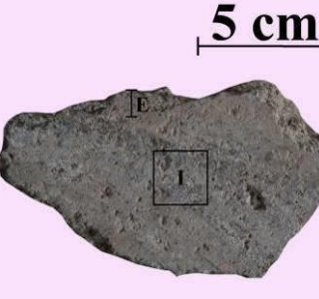


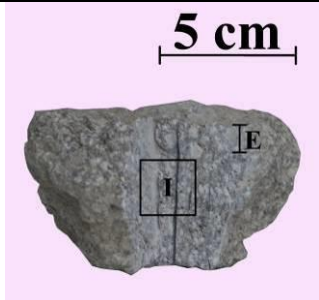


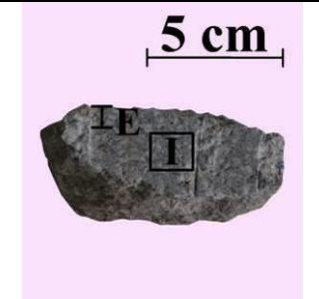


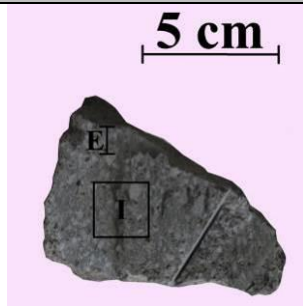


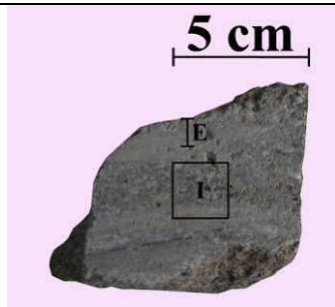

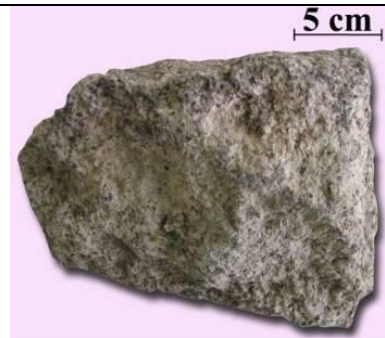
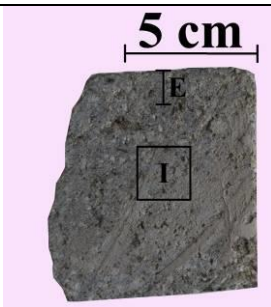

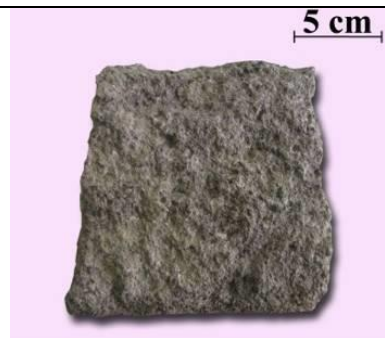
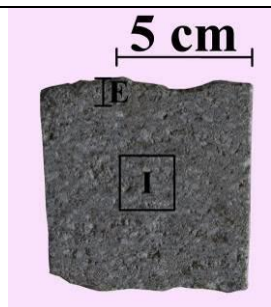
		Location	Sample	Definition	Label	Section	Definition
Soil Samples	AiSo2		—	<p>Southern part of Stoa</p> <p>Excavation year: 2010 Sampling year: 2010</p> <p>Burial depth Shallow burial ≈ 150 cm</p>	<i>AsSo2_Cl</i>	—	Clay fraction of the soil sample.
	AiSo3		—	<p>Southern part of Stoa</p> <p>Excavation year: 2010 Sampling year: 2010</p> <p>Burial depth Shallow burial ≈ 150 cm</p>	<i>AsSo3_Cl</i>	—	Clay fraction of the soil sample.
	AiSo4		—	<p>Southern part of Stoa</p> <p>Excavation year: 2010 Sampling year: 2010</p> <p>Burial depth Shallow burial ≈ 100 cm</p>	<i>AsSo4_Cl</i>	—	Clay fraction of the soil sample.
	AiSo5		—	<p>Southern part of Stoa</p> <p>Excavation year: 2010 Sampling year: 2010</p> <p>Burial depth Shallow burial ≈ 10 cm</p>	<i>AsSo5_Cl</i>	—	Clay fraction of the soil sample.

Table 2.2. Labels and definitions of the samples collected from Assos

		Location	Sample	Definition	Label	Section	Definition
Stone Samples	As1			Eastern part of Bouleuterion Excavation year: 2010-2013 Sampling year: 2010 <u>Burial depth</u> Shallow burial ≈ 180 cm	As1_E		Exterior part of the sample approximately 1.5 cm from its surface to the interior part.
					As1_I		Core of the sample approximately 2x2 cm in dimensions.
					As1_Wd		White deposition on the stone surface.
	As2			Gymnasium Excavation year: 2010 Sampling year: 2010 <u>Burial depth</u> Shallow burial ≈ 50 cm	As2_E		Exterior part of the sample approximately 1.5 cm from its surface to the interior part.
					As2_I		Core of the sample approximately 2x2 cm in dimensions.
					As2_Wd		White deposition on the stone surface.
					As2_Cr		Fine grained particles of the stone in the cracks close to the surface.
	As3			Northern wall of Stoa Excavation year: 2010-2011 Sampling year: 2010 <u>Burial depth</u> Shallow burial ≈ 120 cm	As3_E		Exterior part of the sample approximately 1.5 cm from its surface to the interior part.
					As3_I		Core of the sample approximately 2x2 cm in dimensions.
	As4			Western part of Theatre Excavation year: 1989 Sampling year: 2010 <u>Burial depth</u> Shallow burial ≈ 50 cm	As4_E		Exterior part of the sample approximately 1.5 cm from its surface to the interior part.
					As4_I		Core of the sample approximately 2x2 cm in dimensions.





(cont. on next page)

Table 2.2 (cont.).

	Location	Sample	Definition	Label	Section	Definition
As5			Southern part of Theatre Excavation year: 1989 Sampling year: 2010 Burial depth Shallow burial ≈ 200 cm	As5_E		Exterior part of the sample approximately 1.5 cm from its surface to the interior part.
				As5_I		Core of the sample approximately 2x2 cm in dimensions.
				As5_Cr		Fine grained particles of the stone in the cracks close to the surface.
As6			Necropolis Excavation year: 2010 Sampling year: 2010 Burial depth Shallow burial ≈ 50 cm	As6_E		Exterior part of the sample approximately 1.5 cm from its surface to the interior part.
				As6_I		Core of the sample approximately 2x2 cm in dimensions.
As7			Necropolis Excavation year: 2010 Sampling year: 2010 Burial depth Shallow burial ≈ 100 cm	As7_E		Exterior part of the sample approximately 1.5 cm from its surface to the interior part.
				As7_I		Core of the sample approximately 2x2 cm in dimensions.
				As7_Wd		White deposition on the stone surface.
As8			Necropolis Excavation year: 2010 Sampling year: 2010 Burial depth Shallow burial ≈ 150 cm	As8_E		Exterior part of the sample approximately 1.5 cm from its surface to the interior part.
				As8_I		Core of the sample approximately 2x2 cm in dimensions.

(cont. on next page)

Table 2.2 (cont.).

		Location	Sample	Definition	Label	Section	Definition
Soil Samples	AsSo1		—	Northern wall of Stoa Excavation year: Sampling year: 2010 <u><i>Burial depth</i></u> Shallow burial ≈ 40 cm	<i>AsSo1_Cl</i>	—	Clay fraction of the soil sample.
	AsSo2		—	Theatre Excavation year: 2010 Sampling year: 2010 <u><i>Burial depth</i></u> Shallow burial ≈ 50 cm	<i>AsSo2_Cl</i>	—	Clay fraction of the soil sample.
	AsSo3		—	Western part of Theatre Excavation year: 1980s Sampling year: 2010 <u><i>Burial depth</i></u> Shallow burial ≈ 100 cm	<i>AsSo3_Cl</i>	—	Clay fraction of the soil sample.
	AsSo4		—	Gymnasium Excavation year: 2010 Sampling year: 2010 <u><i>Burial depth</i></u> Shallow burial ≈ 80 cm	<i>AsSo4_Cl</i>	—	Clay fraction of the soil sample.

2.4. Experimental Studies

In this study, physical, microstructural, mineralogical, chemical and thermal analyses were carried out to determine the deterioration problems of buried and excavated andesites. The laboratory analyses were applied to the soil samples, relatively unaltered interior parts and exterior surfaces of the andesites and clay fractions of the soils and andesites.

In the preparation of the stone samples, exterior and interior parts of the andesites were separated by using Buehler low speed saw. As shown in Table 2.1 and Table 2.2, exterior parts of the andesites were taken from approximately 1.5 cm through to their interior part and labeled as Aix_E or Asx_E. Relatively unaltered interior parts of the andesites were taken from their cores approximately 1x1 or 2x2 cm in dimensions according to the size of the sample and labeled as Aix_I or Asx_I.

White deposits observed on the andesite surfaces (Ai1, Ai2, Ai9, Ai11 and As1, As2, As7) and orange-brown deposition observed on Ai1 were taken by using catling and brush from the surfaces and labeled as Aix_Wd, Asx_Wd and Ai1_Od. Clay minerals in the cracks of the andesites were taken by brush and labeled as Aix_Cr or Asx_Cr. The clay fractions of the soil samples (the separation from the soils will be explained in more detail in the following parts) labeled as AiSox_Cl and AsSox_Cl (Table 2.1, Table 2.2).

In the laboratory analyzes;

- Basic physical properties (bulk density and porosity values) of the interior parts and exterior surfaces of the stones were determined by standard test methods (RILEM 1980).
- Mineralogical compositions of the interior parts and exterior surfaces of the andesites were determined by X-ray Diffraction (XRD) and Fourier transformed infrared spectroscopy (FT-IR).
- Elemental and chemical compositions and CO₂ and organic material contents were determined by Scanning Electron Microscope (SEM) equipped with X-Ray Energy Dispersive System (EDS), X-ray fluorescence (XRF), thermal analyses and thermo-gravimetric analysis (TGA).

- Petrographic and microstructural analyses of the interior parts and exterior surfaces of the stones and soils were carried out by Scanning Electron Microscope (SEM) and polarized microscope.
- The salt content in interior parts of the stones and soil samples were determined by ion chromatography (IC).

Deterioration problems of excavated andesites were evaluated by the comparison of the results of these experimental studies mentioned above for interior and exterior parts of the andesites and soils (Table 2.3, Table 2.4).

The chemical deterioration indices of Chemical Index of Alteration (CIA) (Nesbitt and Young 1982) and the Weathering Index of Parker (WIP) (Parker 1970, Hamdan and Burnham 1996) were used with the results of XRF and SEM/EDS analyzes to find out the chemical deterioration of the andesites.

Table 2.3. Laboratory analyses applied to the samples taken from Aigai

Sample	Basic physical properties		Mineralogical composition		Chemical composition			Soluble salt content	Organic material/CO ₂ content	Petrographic and microstructural characteristics	
	<i>Bulk density</i>	<i>Porosity</i>	<i>XRD</i>	<i>FT-IR</i>	<i>SEM/EDS</i>	<i>XRF</i>	<i>TGA</i>	<i>IC</i>	<i>Furnace</i>	<i>SEM</i>	<i>Polarized Microscope</i>
<i>Ai1_E</i>	X	X	X	-	X	X	X	-	X	X	-
<i>Ai1_I</i>	X	X	X	-	X	X	X	X	X	X	-
<i>Ai1_Wd</i>	-	-	X	X	-	-	X	-	X	X	-
<i>Ai1_Od</i>	-	-	X	-	-	-	X	-	X	X	-
<i>Ai2_E</i>	X	X	X	-	X	X	X	-	X	X	-
<i>Ai2_I</i>	X	X	X	-	X	-	-	X	-	X	X
<i>Ai2_Wd</i>	-	-	X	X	-	-	X	-	X	X	-
<i>Ai2_Cr</i>	-	-	X	X	-	-	X	-	X	X	-
<i>Ai3_E</i>	X	X	-	-	X	-	X	-	X	X	-
<i>Ai3_I</i>	X	X	X	-	X	X	-	X	-	X	-
<i>Ai4_E</i>	-	-	-	-	X	-	-	-	-	X	-
<i>Ai4_I</i>	-	-	-	-	X	-	-	X	-	X	-
<i>Ai5_E</i>	X	X	X	-	X	X	X	-	X	X	-
<i>Ai5_I</i>	X	X	X	-	X	-	X	X	X	X	X

(cont. on next page)

Table 2.3 (cont.).

Sample	Basic physical properties		Mineralogical composition		Chemical composition			Soluble salt content	Organic material/CO ₂ content	Petrographic and microstructural characteristics		
	Stone samples	<i>Bulk density</i>	<i>Porosity</i>	<i>XRD</i>	<i>FT-IR</i>	<i>SEM/EDS</i>	<i>XRF</i>	<i>TGA</i>	<i>IC</i>	<i>Furnace</i>	<i>SEM</i>	<i>Polarized Microscope</i>
<i>Ai6_E</i>	X	X	X	–	X	–	–	–	–	–	X	–
<i>Ai6_I</i>	X	X	X	–	X	–	X	X	X	X	X	–
<i>Ai7_E</i>	X	X	X	–	X	–	X	–	–	X	X	–
<i>Ai7_I</i>	X	X	X	–	X	–	X	X	X	X	X	–
<i>Ai8_E</i>	–	–	X	–	X	–	–	–	–	X	X	–
<i>Ai8_I</i>	–	–	–	–	X	–	–	–	X	–	X	–
<i>Ai9_E</i>	X	X	–	–	X	–	–	–	–	–	X	–
<i>Ai9_I</i>	X	X	X	–	X	X	–	–	X	–	X	–
<i>Ai9_Wd</i>	–	–	X	X	–	–	X	–	–	X	X	–
<i>Ai10_E</i>	X	X	–	–	X	–	X	–	–	X	X	–
<i>Ai10_I</i>	X	X	X	–	X	–	X	X	X	X	X	–
<i>Ai11_E</i>	X	X	–	–	X	–	–	–	–	–	X	–
<i>Ai11_I</i>	X	X	X	–	X	X	–	–	X	–	X	–
<i>Ai11_Wd</i>	–	–	X	X	–	–	X	–	–	X	X	–
<i>Ai11_Cr</i>	–	–	X	X	–	–	X	–	–	X	X	–

(cont. on next page)

Table 2.3 (cont.).

Sample	Basic physical properties		Mineralogical composition		Chemical composition			Soluble salt content	Organic material/CO ₂ content	Petrographic and microstructural characteristics	
	<i>Bulk density</i>	<i>Porosity</i>	<i>XRD</i>	<i>FT-IR</i>	<i>SEM/EDS</i>	<i>XRF</i>	<i>TGA</i>	<i>IC</i>	<i>Furnace</i>	<i>SEM</i>	<i>Polarized Microscope</i>
<i>AiSo1</i>	–	–	–	–	–	–	–	X	X	X	–
<i>AiSo1_Cl</i>	–	–	X	–	–	–	X	–	X	–	–
<i>AiSo2</i>	–	–	–	–	–	–	–	X	–	X	–
<i>AiSo2_Cl</i>	–	–	X	–	–	–	X	–	X	–	–
<i>AiSo3</i>	–	–	–	–	–	–	–	X	X	X	–
<i>AiSo3_Cl</i>	–	–	X	X	–	–	X	–	X	–	–
<i>AiSo4</i>	–	–	–	–	–	–	–	X	–	X	–
<i>AiSo4_Cl</i>	–	–	X	–	–	–	X	–	X	–	–
<i>AiSo5</i>	–	–	–	–	–	–	–	X	X	X	–
<i>AiSo5_Cl</i>	–	–	–	–	–	–	–	–	–	–	–

Table 2.4. Laboratory analyses applied to the samples taken from Assos

Sample	Basic physical properties		Mineralogical composition		Chemical composition			Soluble salt content	Organic material/CO ₂ content	Petrographic and microstructural characteristics	
	<i>Bulk density</i>	<i>Porosity</i>	<i>XRD</i>	<i>FT-IR</i>	<i>SEM/EDS</i>	<i>XRF</i>	<i>TGA</i>	<i>IC</i>	<i>Furnace</i>	<i>SEM</i>	<i>Polarized Microscope</i>
<i>As1_E</i>	X	X	X	–	X	–	X	–	X	X	–
<i>As1_I</i>	X	X	X	–	X	–	X	X	X	X	–
<i>As1_Wd</i>	–	–	X	X	–	–	X	–	X	X	–
<i>As2_E</i>	X	X	X	–	X	–	X	–	X	X	–
<i>As2_I</i>	X	X	–	–	X	–	X	X	X	X	–
<i>As2_Wd</i>	–	–	X	X	–	–	X	–	X	X	–
<i>As2_Cr</i>	–	–	X	X	–	–	X	–	X	X	–
<i>As3_E</i>	X	X	X	–	X	X	X	–	X	X	–
<i>As3_I</i>	X	X	X	–	X	X	X	X	X	X	–
<i>As4_E</i>	X	X	X	–	X	X	X	–	X	X	–
<i>As4_I</i>	X	X	–	–	X	X	X	X	X	X	–
<i>As5_E</i>	X	X	X	–	X	X	X	–	X	X	–
<i>As5_I</i>	X	X	X	–	X	X	X	X	X	X	–
<i>As5_Cr</i>	–	–	X	X	–	–	X	–	X	X	–
<i>As6_E</i>	X	X	X	–	X	X	X	–	X	X	–
<i>As6_I</i>	X	X	–	–	X	X	X	X	X	X	–

(cont. on next page)

Table 2.4 (cont.).

Sample	Basic physical properties		Mineralogical composition		Chemical composition			Soluble salt content	Organic material/CO ₂ content	Petrographic and microstructural characteristics	
	<i>Bulk density</i>	<i>Porosity</i>	<i>XRD</i>	<i>FT-IR</i>	<i>SEM/EDS</i>	<i>XRF</i>	<i>TGA</i>	<i>IC</i>	<i>Furnace</i>	<i>SEM</i>	<i>Polarized Microscope</i>
<i>Stone samples</i>											
<i>As7_E</i>	X	X	–	–	X	–	–	–	–	X	–
<i>As7_I</i>	X	X	X	–	X	–	X	X	X	X	–
<i>As7_Wd</i>	–	–	–	X	–	–	X	–	X	X	–
<i>As8_E</i>	X	X	–	–	X	–	–	–	–	X	X
<i>As8_I</i>	X	X	–	–	X	–	X	X	X	X	X
<i>Soil samples</i>											
<i>AsSo1</i>	–	–	–	–	X	–	–	X	X	X	–
<i>AsSo1_Cl</i>	–	–	–	–	–	–	–	–	–	–	–
<i>AsSo2</i>	–	–	–	–	–	–	–	X	X	X	–
<i>AsSo2_Cl</i>	–	–	–	–	–	–	–	–	–	–	–
<i>AsSo3</i>	–	–	–	–	–	–	–	X	–	X	–
<i>AsSo3_Cl</i>	–	–	–	–	–	–	–	–	–	–	–
<i>AsSo4</i>	–	–	–	–	–	–	–	X	X	X	–
<i>AsSo4_Cl</i>	–	–	X	X	–	–	X	–	X	–	–

2.4.1. Determination of Basic Physical Properties of Interior and Exterior Parts of the Stones

In order to find out the physical characteristics of interior and exterior parts of the stones and evaluate the physical deterioration of the andesites, bulk density and porosity values of the samples were determined. For the determination of values of bulk density (g/cm^3), which is the ratio of the mass to its bulk volume, and porosity (%), which is the ratio of the pore volume to the bulk volume of the sample, the RILEM standard test methods were used (RILEM 1980). The interior parts of the andesite samples used in the analysis were in the sizes of approximately 2×2 cm and the exterior parts were in the sizes of 1.5×1.5 cm dimensions. The analysis was applied all the samples except Ai4 and Ai8, which are the thinnest andesite sample (approximately 2 cm) (Table 2.3, Table 2.4). Analyzed andesites were first dried in an oven at 40°C for 24 hours, and their dry weights (M_{dry}) were determined by a precision balance (AND HF-3000G). Then, the samples were saturated with distilled water in a vacuum oven (Lab-Line 3608-6CE Vacuum Oven) and then were weighed by a precision balance using hydrostatic weighing method in distilled water to determine their saturated weights (M_{sat}) and archimedes weights (M_{arch}). The bulk densities (D) and porosities (P) of the samples were determined using the formulas below:

$$D (\text{g/cm}^3) = M_{\text{dry}} / (M_{\text{sat}} - M_{\text{arch}})$$

$$P (\%) = [(M_{\text{sat}} - M_{\text{dry}}) / (M_{\text{sat}} - M_{\text{arch}})] \times 100$$

where;

M_{dry} : Dry Weight (g)

M_{sat} : Saturated Weight (g)

M_{arch} : Archimedes Weight (g)

$M_{\text{sat}} - M_{\text{dry}}$: Pore Volume

$M_{\text{sat}} - M_{\text{arch}}$: Bulk Volume

SEM analysis was also used for the determination of the basic physical properties for both interior and exterior parts of the andesites (Table 2.3, Table 2.4). For the analysis, the thin sections of the andesites from their exterior surfaces to the interior parts were prepared to analyze the cracks and pore formations in the andesite structures.

2.4.2. Determination of Soluble Salt Contents in Soils and Andesites

In order to evaluate the possible deterioration problems of andesites and possible effects of being near the seashore for Assos archaeological site, percent soluble salts in soil and andesite samples were determined by ion chromatography (IC) which is highly sensitive and more sophisticated method for the determination not only type, but also the amount of soluble salts in the materials precisely (Borrelli 1999, Eith et al. 2001, Doehne and Price 2010) (Table 2.3, Table 2.4).

For this analysis, 1.00 g of finely-ground soil samples and powdered andesite samples of less than 53 μm from interior parts of the stones were mixed with 50 ml deionised water. After stirring thirty minutes, the mixtures were waited two weeks for the precipitation of the particles and then they were filtered less than 0.20 μm . In the analysis, the principle anions such as sulphate (SO_4^{2-}), chloride (Cl^-), nitrate (NO_3^-), carbonate (CO_3^{2-}) and phosphate (PO_4^{3-}) in the solutions were determined. The instrument used in the analysis is equipped with Dionex GP50 gradient pump, LC25 chromatography oven, IonPac CS12A (4x250mm) cation exchanger column, IonPac AS9-HC (4x250mm) anion exchanger column and ED50 electrochemical detector. In the analysis of andesite and soil samples, the amounts of soluble salts in the concentrations in IC gathered as ppm (mg/L) and converted to percentage.

The results of soil and andesite samples were compared to find out possible penetration of the soluble salts to the andesites from the surrounding soil.

2.4.3. Thermal Analysis of Soil and Stone Samples

Organic material, carbonate and clay mineral contents of andesite samples of both interior and exterior parts of the andesites and soil samples were evaluated by thermal analysis. Thermal analyses of the samples were carried out by analysis (TG/DTA) by using Pelkin Elmer Diomand TG/DTA and by heating the samples in the furnace (Table 2.3, Table 2.4).

The thermogravimetric analysis was carried out in static nitrogen atmosphere at a temperature range of 25-1000°C with a controlled heating rate of 10°C/min. During this heating, TGA instrument recorded loss of hygroscopic (adsorbed) water (< 103°C),

loss of structural water bounded to hydraulic components and loss of organic materials and clay fractions (103°C-550°C), and loss of carbon dioxide gas due to decomposition of carbonates (> 900°C) (Wang, Odlyha and Cohen 2000).

For the analysis carried out by heating the samples in the furnace, three soil and three exterior surfaces of andesite samples (approximately 1.5x1.5 cm in sizes) from each site were selected according to where they were taken. In this analysis, one gram fine ground sample was heated in the crucible at 103°C for 1 day, at 550°C for 1 hour and at 900°C for 1 hour. Weight losses at these temperatures were then precisely measured to determine the hygroscopic (adsorbed) water, organic material and carbonate contents and dehydroxilation of some types of clays (Tylecote 1979).

2.4.4. Separation of Clay Fraction from Soil Samples

In order to find out the possible effects of the clay minerals in the deterioration of buried and excavated andesites, the presence and the characteristics of the clays in the soil structures have be known. Thus, the clay fractions of the soil samples were separated from the soil samples in order to find out the type of the clays in the soil structure.

In this process, “Filtration Method” was used for providing uniform specimens (Iijima, Jimenez-Espejo and Sakamoto 2005). 30 grams of each soil sample was soaked in 50 ml of distilled water and stirred for approximately 10 minutes. Then, the mixtures were sieved through a series of sieves (Retsch mark) having the sieve sizes of 53 µm, 125 µm, 250 µm, 500 µm, 1180 µm by using an analytical sieve shaker (Retsch AS200). This process of sieving was carried out until distilled water was obtained after sieving. For every soil sample, the mixtures which are less than 53 µm were filtered and left for more than 20 days for the precipitation of clay fraction and for the evaporation of the water. After the evaporation of water, clay fractions in soil samples were obtained.

2.4.5. Determination of Mineralogical Characteristics

For the characterization and the evaluation of the deterioration of the andesites, mineralogical compositions of interior and exterior parts of the andesite samples, white depositions of the andesites and clay fractions of andesite and soil samples were determined by X-ray Diffraction (XRD) analysis performed by using a Philips X-Pert Pro X-ray Diffractometer (Table 2.3, Table 2.4). The instrument was operated with CuK α radiation with Ni filter adjusted to 40 kV and 40mA in the range of 2-60° with a scan speed of 1.60 per minute. The analyses were performed on powdered samples of less than 53 μm and the clay fractions of the samples. In the mineralogical analysis of the andesite samples, exterior parts and inner cores of the andesites were analyzed separately to find out the mineralogical differences between the sound and deteriorated parts. To identify the mineral phases in each X-ray diffraction spectrum, The Philips X-pert Graphics and Identity software program was used.

Mineralogical compositions of the white depositions and clay content of the andesite samples were also determined by FTIR analysis (Table 2.3, Table 2.4). Powdered samples of less than 53 μm were mixed with KBr in the proportion of 1 sample/100 KBr and pressed into pellets under approximately 10 tons/cm² pressure. The spectral measurements were carried out on a PerkinElmer-FT-IR System Spectrum BX spectrometer. Four scans were recorded for each sample.

2.4.6. Determination of Chemical Compositions of Interior and Exterior Parts of the Stones

Chemical compositions of interior and exterior parts of the andesites were determined in order to compare the results and to find out the possible deterioration products (Table 2.3, Table 2.4). The results of chemical analysis of the interior and exterior parts of the andesites were also used in the chemical weathering indices, which will be explained in more detail in the following parts.

Chemical compositions of andesite samples were determined by Philips XL 30S-FEG Scanning Electron Microscope (SEM) equipped with X-Ray Energy Dispersive System (EDS). The analyses were performed on pellets of finely ground samples less than 53 μm prepared by pressing the samples under 10 tons/cm². SEM-EDS analyses were carried out in three different zones which were 2.4675 sqmm (1.75 mm x 1.41 mm) in surface area of each sample.

Major, minor and trace element compositions of the samples were also assessed by X-ray fluorescence spectroscopy (XRF) (Table 2.3, Table 2.4). Because XRF analysis provides depth elemental characterization of the materials while SEM/EDS provides surface elemental distribution (Komatani et al. 2013). XRF analyses were carried out by a Spectro IQ II on melt tablets of powdered samples less than 53 μm diluted with lithium tetraborat.

2.4.7. Petrographic and Microstructural Analysis

Microstructural and petrographic analyses were carried out on interior parts and exterior surfaces of the andesite samples in order to find out the mineralogical characteristics and physical changes of the andesites from their surfaces through interior parts.

For the microstructural analysis; coarse andesites and thin sections of the samples were used. Andesite samples were first covered with epoxy resin and cut into thin sections with Buhler low speed saw. The samples were analyzed from their exterior surfaces through the interior parts to compare the microstructural characteristics such as density and width of pores and cracks. For the coated ones, andesite samples were first covered with epoxy resin in Lab-Line 3608-6CE Vacuum Oven for 24 hours. Then, the samples were cut to 2 mm or 3 mm thick slices using BUEHLER Low Speed Saw and finally coated with gold. Together with the coated samples, coarse stone samples were also used. Scanning Electron Microscope (SEM) analysis was also performed on soil samples in order to find out the presence of the diatoms and organic materials in the samples.

As the microstructural analyses, petrographic analyses of the andesites were also performed from the exterior surfaces through interior by using Leika Polarizing Microscope with the thin sections of the stones less than 30 μm .

2.4.8. Calculation of Chemical Weathering Indices

The chemical deterioration of the andesites was evaluated by using chemical weathering indices with the results of SEM/EDS and XRF analyses (Reiche 1943, Ruxton 1968, Parker 1970, Nesbitt and Young 1982, Gupta and Rao 2001, Bahlburg and Dobrzinski 2009). Although XRF is more sensitive method than SEM/EDS analysis in the determination of chemical characteristics (Komatani et al. 2013), both results were used in the weathering indices and the results were compared. In the evaluation, the Chemical Index of Alteration (CIA) (Nesbitt and Young 1982) and the Weathering Index of Parker (WIP) (Parker 1970, Hamdan and Burnham 1996), which are the two commonly applied chemical weathering indices by the geologists, were applied to interior and exterior parts of the andesites and the results were compared (Shao et al. 2012).

Weathering Index of Parker (WIP) considers mirroring the changes in Mg^{2+} , Ca^{2+} , K^+ and Na^+ as a major process of chemical deterioration with the formula of:

$$WIP = [(Na^*/0.35) + (Mg^*/0.9) + (K^*/0.25) + (Ca^*/0.7)] \times 100$$

or

$$WIP = [(2Na_2O/0.35) + (MgO/0.9) + (2K_2O/0.25) + (CaO/0.7)] \times 100$$

where the cations* represent the atomic percentage of an element divided atomic weight (Parker 1970, Bahlburg and Dobrzinski 2009).

Results of WIP are commonly between ≥ 100 and 0 and the smaller WIP values indicate stronger chemical deterioration (Table 1.4) (Parker 1970, Hamdan and Burnham 1996). However, WIP lacks of consideration of a relatively immobile Al_2O_3 in formula which would help to monitor the changes of composition of the relevant mineral components (Bahlburg and Dobrzinski 2009, Shao et al. 2012).

This disadvantage of WIP was overcome in the Chemical Index of Alteration (CIA). CIA is based on monitoring the hydrolysis of feldspar and volcanic glass and their conversion to clays as a result of chemical deterioration (Shao et al. 2012). It represents a ratio of predominantly immobile Al_2O_3 to the mobile cations Ca^{2+} , K^+ and Na^+ as oxides. It is defined as:

$$CIA = \left(\frac{Al_2O_3}{Al_2O_3 + Na_2O + K_2O + CaO} \right) \times 100$$

where the major element oxides are given in molecular proportions. In contrary to WIP values, highest degree of deterioration in CIA has a value of 100 and represents kaolinite. Illite is between 75 and 90, muscovite is 75, the feldspars are 50 and fresh igneous rocks have the values between 30 and 55 according to their chemical characteristics (Table 1.4) (Nesbitt and Young 1982, Fedo et al. 1995, Bahlburg and Dobrzinski 2009).

CHAPTER 3

RESULTS AND DISCUSSIONS

Results of the visual analysis of andesite deteriorations and experimental studies, which were carried out on andesite and soil samples, are given and discussed in this part. Basic physical, chemical, mineralogical and microstructural characteristics of interior and exterior parts of the andesites, soils and deposits observed on the andesites are described, compared and discussed. The comparison of the andesite surfaces documented in 2010 and 2014 with the photos and the results of the experimental studies revealed the deterioration of the excavated andesites. Estimations about the deterioration of buried andesites and possible effects of being near seashore were made upon soluble salt, clay, organic material and carbonate content analyses.

As the results of the experimental studies, this part also includes the results of WIP and CIA analyses, which were used to evaluate the chemical deterioration of the andesites, with the results of SEM/EDS and XRF analyses.

3.1. Visual Analysis of Stone Deteriorations Observed on the Andesites

Visual analysis of the andesite deteriorations was carried out with the site surveys in 2010 and 2014 and documented with the photos. The surfaces of the exposed standing andesites, which are approximately exposed to atmospheric conditions since 2500 years for both archaeological sites, completely excavated andesites and exposed standing and recently excavated parts of the partially excavated andesites were compared.

Comparison was carried out and in two phases:

- In the first phase, recently excavated and exposed standing parts of the partially excavated andesites were compared.
- Second phase of the comparison consisted of completely exposed standing and excavated andesites and partially excavated andesites between 2010 and 2014. Progresses of the andesite deteriorations in four years period were evaluated.

In the comparisons, visible deterioration types such as crack formation, progress of the current cracks, spalling, pitting or loss of stone material, biological growth and discoloration were examined on the andesites.

In the tables of comparison, excavated parts and exposed standing parts of the excavated andesites are separated with red dashed lines and deterioration types determined on the andesites are shown with red arrows. Locations of the detail photos framed with black rectangles. In the definition line of the tables, information about the andesite surfaces and determined deterioration are given (Table 3.1, Table 3.2, Table 3.3, Table 3.4).

In the first phase, results of the comparison of recently excavated and exposed standing parts of the partially excavated Aigai and Assos andesites by visual observations show less deterioration of the buried parts of the andesites, which is visible by naked eye. As seen in Table 3.1 and Table 3.2, exposed standing parts of the andesites have more biological formations on the surfaces while the recently excavated andesite surfaces almost fresh. Only white deposits, which can not be observed on exposed standing parts, are observed on recently excavated parts of the andesites. Thus, as supporting the data coming from the literature (Cronyn 2002), visual observations of the excavated andesites also show better preservation of stones in the burial environment.

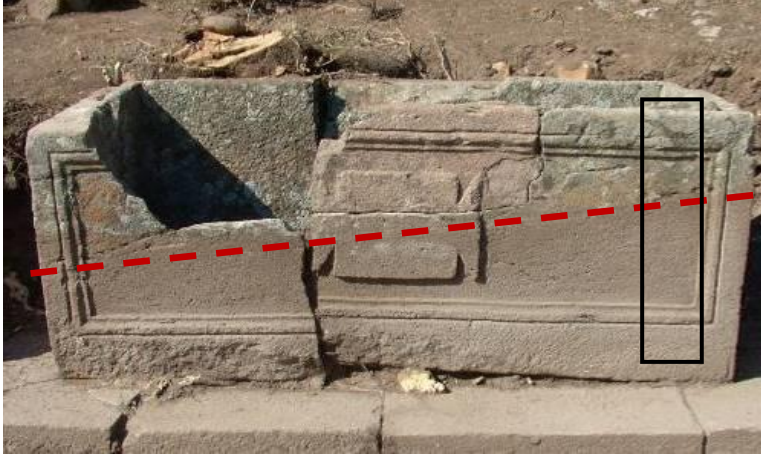

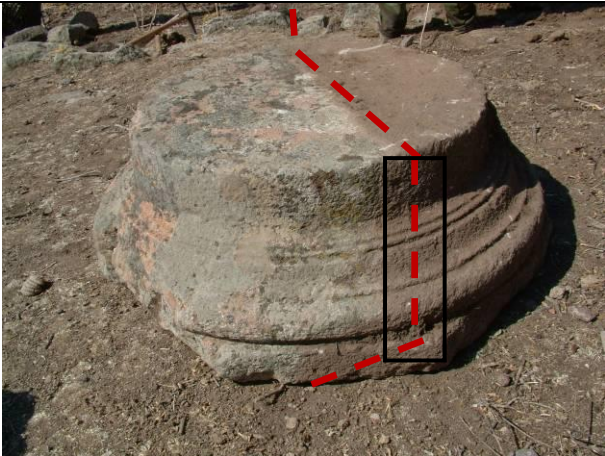



In the second phase of the visual analysis, comparison of completely exposed standing and excavated andesites and, exposed standing and recently excavated parts of the partially excavated andesites between 2010 and 2014 show slightly deterioration progresses of all the andesites in four years period (Table 3.3, Table 3.4). Increase in the white deposits on the andesite surfaces through the years also could not be observed on both Aigai and Assos andesites. Recently formed deteriorations are especially determined in the recently excavated parts when compared with the exposed standing parts of the andesites (Table 3.3, Table 3.4).

Recently formed deteriorations on the andesites are discoloration, pitting, biological forms and moisture on the andesite surfaces, progress of the cracks and loss of stone materials. Although loss of stone material and progress of the cracks are serious problems, they were rarely observed on the andesites. Except the deteriorations observed on the andesite surfaces, discharge of the soil, which was used to combine the andesites in both sites, is also observed on the walls.

The reasons of the stone deteriorations will be explained in the following parts with the results of the experimental studies. However, visual observations at the sites also showed that one of the reasons of the andesite deteriorations in both sites is lack of site maintenance after archaeological excavations. Accumulation of the rain water on the ground of excavated monuments resulted in wet andesite surfaces and generation of biological forms on recently excavated andesites in both sites.

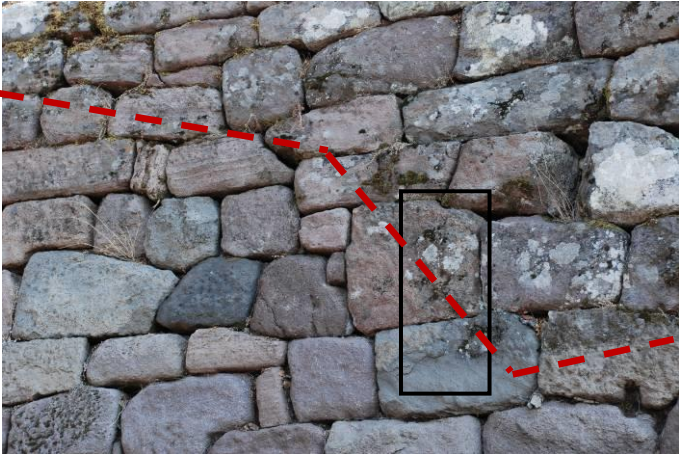

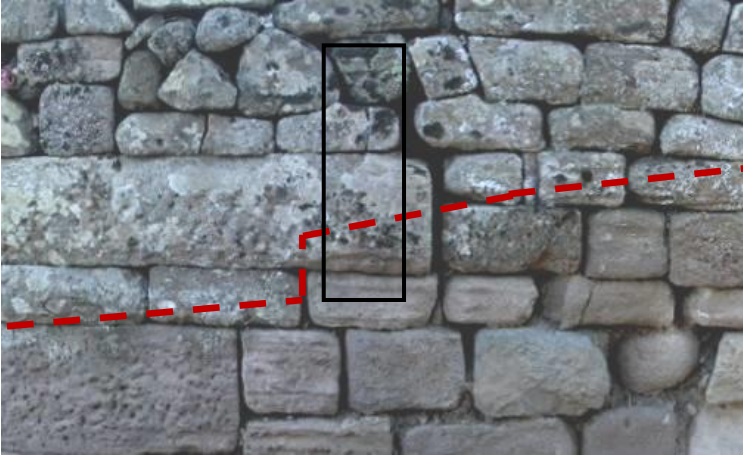

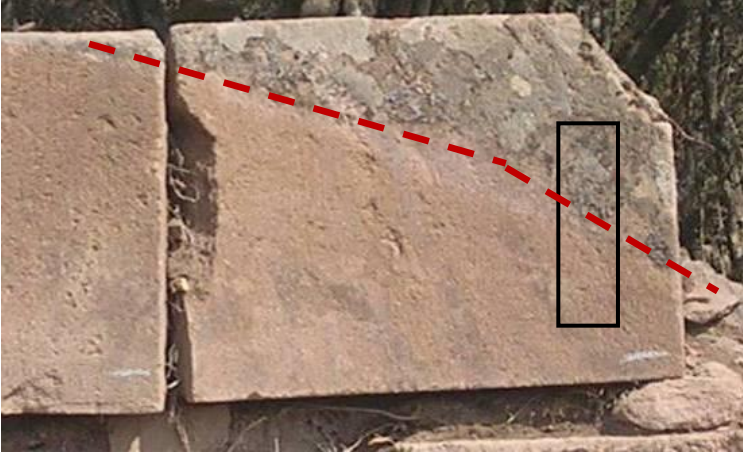

To prevent the generation of the biological forms on recently excavated andesites, which have physical and chemical effects on the stones, necessary environmental arrangements such as drainage have to be supplied and biocides have to be implemented on the stone surfaces. Biocide, which will be implemented on the stones, must be compatible with the andesites. In other words, it must not harm the stone structure and must not change the appearance. The material also has to be appropriate to environmental conditions such as rain and wind.

Table 3.1. Visual analysis of exposed standing and excavated parts of the partially excavated andesites in Aigai archaeological site

	Image	Detail
<p style="writing-mode: vertical-rl; transform: rotate(180deg);">Necropolis: Excavated in 2006</p>		
		
		
<p>Visible deterioration: Biological growth on exposed standing parts is observed.</p>		

(cont. on next page)

Table 3.1 (cont.).

<p>Iron Gate: Excavated in 2005 and 2006</p>		<p>Exposed Standing</p>  <p>Excavated</p>
		<p>Exposed Standing</p>  <p>Excavated</p>
<p>Bouleuterion: Excavated between 2004 and 2006.</p>		<p>Exposed Standing</p>  <p>Excavated</p>
<p><i>Visible deterioration: Biological growth on exposed standing parts is observed.</i></p>		

(cont. on next page)

Table 3.1 (cont.).

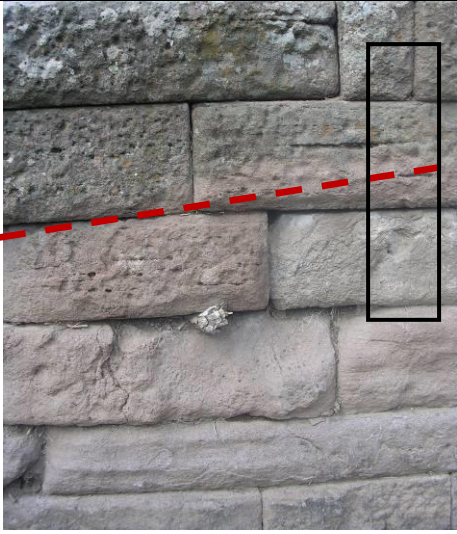

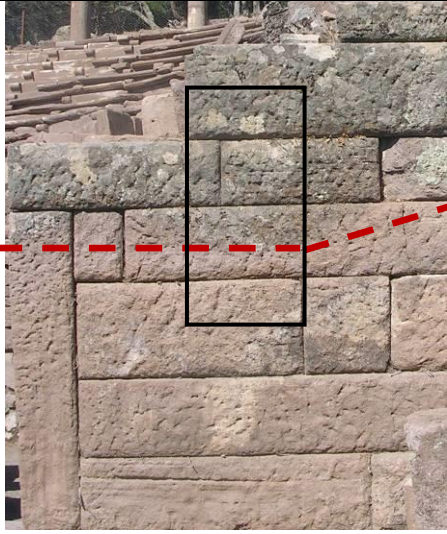

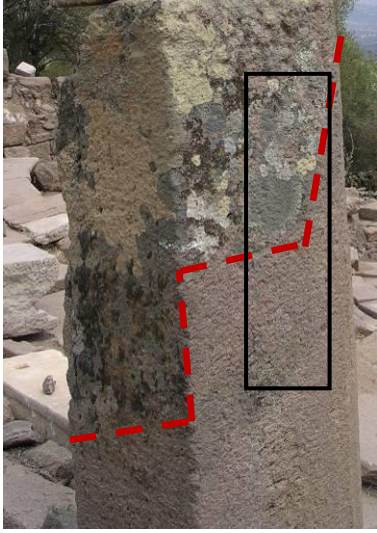

<p>Boulevardierion: Excavated between 2004 and 2006.</p>		<p>Excavated</p> 
		<p>Excavated</p> 
		<p>Excavated</p> 
<p><i>Visible deterioration: Biological growth on exposed standing parts is observed.</i></p>		

Table 3.2. Visual analysis of exposed standing and excavated parts of the partially excavated andesites in Assos archaeological site

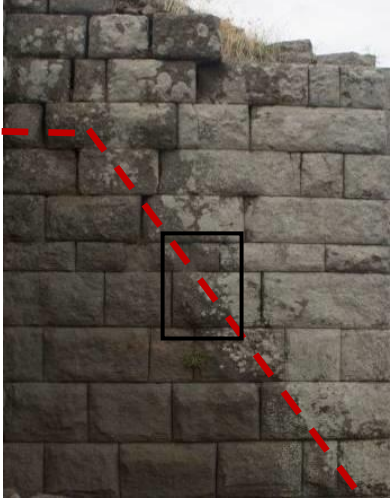

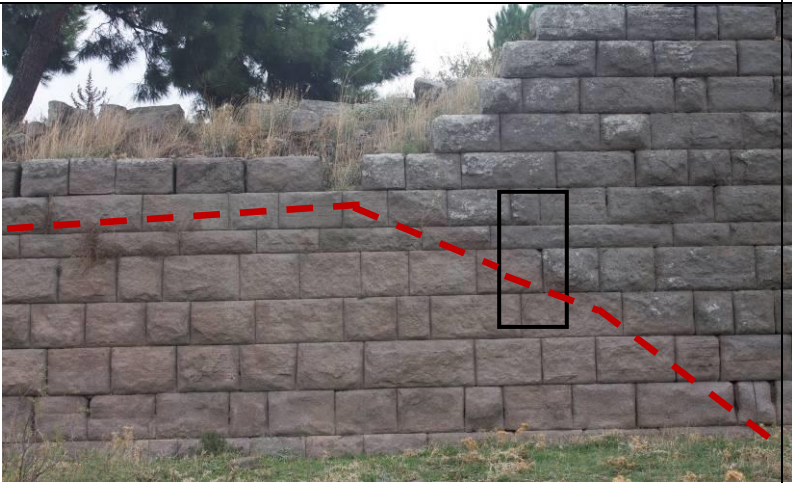

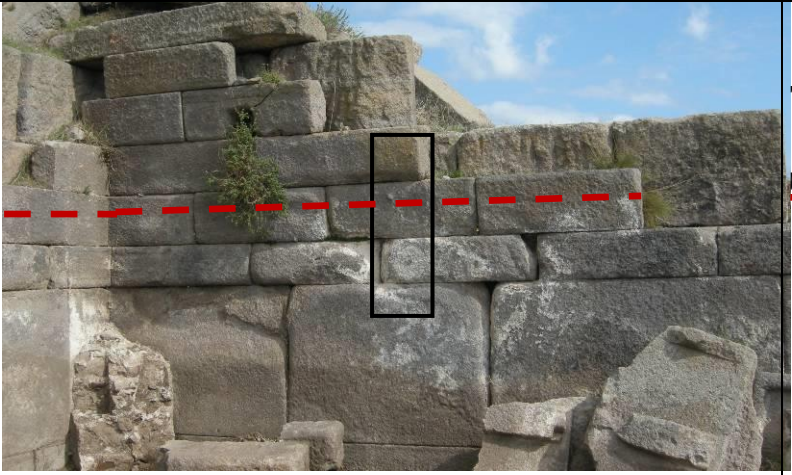

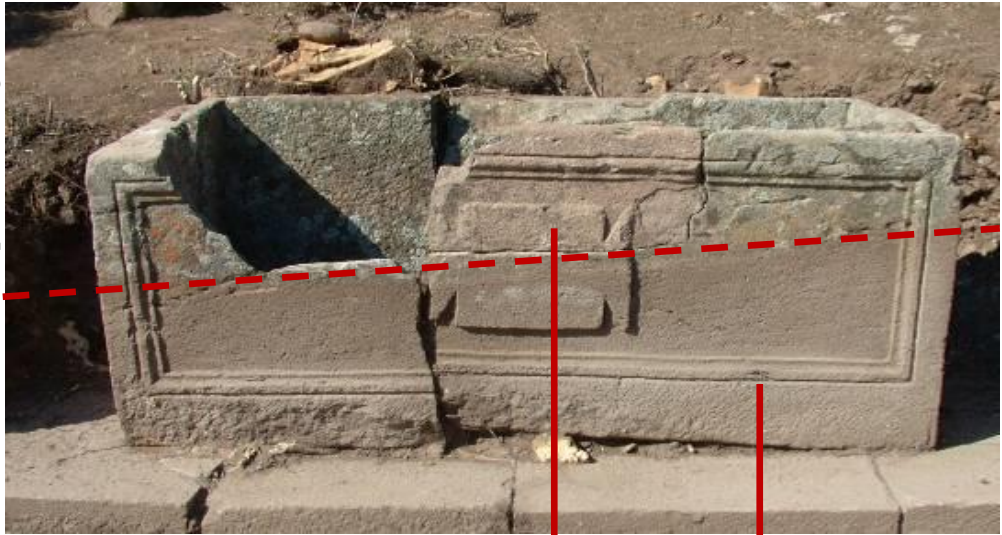


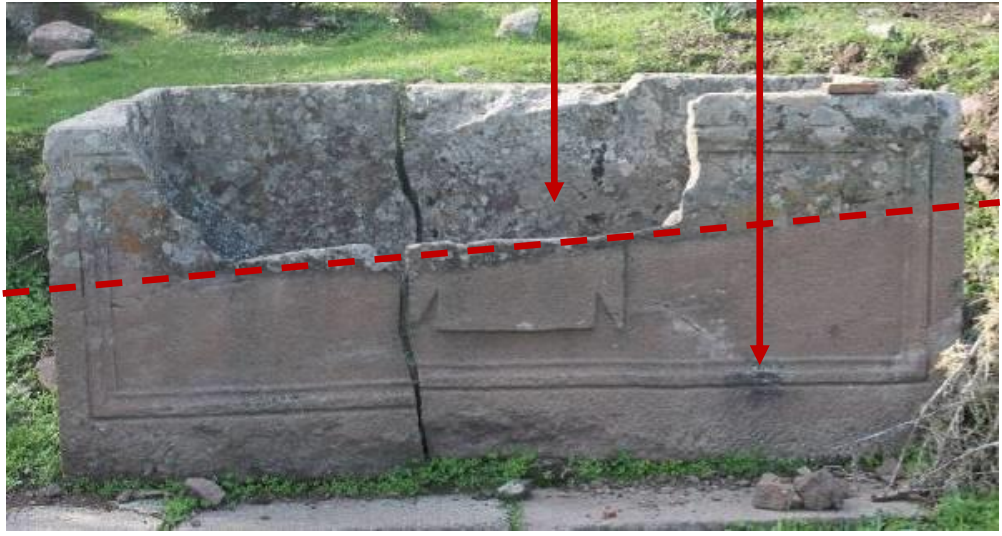

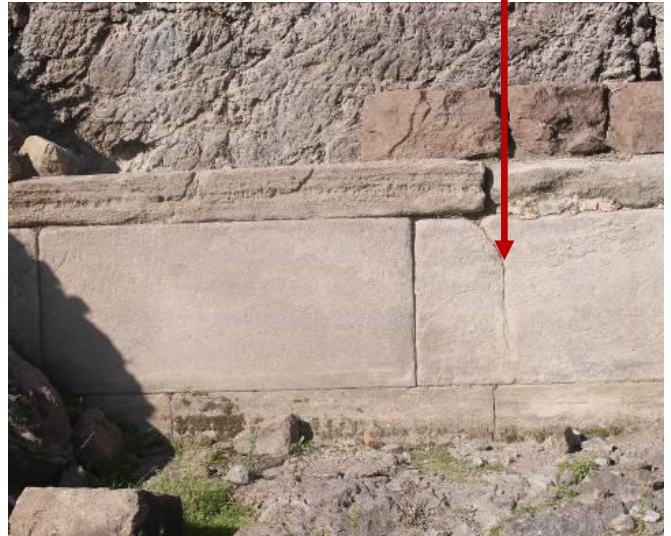

<p>Fortification Wall: Excavated in 2010</p>		<p>Exposed Standing</p>  <p>Excavated</p>
<p>Fortification Wall: Excavated in 2010</p>		<p>Exposed Standing</p>  <p>Excavated</p>
<p>Bouleuterion Excavated between 2010-2013</p>		<p>Exposed Standing</p>  <p>Excavated</p>
<p><i>Visible deterioration: Biological growth on exposed standing parts and white deposition on recently excavated parts are observed.</i></p>		

Table 3.3. Comparison of deterioration progresses observed on the andesites in Aigai archaeological site between the years 2010 and 2014

<p style="writing-mode: vertical-rl; transform: rotate(180deg);">October 2010</p>	<p style="writing-mode: vertical-rl; transform: rotate(180deg);">Exposed standing</p>  <p style="writing-mode: vertical-rl; transform: rotate(180deg);">Excavated</p>		
<p style="writing-mode: vertical-rl; transform: rotate(180deg);">October 2014</p>	<p style="writing-mode: vertical-rl; transform: rotate(180deg);">Exposed standing</p>  <p style="writing-mode: vertical-rl; transform: rotate(180deg);">Excavated</p>		
<p style="writing-mode: vertical-rl; transform: rotate(180deg);">Definition</p>	<p>Necropolis: Partially excavated in 2006. Visible deterioration: Collapse of restored piece of the grave and discolouration are observed.</p>	<p>Agora: Completely exposed standing since approximately 2500 years. Visible deterioration: Pitting on the andesite surfaces is observed.</p>	<p>Western Stoa: Completely excavated in 2009. Visible deterioration: Progress of the current crack is observed.</p>

(cont. on next page)

Table 3.3 (cont.).

<p>October 2010</p>			
<p>October 2014</p>			
<p>Definition</p>	<p>Western Stoa: Completely excavated in 2009. <i>Visible deterioration:</i> Discharge of the soil, which was used to combine the andesites, is observed.</p>		







(cont. on next page)

Table 3.3 (cont.).

<p>October 2010</p>			
<p>October 2014</p>			
<p>Definition</p>	<p>Western Stoa: Completely excavated in 2009.</p> <p><i>Visible deterioration:</i> Biological growth on the ground and discharge of the soil, which was used to combine the andesites, are observed.</p>		







(cont. on next page)

Table 3.3 (cont.).

<p>October 2010</p>			
<p>October 2014</p>			
<p>Definition</p>	<p>Western Stoa: Completely excavated in 2009. <i>Visible deterioration:</i> Biological growth and accumulation of water on the ground are observed.</p>		<p>Bouleuterion: Partially excavated between 2004 and 2006. <i>Visible deterioration:</i> Collapse of the andesite surface on the wall is observed.</p>



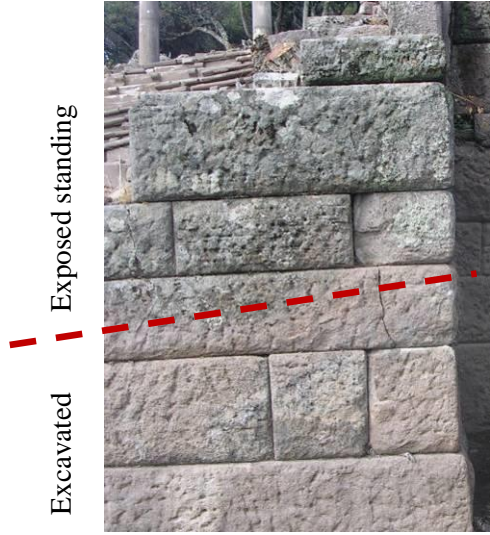


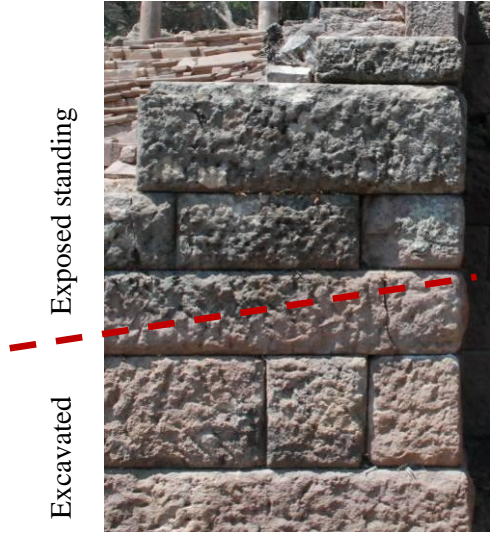
(cont. on next page)

Table 3.3 (cont.).

<p style="writing-mode: vertical-rl; transform: rotate(180deg);">October 2010</p>			
<p style="writing-mode: vertical-rl; transform: rotate(180deg);">October 2014</p>			
<p style="writing-mode: vertical-rl; transform: rotate(180deg);">Definition</p>	<p>Bouleuterion: Partially excavated between 2004 and 2006. <i>Visible deterioration:</i> Biological growth on the ground is observed.</p>		




(cont. on next page)

Table 3.3 (cont.).

<p>October 2010</p>			
<p>October 2014</p>			
<p>Definition</p>	<p>Bouleuterion: Partially excavated between 2004 and 2006. <i>Visible deterioration:</i> Biological growth and pitting on the ground is observed.</p>		

(cont. on next page)

Table 3.3 (cont.).

<p>October 2010</p>			
<p>October 2014</p>			
<p>Definition</p>	<p>Shop: Completely excavated in 2008. <i>Visible deterioration:</i> Biological growth on the wall is observed.</p>	<p>Public Bath Wall: Completely excavated in 2008. <i>Visible deterioration:</i> Discharge of the soil, which was used to combine the andesites, is observed.</p>	

(cont. on next page)

Table 3.3 (cont.).

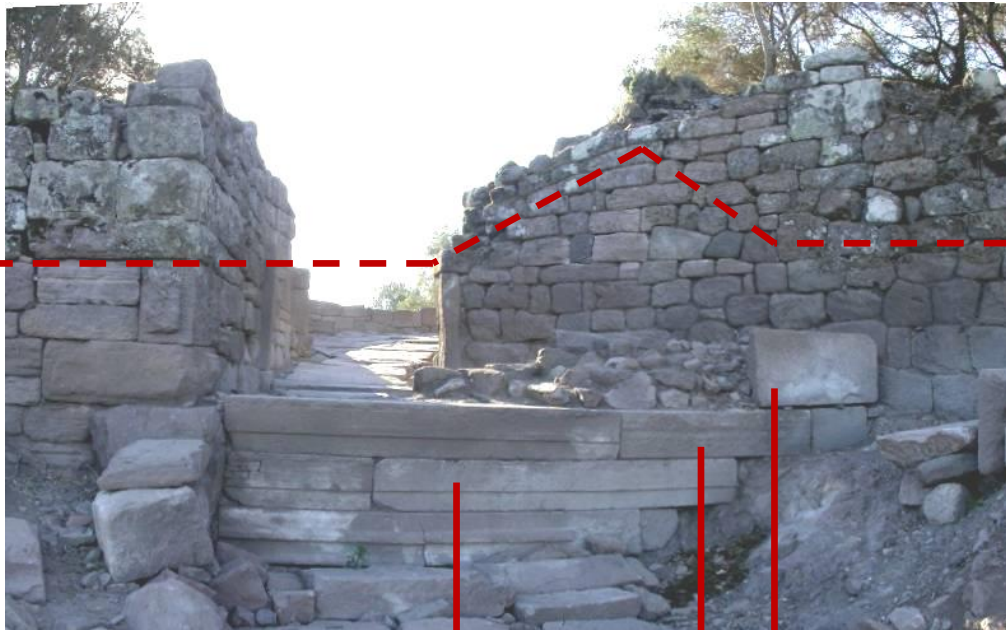

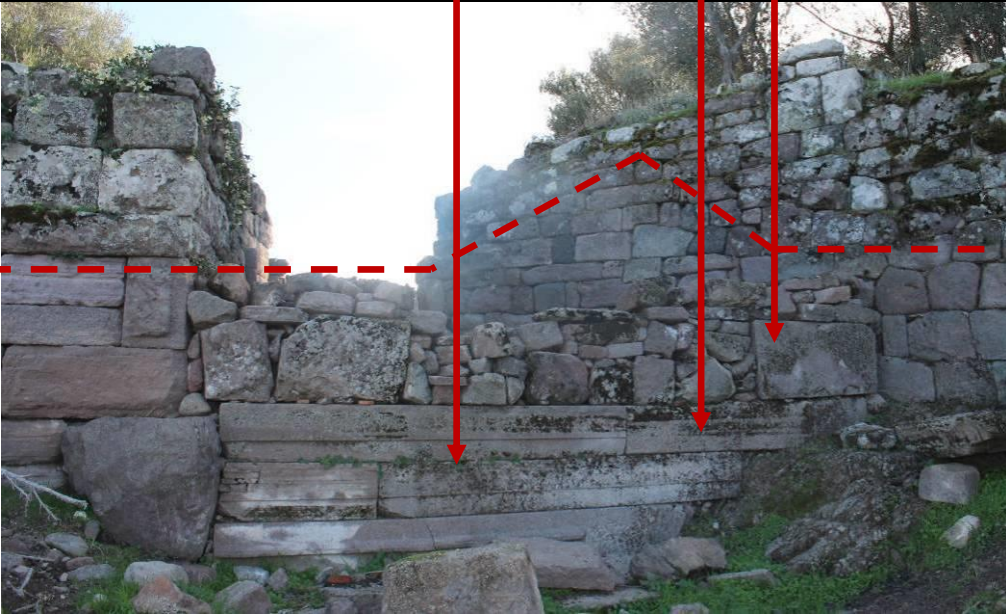
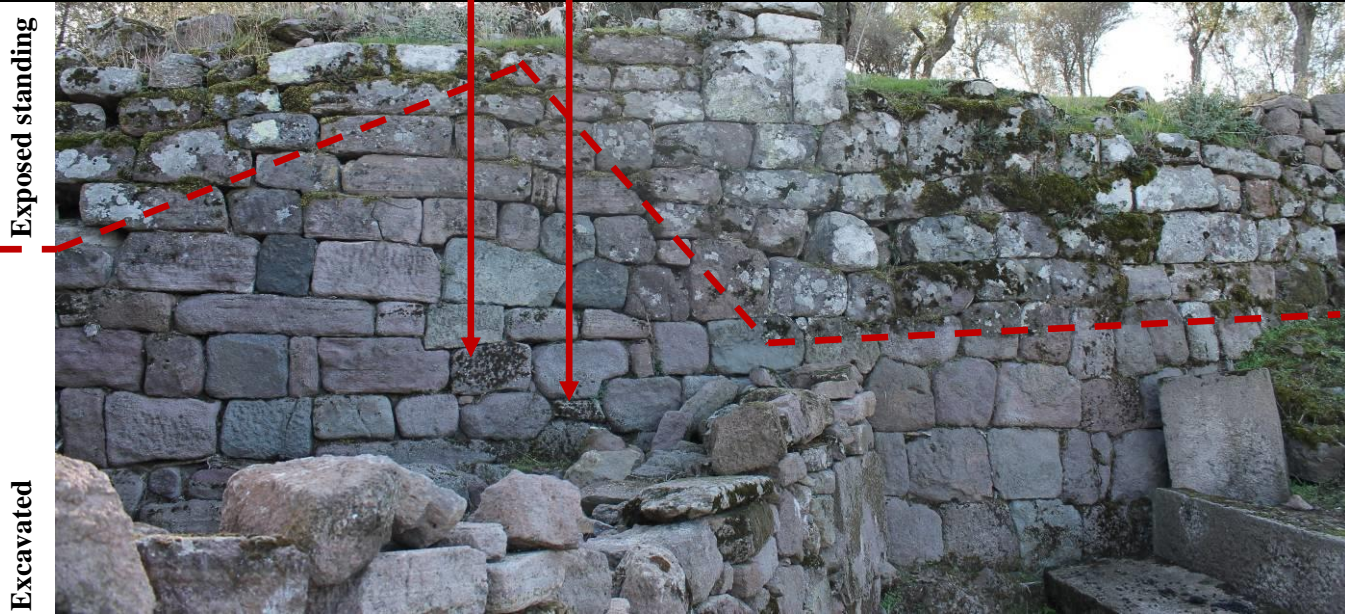







<p>October 2010</p>	<p>Exposed standing</p>  <p>Excavated</p>	<p>Exposed standing</p>  <p>Excavated</p>
<p>October 2014</p>	<p>Exposed standing</p>  <p>Excavated</p>	<p>Exposed standing</p>  <p>Excavated</p>
<p>Definition</p>	<p>Iron Gate: Partially excavated in 2005 and 2006. <i>Visible deterioration:</i> Biological growth on the excavated parts of the wall is observed.</p>	

Table 3.4. Comparison of deterioration progresses observed on the andesites in Assos archaeological site between the years 2010 and 2014

<p style="writing-mode: vertical-rl; transform: rotate(180deg);">October 2010</p>			
<p style="writing-mode: vertical-rl; transform: rotate(180deg);">October 2014</p>			
<p style="writing-mode: vertical-rl; transform: rotate(180deg);">Definition</p>	<p>Fortification wall: Exposed standing. <i>Visible deterioration:</i> Deterioration of the andesites was not observed.</p>		<p>Gymnasium wall: Completely excavated in 2014. <i>Visible deterioration:</i> Deterioration of the andesites was not observed.</p>

(cont. on next page)

Table 3.4 (cont.).

<p>October 2010</p>			
<p>October 2014</p>			
<p>Definition</p>	<p>Necropolis: Completely excavated between 2008 and 2014. <i>Visible deterioration:</i> Loss of andesite street floor coverings is observed.</p>		<p>Monumental tomb: Exposed standing. <i>Visible deterioration:</i> Wet andesite surfaces are observed.</p>

(cont. on next page)

Table 3.4 (cont.).

<p>October 2010</p>			
<p>October 2014</p>			
<p>Definition</p>	<p>North Stoa: Partially excavated between 2009 and 2014. <i>Visible deterioration:</i> Discoloration of andesite surfaces is observed.</p>		





(cont. on next page)

Table 3.4 (cont.).

<p>October 2010</p>			
<p>October 2014</p>			
<p>Definition</p>	<p style="text-align: center;">Theatre: Completely excavated in 1989. <i>Visible deterioration:</i> Loss of andesite is observed on the scene wall.</p>		

(cont. on next page)

Table 3.4 (cont.).

October 2010		
October 2014		
Definition	<p>Bouleuterion: Completely excavated between 2009 and 2013. <i>Visible deterioration:</i> Biological growth on the excavated parts of the wall is observed.</p>	

3.2. Subsoil Characteristics of Aigai and Assos

The importance of the characteristics of subsoil environments such as clay, carbonate, organic material and soluble salt contents in the deterioration of buried materials was mentioned before. Because the andesite samples were collected from the regions which were in shallow burial parts of the subsoil environments before the excavations, soil samples of these parts were also collected and analyzed to find out the main characteristics of subsoil environments, where the deterioration of buried andesites occurred.

Shallow burial environments are composed of sand, organic materials, silt, clay and soluble salts (Amundson 2003, Velde and Meunier 2008). Thus, shallow burial areas support the penetration of clays, soluble salts and organic materials in the buried materials (Curran et al 2002, Cronyn 2002). While salt and clay minerals penetrate the materials during burial, they do not have direct effects before excavation of the materials. As an indirect effect, the water holding capacities of clays increase the rate of interaction between water and material minerals (Thorn et al. 2002). When rapid temperature and humidity changes start to occur after the excavations, deposited clay and soluble salts may lead to a rapid deterioration of stone which is faster than exposed standing stones (Power 1989, Thorn et al. 2002, Cronyn2002, Warke et al 2010). The crystallization of soluble salts in the stone structure and results in the crack formations as a physical deterioration (Cronyn 2002). In some cases, salts also enhance the swelling potential of clay minerals in the stone structure (Snethlage and Wendler 1997, Rodriguez-Navarro et al. 1998, Scherer 2006, Scherer and Jimenez-Gonzales 2008, Doehne and Price 2010). As promoting physical deterioration, salt solutions also promote the alteration of quarts (Young 1987) and feldspars (Bernabe et al. 1995) which are the main minerals of the andesites.

Physical deterioration of the excavated stones is also supported by the swelling and shrinkage of the clay minerals in the cracks of the stones with wetting-drying processes (Press and Siever 2002, Scherer 2006). As far as promoting physical deterioration, clay minerals also constitute appropriate environment for biological formations, which also support physical and chemical deterioration of the stones (Press and Siever 2002, Chen et al. 1999).

Thus, important parameters such as clay, carbonate, organic material and soluble salt contents of the subsoil environments of Aigai and Assos archaeological sites were determined. In the following parts, mineralogical characteristics of the clay fractions of soil samples, organic material, carbonate and soluble salt contents of the soil samples are explained.

3.2.1. Mineralogical Characteristics

Mineralogical characteristics of the clay fractions of the soil samples were studied by XRD and FT-IR spectroscopic analysis. Infrared spectra were recorded in the 4000-400 cm^{-1} with KBR pellets of the samples and observed bands have been tentatively assigned. In the FT-IR analysis of the soil samples, OH stretching absorption bands found between 3423 cm^{-1} and 3700 cm^{-1} may show the presence of clay minerals, halloysite, illite, kaolinite, montmorillonite and saponite in the IR spectrums of the samples (Gadsden 1975) (Figure 3.1). Except kaolinite, all the other clay minerals were also determined by the XRD analysis of the soil samples (Figure 3.2, Figure 3.3).

During burial, clays in the soil structure increase water retention of the subsoil environment and thus chemical deterioration rate increase (Thorn et al. 2002). Besides, they constitute appropriate environment for biological formations which have both physical and chemical effects on the stones as previously mentioned (Press and Siever 2002, Chen et al. 1999). Hence, presence of clay minerals in the soil structure may be one of the reasons of andesite deteriorations during burial. Their presence may also be effective in the generation of biological forms on the andesite surfaces after their excavations as mentioned in visual analysis part.

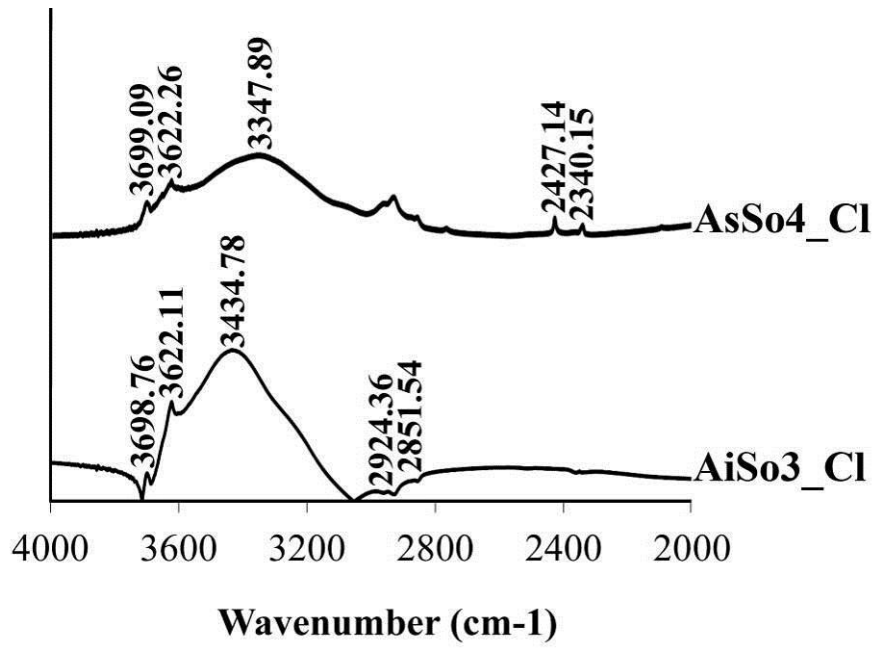
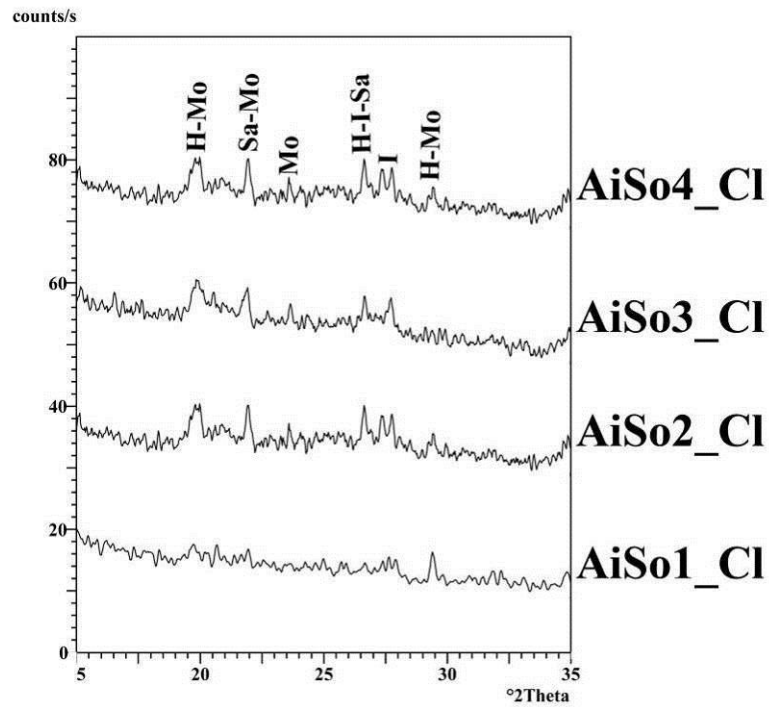
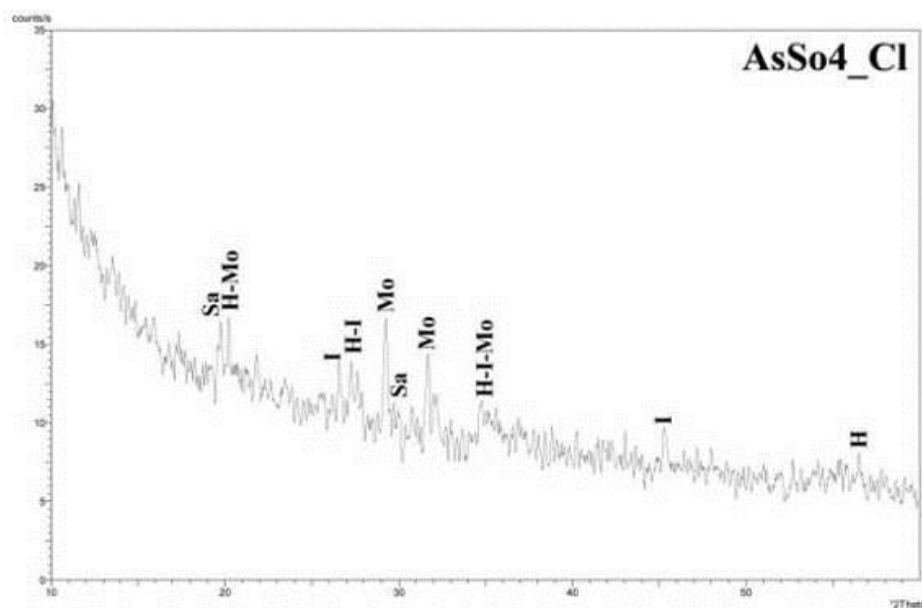


Figure 3.1. FT-IR spectrum of clay fraction of AiSo3 and AsSo4



H: Halloysite, I: Illite, Mo: Montmorillonite, Sa: Saponite

Figure 3.2. XRD spectrums of clay fractions of AiSo1, AiSo2, AiSo3 and AiSo4



H: Halloysite, I: Illite, Mo: Montmorillonite, Sa: Saponite

Figure 3.3. XRD spectrum of clay fraction of AiSo4

3.2.2. Organic Material and Carbonate Contents

Organic material and carbonate contents of the soil samples were analyzed and compared with the andesite samples to find out the possible deterioration factors during burial of the andesites. The results of the analysis for the average values of the organic material proportions of the soil samples of both Aigai and Assos shows low amounts of organic material contents. The amount of organic material content is 8.9 % for the soil samples of Aigai and 7.91 % for the ones of Assos (Figure 3.4). Supporting the results of organic material content analyses, IR spectrums of the clay fractions of the soil samples, the absorption bands between 2400 cm^{-1} and 2800 cm^{-1} and SEM analyses of the soil samples show the presence of organic materials in the soil structure (Figure 3.1, Figure 3.5).

The presence of organic materials in soil structure generally originates from biological sources of living or abiotic plants, microbial materials and animals and they have both physical and chemical effects on the buried stones (Chen et al. 1999, Press and Siever 2002, Mortatti and Probst 2003, Doehne and Price 2010). The activities of organic materials in the soil structure by the excretion of various enzymes and acids,

such as carbonic acid promote the dissolution (chemical deterioration) of stone forming minerals (Chen et al. 1999, Press and Siever 2002, Mortatti and Probst 2003). As a physical effect, their hyphae penetration through the voids of the materials and swelling/shrinkage action of the hyphae in the voids cause new micro-cracks in the material structures (Chen et al. 1999). Thus, the organic materials in the soil structure may be effective in the physical and chemical deterioration of the studied andesites.

As the presence of organic materials, carbonate contents of the soils were also analyzed by carbonate content analysis and the results for the carbonate contents were compared for andesite and soil samples. The results of the carbonate content analysis show that the soil samples of the Aigai and Assos contain low amounts of carbonate content ranging between 0.9- 4.5 % (Figure 3.4).

Similar values of organic material and carbonate contents of the soil samples taken from Aigai and Assos archaeological sites may be resulted from the locations of the samples. Because the soil samples were all collected from the shallow burial parts of the subsoil environments, before the excavations.

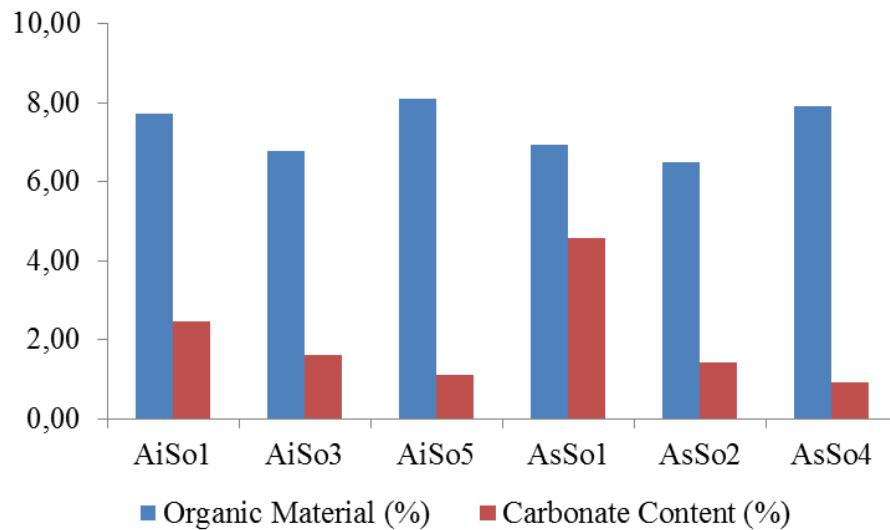


Figure 3.4. % Organic material and carbonate contents of soil samples of Aigai and Assos

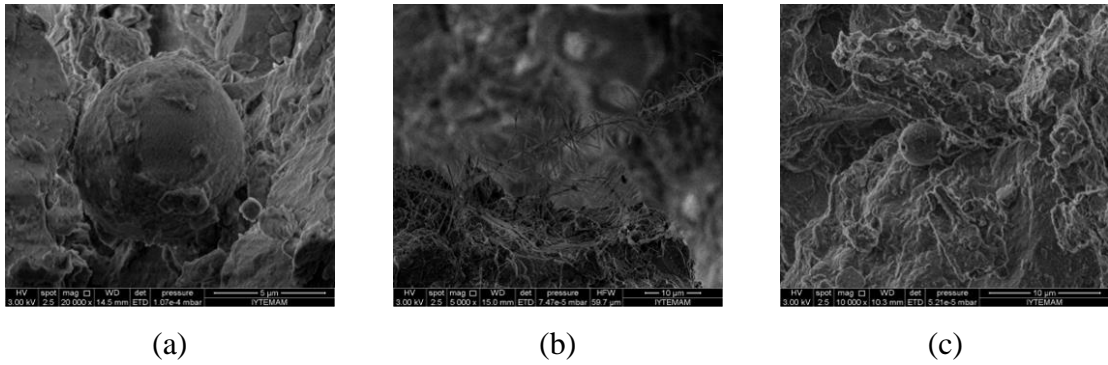


Figure 3.5. SEM images of organic materials in AiSo1 (a) (b) and AsSo1 (c)

3.2.3. Soluble Salt Contents

In order to evaluate the possible deterioration problems of andesites and possible effects of being near seashore in Assos archaeological site, percent soluble salts in soil and andesite samples were determined by ion chromatography (IC) (Doehne and Price 2010).

As previously mentioned, the presence of soluble salts in the stone structure is one of the most important factors in the deterioration of stones and it is mainly supported by the surrounding soil (Power 1989, Cronyn 2002). While salt penetration to the materials occur during burial, they are more likely to be excessive after excavation when rapid temperature and humidity changes start to occur (Wüst and McLane 2000, Curran et al 2002, Cronyn 2002, Warke et al 2010). As a result of these changes, deposited soluble salts may lead to a rapid deterioration of stone which is faster than exposed standing stones (Power 1989, Thorn et al. 2002, Cronyn 2002, Thorn et al. 2006, Warke et al 2010).

The results of the IC analyses show that studied soil samples which were collected from Aigai and Assos archaeological sites contain trace amounts of soluble salts (Figure 3.6, Appendix A). Although Assos is a coastal archaeological site, soil samples collected from Assos contain trace amounts of soluble salts either. Thus, the results of the analyses show that the soluble salts may be less effective in the deterioration of buried Aigai and Assos andesites.

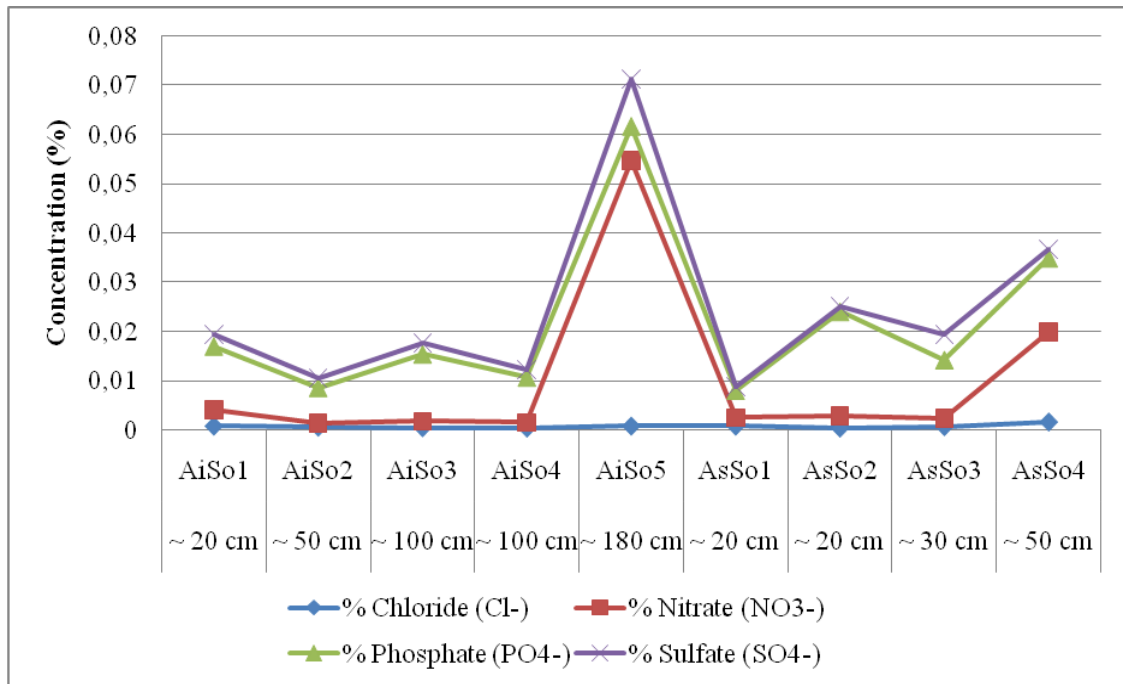


Figure 3.6. % Soluble salt contents of the soil samples

3.3. Characteristics of Interior and Exterior Parts of the Andesites

In the following parts, basic physical, microstructural petrographic, mineralogical and chemical characteristics of interior parts and exterior surfaces of andesite samples are described and compared.

3.3.1. Basic Physical Characteristics

RILEM standard test methods show that the average density and porosity values of the interior parts of the andesite samples of Aigai is 2.3 g/cm³ and 10.1% by volume respectively (Figure 3.7). For the interior parts of the andesite samples of Assos, the average density value is 2.3 g/cm³ and porosity value is 11.3% by volume (Figure 3.8). In the exterior parts of the andesites (which were taken from their exterior parts approximately 1.5 cm through to their interior parts), the average density values decrease to 2.2 g/cm³ and the average porosity values increase to 12.2% and 13.2% by volume for Aigai and Assos andesites respectively (Figure 3.7, Figure 3.8, Appendix

B). Higher porosity and lower density values of the exterior parts of the stones resulted from the crack and pore formations in the stone structures as a physical deterioration and results in the decrease of the stone strength (Jaeger and Cook 1979, Brady and Brown 2004, Arıkan et al. 2007).

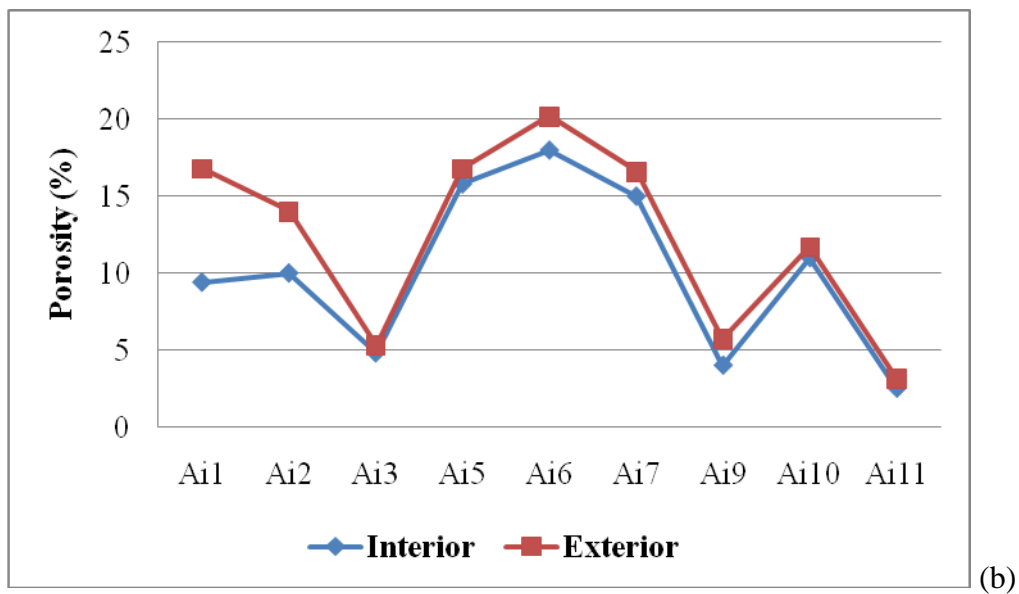
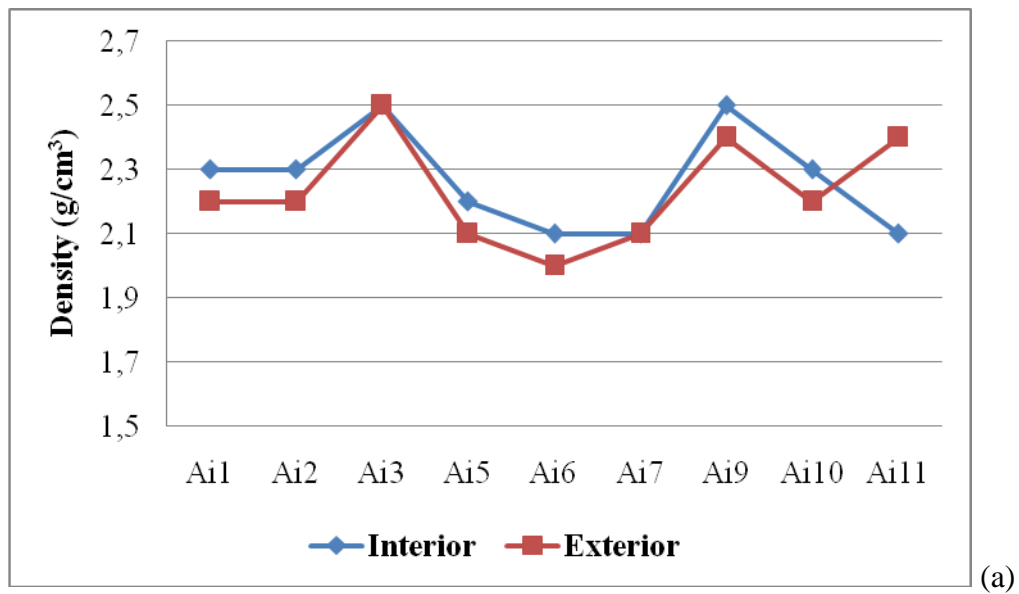


Figure 3.7. Density (g/cm^3) (a) and porosity (%) (b) values of Aigai Andesites

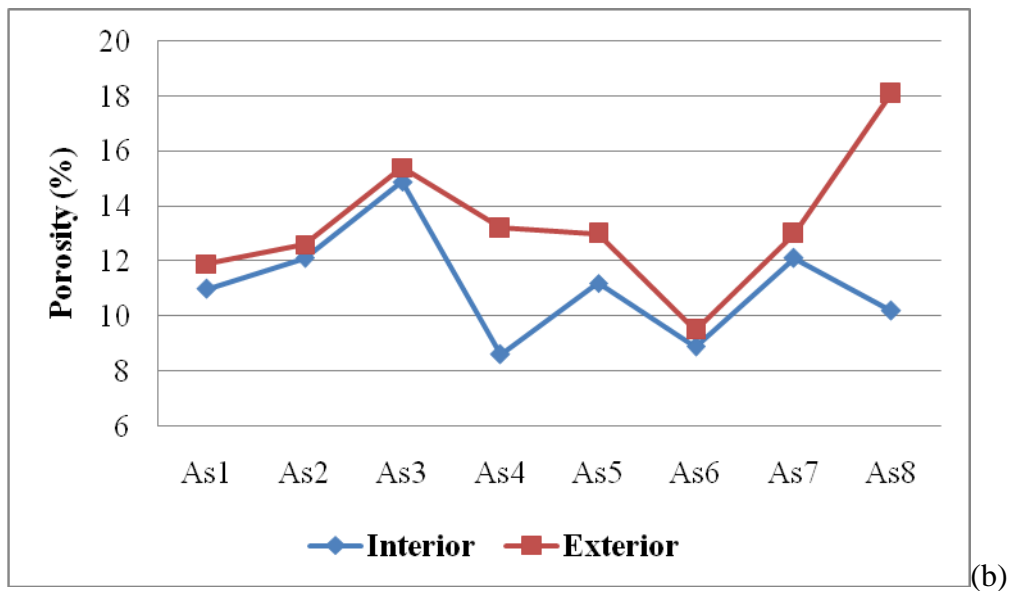
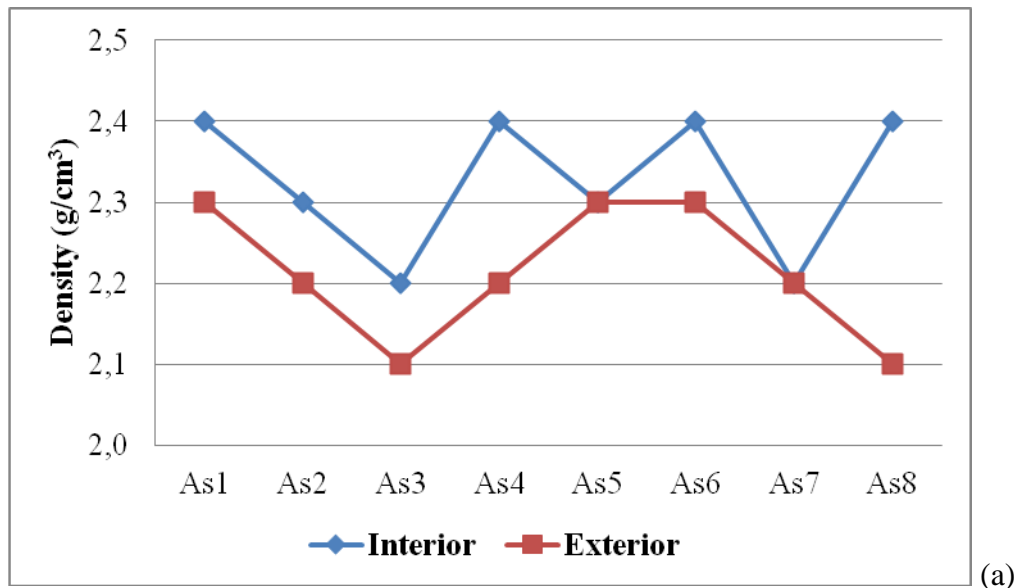


Figure 3.8. Density (g/cm^3) (a) and porosity (%) (b) values of Assos Andesites

Physical deterioration of the stones are related to their porosity and density values and thereby related to the strength of the materials. A low density and high porosity of the stones leads to high permeability for the deterioration factors such as clays and water and results in the decrease of the stone strength (Jaeger and Cook 1979, Brady and Brown 2004).

As mentioned before, the average density of the andesites is in the range of between 2.5 to 2.8 and the porosity values vary between 0.2 to 8.0 percent (Jaeger and Cook 1979, Howe 2001, Brady and Brown 2004). When the average density and porosity values of the sound andesites gathered from the literature are compared with the average density and porosity values of the interior parts of the studied andesites, higher values of the studied andesites can be seen. However, when the density and porosity values of the interior and exterior parts of the andesites are compared; decrease in the density and increase in the porosity values of the andesites in the exterior parts was determined. As mentioned above, higher porosity and lower density values of the stones are resulted from physical deterioration of the materials and results in the decrease of the stone strength (Jaeger and Cook 1979, Brady and Brown 2004, Arıkan et al. 2007).

Increase of the porosity of the andesites from their cores through the surfaces, in other words, physical deterioration of the andesites, is also observed in microstructural analysis of the samples, which will be explained in the following parts.

3.3.2. Microstructural and Petrographic Characteristics

Thin sections of andesite samples were analyzed by Scanning Electron microscope (SEM) and polarized microscope to find out their microstructural and petrographic characteristics and also microstructural differences of exterior and interior parts of the andesites. Thicknesses of the andesite sections were approximately 2 mm for SEM analysis and 30 μm for petrographic analysis.

The analyses show that Aigai and Assos andesites have similar petrographic characteristics. All the textures of the studied andesites are aphanitic (fine grained) (Howe 2001). Supporting the results of mineralogical analyses, which will be explained in following parts, the studied andesites consist predominantly of plagioclase feldspar with lower amounts of quartz (Figure 3.9, Figure 3.10, Figure 3.11, Figure 3.12).

In the stone matrix, with the presence of single mineral grains, stone-forming minerals also show both twinning (intergrowth of two or more different crystals by sharing some of their boundaries) and oscillatory zoning (single or multiple zoning cycles of the minerals) (Figure 3.13) (Ray et al. 2011). Zoning is widespread among calcium feldspars and ferromagnesian minerals (Figure 3.13). Twinning is widespread

among different ferromagnesian minerals such as hornblende and biotite and andesine as calcium feldspar (Figure 3.13). Less commonly than the other crystal textures, corona texture (covering of a mineral crystal by one or more another crystals) with calcium feldspar core and ferromagnesian rim was observed in As2 and Ai6 (Figure 3.14) (Ray et al 2011).

BSE and polarized microscope images of the mineral grains show that all the feldspars are subhedral or anhedral in shape and averages 0.05 to 1.5 mm in size for Aigai andesites and 0.05 to 2.5 mm in size for Assos andesites. In other words, larger mineral (feldspars and ferromagnesian minerals) grains were observed in the Assos andesites. Size of the mineral grains in the stones show the cooling process of the stones during their formation. When magma cools slowly, the minerals have enough time to combine and form bigger minerals in size (Press and Siever 2002). As a result, bigger minerals observed in the Assos andesites show that the cooling process of Assos andesites proceeded slower than the Aigai andesites during their formation.

With the stone-forming minerals, volcanic matrix with the glassy phase of the andesites was also observed in all the samples (Figure 3.9, Figure 3.11, Figure 3.13, Figure 3.14).

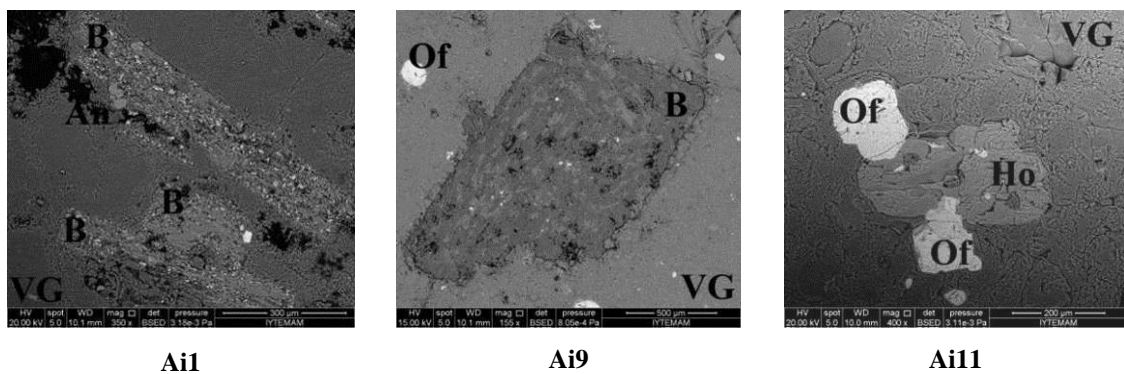


Figure 3.9. BSE images of the minerals in the interior parts of Aigai andesites (VG: volcanic glass, B: biotite, Ho: hornblende, Of: orthoferrosillite)

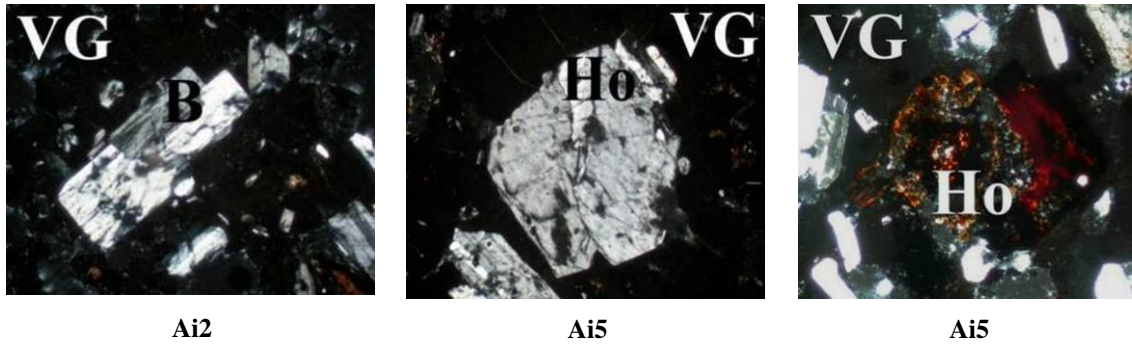


Figure 3.10. Photomicrograph of interior parts of Ai2 and Ai5 (VG: volcanic glass, B: biotite, Ho: hornblende, Of: orthoferrosillite)

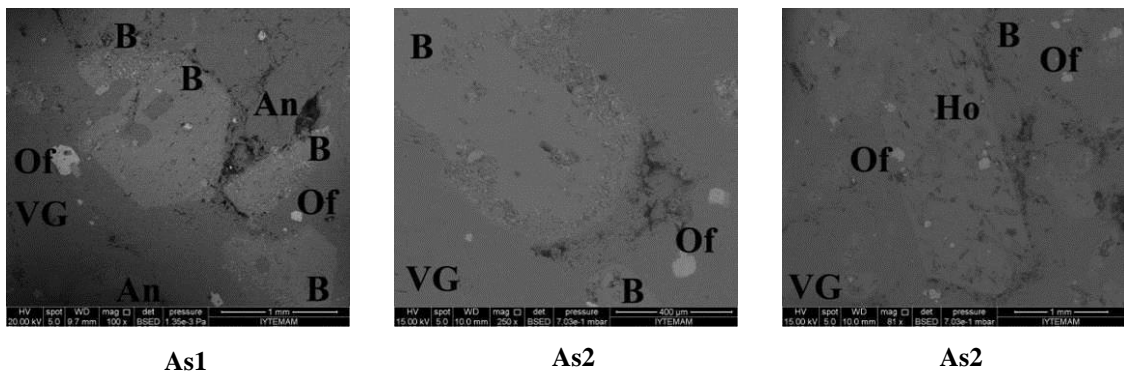


Figure 3.11. BSE images of the minerals in the interior parts of Assos andesites (VG: volcanic glass, An: andesine, B: biotite, Ho: hornblende, Of: orthoferrosillite)

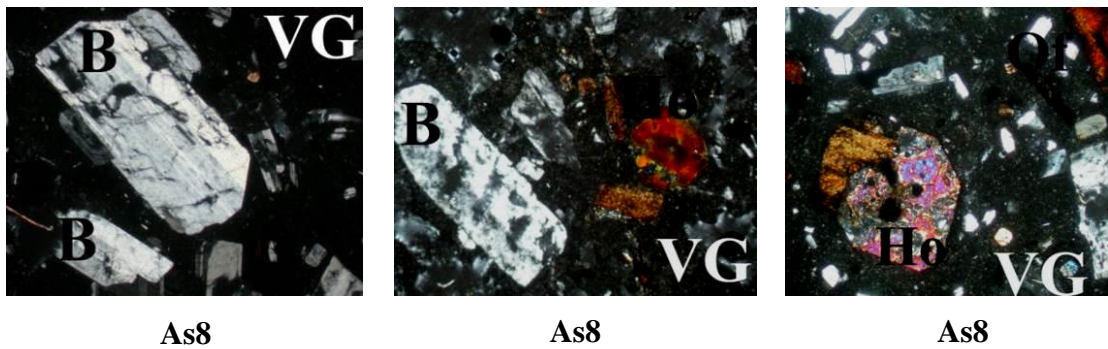


Figure 3.12. Photomicrograph of As8 (VG: volcanic glass, An: andesine, B: biotite, Ho: hornblende, Of: orthoferrosillite)

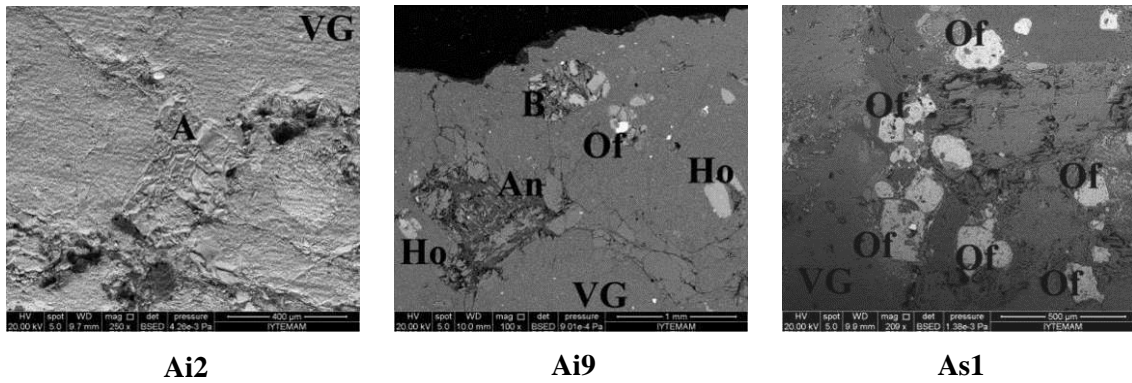


Figure 3.13. BSE images of the single mineral grain observed in Ai2, twinning minerals in Ai9 and oscillatory zoning observed in As1 (VG: volcanic glass, A: albite, B: biotite, Ho: hornblende, Of: orthoferrosillite)

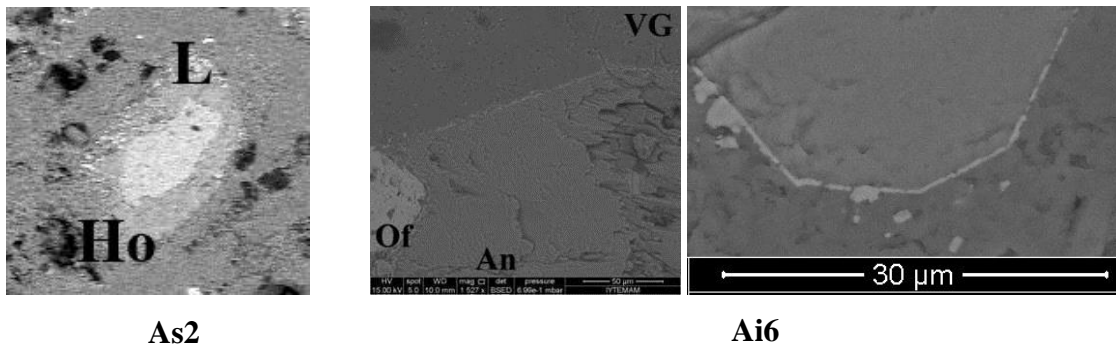
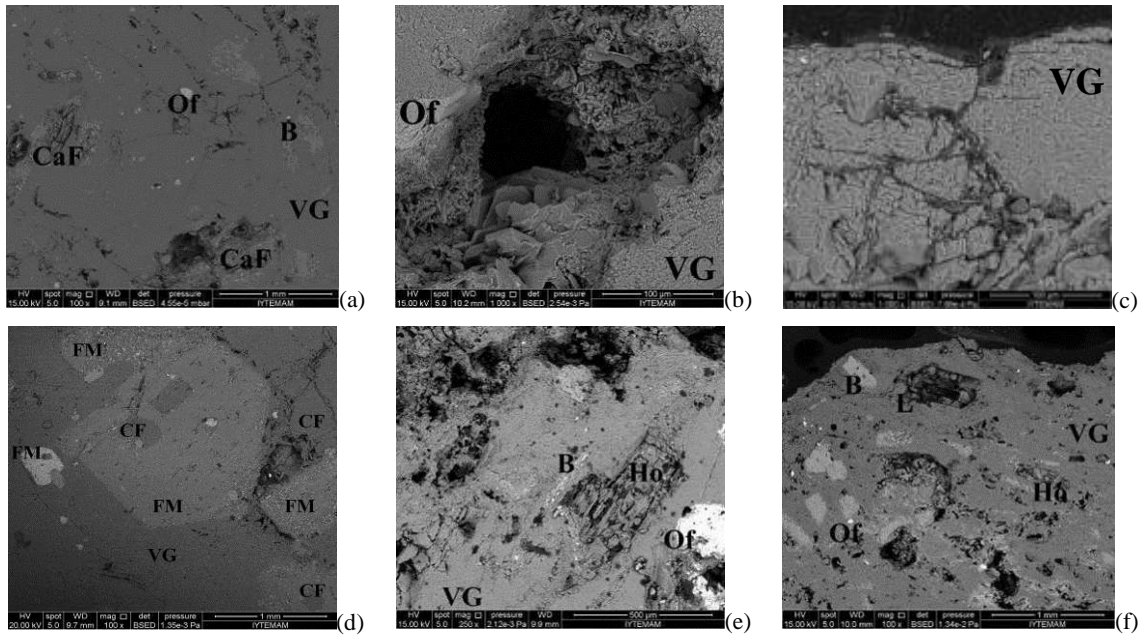


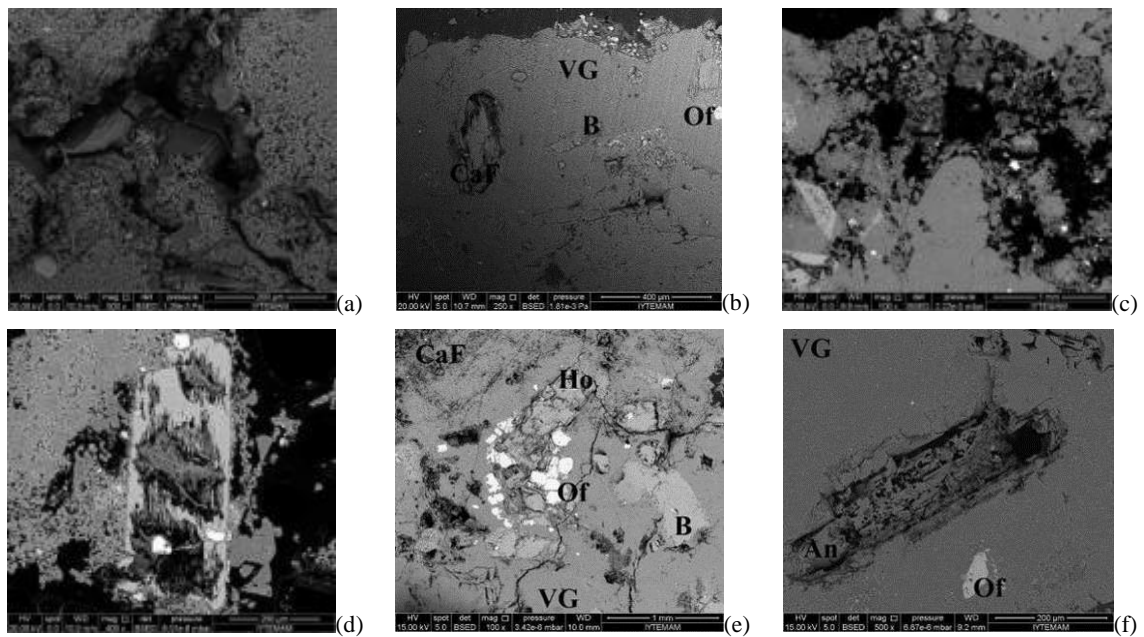
Figure 3.14. BSE images of the corona mineral texture of As2 and Ai6 (VG: volcanic glass, An: andesine, L: labradorite, Ho: hornblende, Of: orthoferrosillite)

The comparison of microstructural characteristics of interior and exterior parts of the andesites, which was analyzed with SEM analyses show micro-cracks ($\leq 55 \mu\text{m}$) and pore formation in the stone structures by the deterioration of stone forming minerals and volcanic glass as matrix (Figure 3.15, Figure 3.16). Supporting the results of basic physical property analyses, density of the pores and micro-cracks are higher in the sections close to the surface of the stones and they decrease through the inner parts.



B: Biotite, CaF: Calcium Feldspar, L: Labradorite, Ho: Hornblende,
Of: Orthoferrosilite, VG: Volcanic Glass

Figure 3.15. SEM images of pore formation and micro-cracks of exterior parts of Ai1 (a), Ai2 (b) (c), Ai6 (d), Ai8 (e) and Ai9 (f)



B: Biotite, CaF: Calcium Feldspar, An: Anorthite, Ho: Hornblende,
Of: Orthoferrosilite, VG: Volcanic Glass

Figure 3.16. SEM images of pore formation and micro-cracks of exterior parts of As1 (a) (b), As2 (c) (d), As5 (d) and As7 (f)

For both Aigai and Assos andesites, the widths of the micro-cracks change between 10 and 55 μm (Figure 3.17). As micro-crack dimensions, the widths of the pores have a great variety changing between 100 μm and 2.5 mm. Having the larger mineral grains, the pores of Assos andesites are larger than the ones of Aigai. While the largest pores observed in Aigai andesites are approximately 1.3 mm (Ai1, Ai11), it increase to 2.5 mm in Assos andesites (As5) (Figure 3.18).

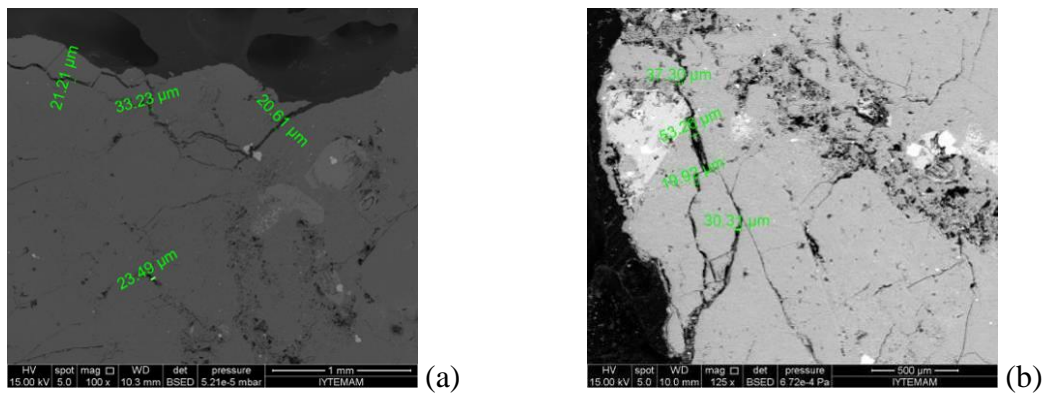


Figure 3.17. BSE images with the dimensions of the cracks observed on Ai1 (a) and As4 (b)

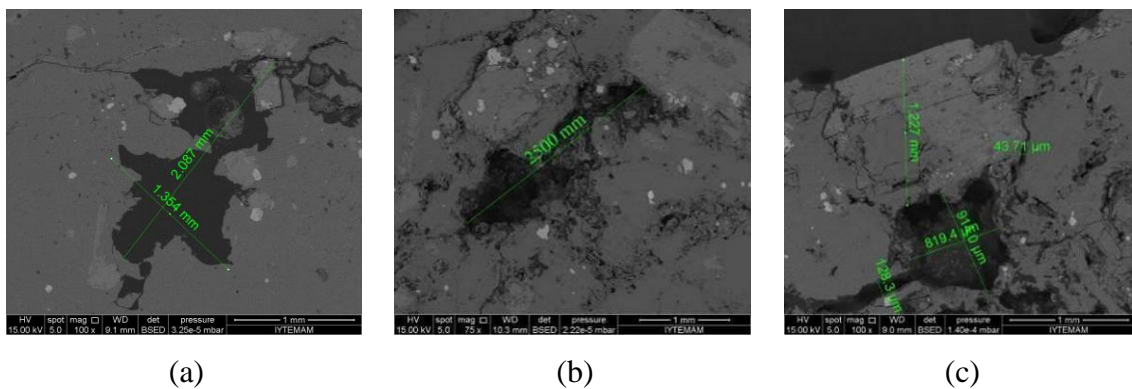


Figure 3.18. BSE images with the dimensions of the pores observed on Ai11 (a), As5 (b) and As7 (c)

Micro-crack formations are generally seen around the mineral boundaries which are generally formed as a result of chemical deterioration of the stone forming minerals (Press and Siever 2002), or through the stone surface to the interior parts (Figure 3.19). Mapping of some of the pores based on their chemical characteristics contain the remains of the deteriorated minerals. The analyses show that these pores in the andesites are generally formed as a result of chemical deterioration of calcium feldspars and pyroxenes, which will be explained in more detail in the following parts.

Physical deterioration of the samples was observed by the examination of the andesite sections from their surfaces through interior parts by SEM. As a technical constraint of the SEM, the sections which are longer than 5.3 cm could not analyzed. Visual observation of the combined BSE images of the andesite sections also show the presence of micro-cracks and pore formations in the interior parts of the samples (Figure 3.20, Figure 3.21). As determined in the sections close to the andesite surfaces and mentioned above, micro-crack formations are also generally seen around the mineral boundaries and through the interior parts of the andesites in the interior parts either.

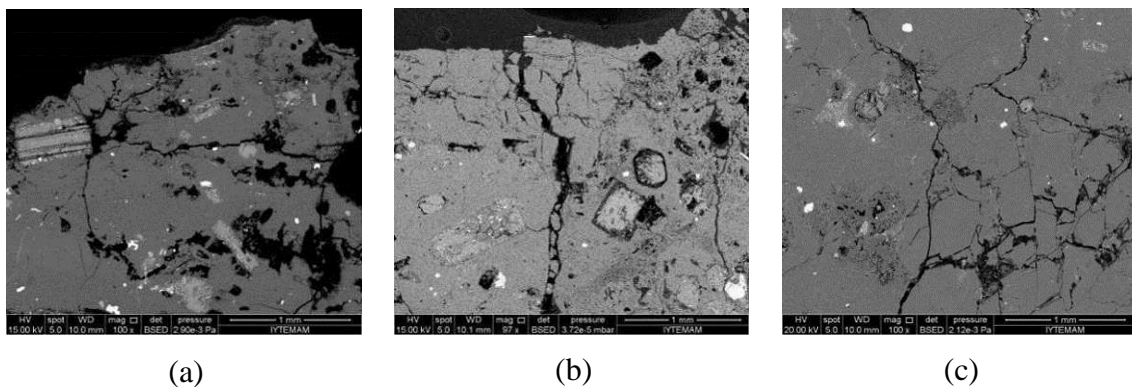


Figure 3.19. BSE images of the cracks observed on Ai2 (a), As3 (b) and As6 (c)

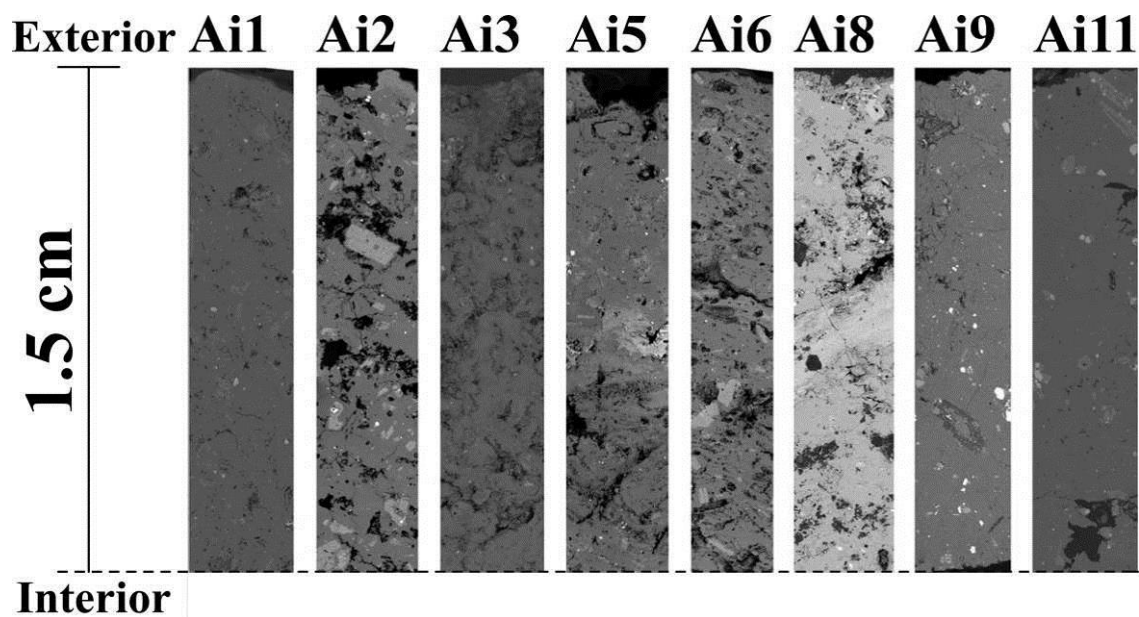


Figure 3.20. BSE images of Aigai andesites from surfaces to the inner cores

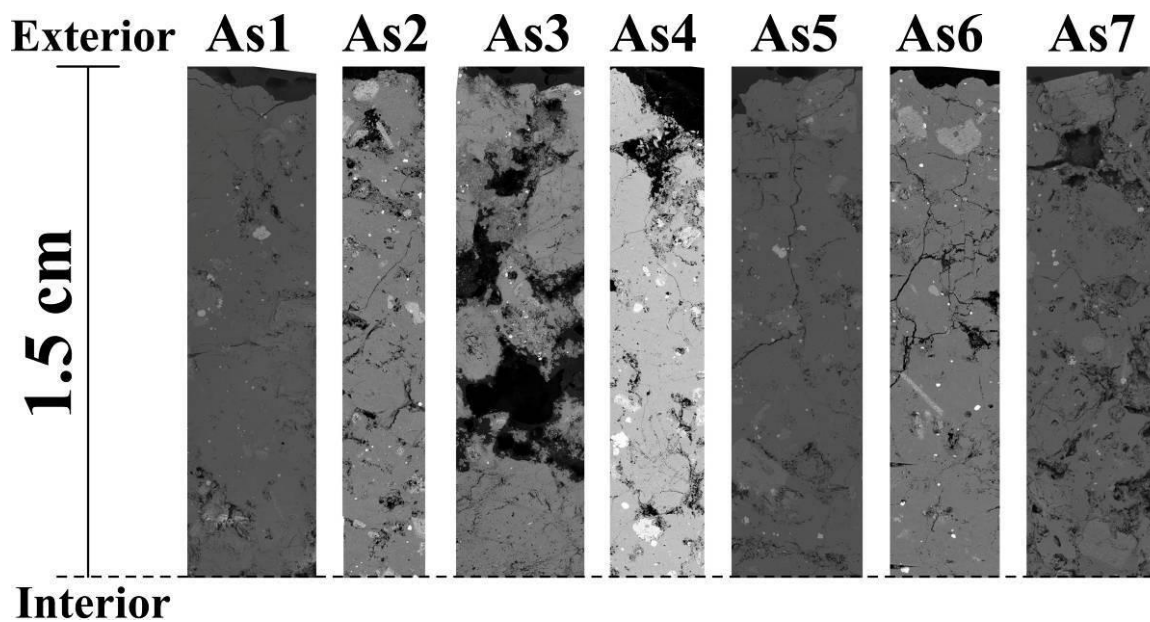
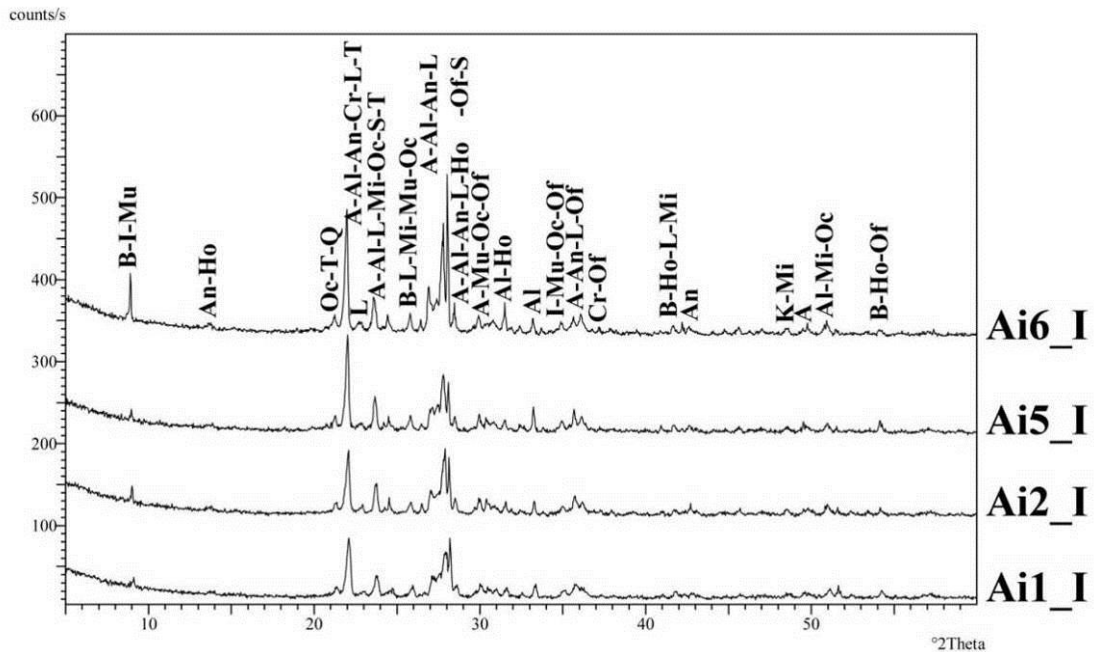


Figure 3.21. BSE images of Assos andesites from surfaces to the inner cores

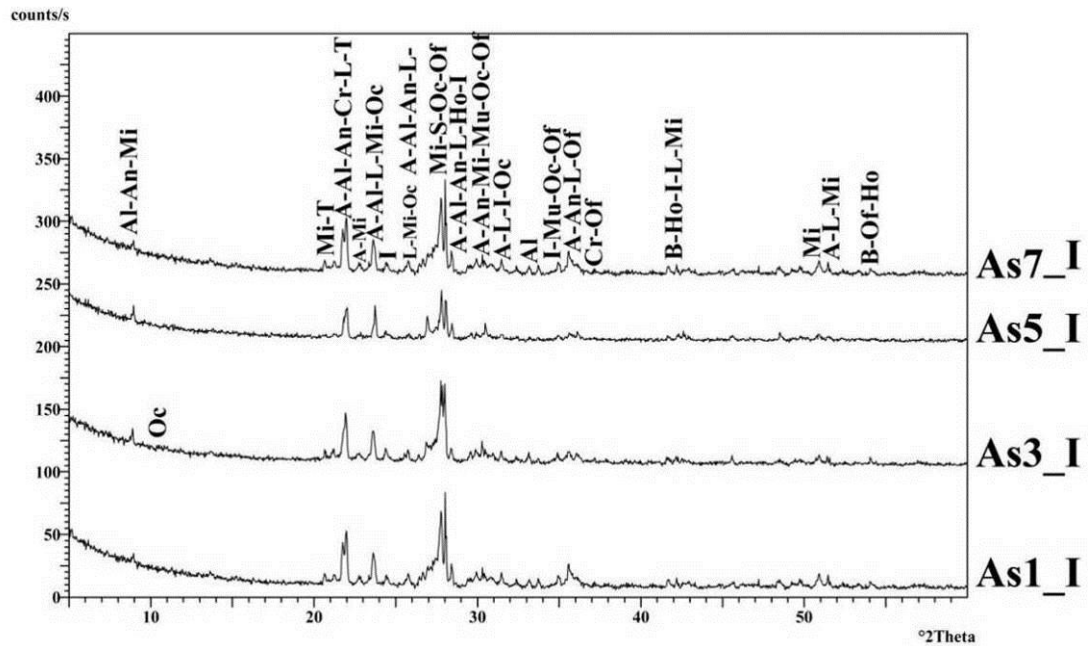
3.3.3. Mineralogical Characteristics

Mineralogical characteristics of both interior and exterior parts of the andesites were determined by XRD analysis. XRD analyzes of the interior parts of the studied andesite sample show that the andesites are dominated by the minerals of microcline, orthoclase and sanidine as potassium feldspars, albite as sodium feldspar, andesine, labradorite and anorthite as plagioclase feldspars, muscovite as mica, cristobalite, tridymite and quartz as quartz minerals, kyanite and mullite as aluminum silica and biotite, hornblende (amphibole) and orthoferrosilite (pyroxene) as ferromagnesian minerals (Figure 3.22, Figure 3.23, Table 3.5, Table 3.6).



microcline (Mi), ortoclase (Oc), albite (Al), andesine (A), labradorite (L), anortite (An), biotite (B), muskovite (M), cristobalite (Cr), tridymite (T), quarts (Q), kyanie (K), ortoferrosilite (Of), hornblende (Ho), sanidine (S)

Figure 3.22. XRD patterns of interior parts of andesite samples of Aigai (Aix_I)



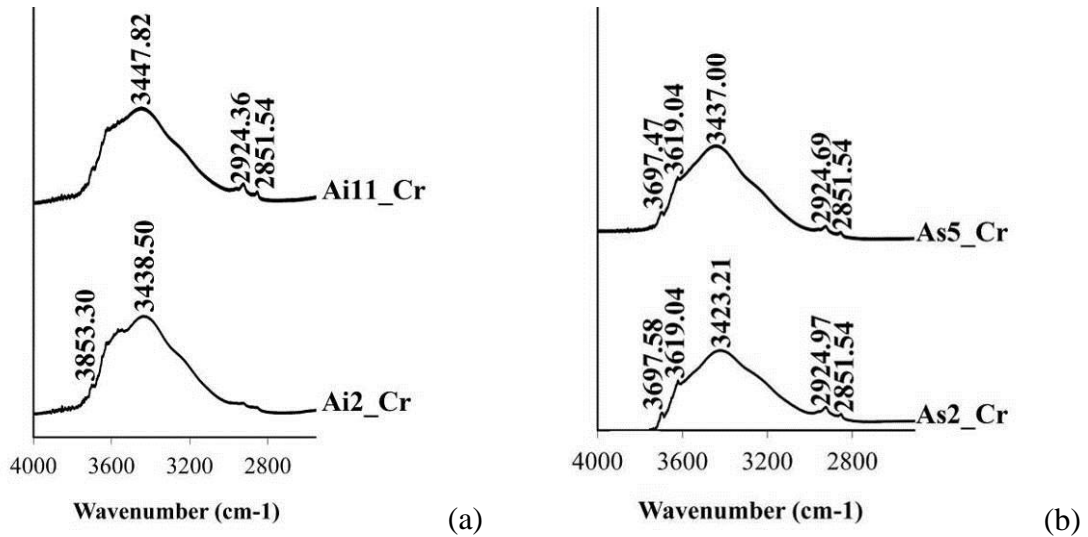
microcline (Mi), orthoclase (Oc), albite (Al), andesine (A), labradorite (L), anortite (An), biotite (B), muskovite (M), cristobalite (Cr), tridymite (T), quartz (Q), kyanite (K), ortoferrosilite (Of), hornblende (Ho), sanidine (S)

Figure 3.23. XRD patterns of interior parts of andesite samples of Assos (Asx_I)

With the presence of other andesite-forming minerals mentioned above, mineralogical analyses of andesite surfaces by XRD also show the presence of clay mineral of illite on the andesite surfaces (Figure 3.22, Figure 3.23, Table 3.5, Table 3.6). The clay fractions of stone were also studied by FT-IR analysis to determine types of clay minerals (Gadsden, J. A. 1975). In the determination of clay minerals, the absorption bands due to structural OH and Si–O groups play an important role in the differentiation of clay minerals from each other (Gadsden 1975, Majedova 2002). Infrared spectra were recorded in the 4000-400 cm^{-1} with KBR pellets of the samples and observed bands have been tentatively assigned.

Mineralogical analyses of the exterior surfaces of andesites by FT-IR analysis also show the presence of clay minerals in the stone structures with the other minerals. OH stretching absorption bands found between 3423 cm^{-1} and 3700 cm^{-1} may show the presence of clay minerals, illite, kaolinite and montmorrillonite in Aigai andesites and halloysite, illite, kaolinite, montmorrillonite and saponite in the IR spectrums of the Assos andesites (Gadsden 1975) (Figure 3.24, Table 3.5, Table 3.6).

The other absorption bands between 2400 cm^{-1} and 2800 cm^{-1} , which show the presence of organic materials, will be mentioned in the following sections (Figure 3.24).



H: Halloysite, I: Illite, Ka: Kaolinite, Mo: Montmorillonite, Sa: Saponite

Figure 3.24. FT-IR spectrum of surface crack of Ai2 - Ai11 (a) and As2 - As5 (b)

Table 3.5. Mineralogical Characteristics of Interior Parts and Exterior Surfaces of Aigai Andesites

	Interior Parts		Exterior Surfaces		
	Sample	XRD	Sample	XRD	FT-IR
Aigai Andesites	Ai1_I	Microline	Ai1_E	Illite	-
		Orthoclase	Ai2_E		
	Ai2_I	Sanidine	Ai5_E		
		Albite	Ai6_E		
	Ai3_I	Andesine	Ai7_E		
		Labradorite	Ai8_E		
	Ai5_I	Anorthite	Ai2_Cr	-	Illite, Kaolinite, Montmorillonite
		Muscovite	Ai5_Cr		
	Ai6_I	Cristobalite	Ai11_Cr		
		Tridymite			
	Ai7_I	Quartz			
		Kyanite			
	Mullite				
	Biotite				
	Hornblende				
	Orthoferrosilite				
<p style="text-align: center;">potassium feldspar, sodium feldspar, plagioclase feldspar, mica mineral, quartz mineral, aluminum silica, ferromagnesian mineral, clay minerals</p>					

Table 3.6. Mineralogical Characteristics of Sound Interior Parts and Deteriorated Exterior Surfaces of Assos Andesites

	Interior Parts		Exterior Surfaces		
	Sample	XRD	Sample	XRD	FT-IR
Assos Andesites	As1_I	Microline	As1_E	Illite	-
		Orthoclase	As2_E		
	As2_I	Sanidine	As3_E		
		Albite	As4_E		
	As3_I	Andesine	As5_E		
		Labradorite	As6_E		
	As4_I	Anorthite	As2_Cr	-	Halloysite, Illite, Kaolinite, Montmorillonite
		Muscovite			
	As5_I	Cristobalite	As5_Cr		
		Tridymite			
	As6_I	Quartz			
		Kyanite			
	As7_I	Mullite			
		Biotite			
Ai8_I	Hornblende				
	Orthoferrosilite				
potassium feldspar, sodium feldspar, plagioclase feldspar, mica mineral, quartz mineral, aluminum silica, ferromagnesian mineral, clay minerals					

All the clay minerals found in andesites are swelling minerals with high water holding capacity (Velde and Meunier 2008). After excavation of the andesites, clay minerals swell and shrink with wetting and drying processes. In the process of swelling and shrinkage, cracks further propagate in the pores of the stone (Press and Siever 2002, Scherer 2006). Thus, the presence of clay minerals in the stone structure may be one of the reasons of the formation of micro-cracks in the andesite structures.

As far as promoting physical deterioration, clay minerals also constitute appropriate environment for biological growth which have both physical and chemical effects on the stones (Press and Siever 2002, Chen et al. 1999). Evidencing the generation of biological forms, FT-IR analysis of the exterior parts of the andesites, absorption bands between 2400 cm^{-1} and 2800 cm^{-1} , show the presence of organic materials and biologic tissues in the stones as mentioned before. As a chemical deterioration, the activities of organic materials in the soil and stone structure by the excretion of various enzymes and acids, such as carbonic acid promote the dissolution of stone forming minerals (Chen et al. 1999, Press and Siever 2002, Mortatti and Probst 2003). Supporting FT-IR analyses, SEM analysis of the exterior surfaces of the andesites show the presence of biological tissues and their penetration to the interior of the andesites (Figure 3.25). As promoting the chemical deterioration of the stones, biologic tissues in the stone structures have also physical effects on the materials. Their hyphae penetration through the voids of the materials and swelling/shrinkage action of the hyphae in the voids cause new micro-cracks in the material structures (Chen et al. 1999, Press and Siever 2002). Thus, presence of biological forms, which is caused by the presence of clay minerals and water in the andesite structure, may be one of the reasons for the chemical deterioration of the stone forming minerals and formation of clay minerals which was mentioned before. They may also promote the physical deterioration of the andesites with their hyphae penetration through the interior parts of the stones.

As supported with the experiments, both in Aigai and Assos, biological formations in micro and macro scale can be seen on the excavated stone surfaces (Figure 3.26, Table 3.3, Table 3.4). The comparison of the photographs taken in 2010 and 2014 in Aigai and Assos archaeological sites also show the generation of biological forms on the andesite surfaces and loss of stone materials resulted from the presence of clay minerals and water as mentioned before (Table 3.3, Table 3.4).

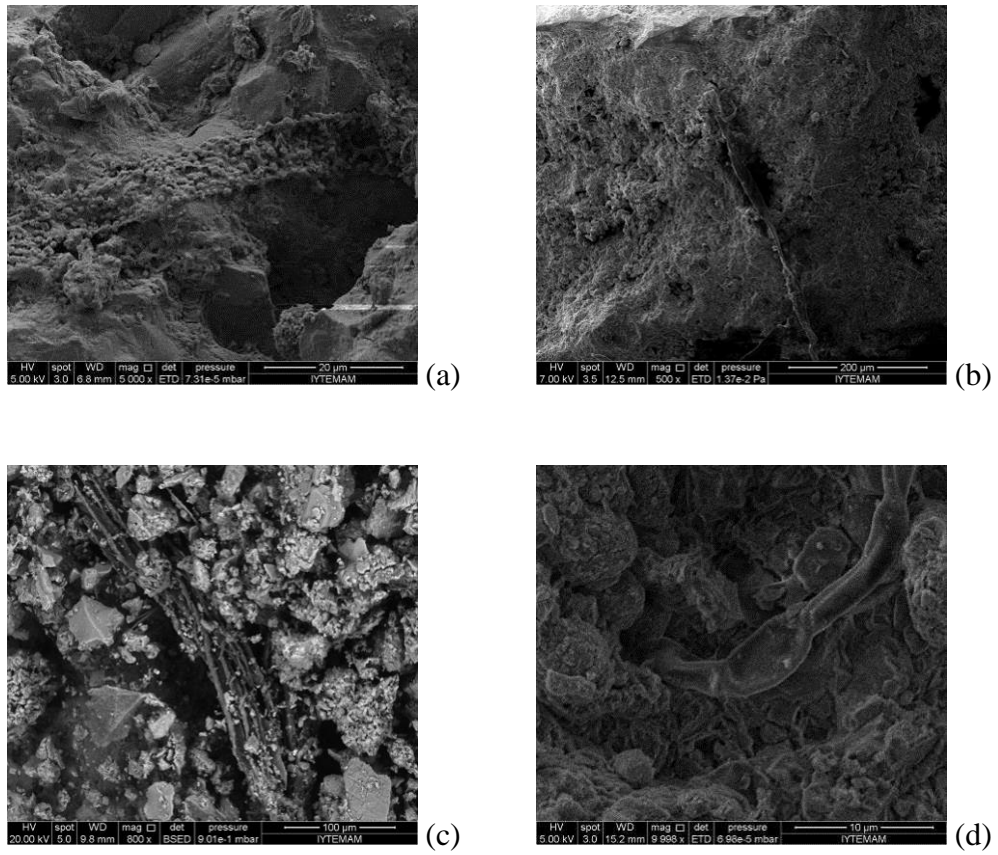


Figure 3.25. SEM images of hyphae observed on Ai2 (a), Ai3(b), As5 (c) and As8 (d)

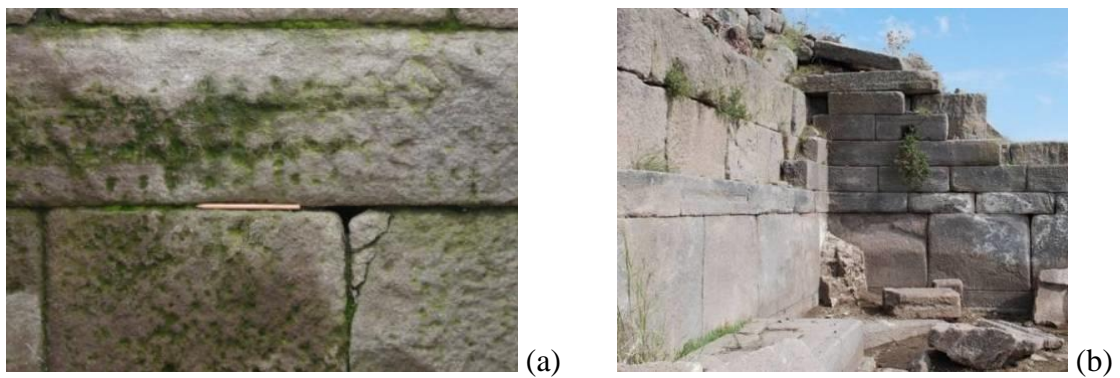


Figure 3.26. Biological forms observed on the walls of bouleuterion of Aigai (a) and stoa Assos (b)

3.3.4. Chemical Characteristics

Chemical characteristics of the interior parts and exterior surfaces of the andesite samples were determined by SEM/EDS, XRF and TGA analyses. The results of SEM/EDS and XRF analyses were also used in chemical weathering indices. In the following parts, the results of these analyses and indices will be explained.

3.3.4.1. SEM/EDS and XRF Analysis

Further sensitivity of XRF analysis than SEM/EDS analysis in the determination of chemical characteristics was mentioned before. While XRF analysis provides depth elemental characterization of the materials, SEM/EDS provides surface elemental distribution (Komatani et al. 2013). However, both analyzes used in the chemical analyzes and in the weathering indices to compare the results.

SEM/EDS and XRF analyses of the interior parts of the andesite samples show that the andesites of both Aigai and Assos were composed primarily of silicon dioxide (SiO_2), aluminum oxide (Al_2O_3) and iron oxide (Fe_2O_3). The minor elements were sodium oxide (Na_2O), potassium oxide (K_2O), magnesium oxide (MgO) and calcium oxide (CaO). The samples also contain trace amounts of titanium oxide (TiO_2) and phosphorus pentoxide (P_2O_5) (Figure 3.27, Figure 3.28, Table 3.7). The amounts of silica (SiO_2) content in both samples are in the range of 58.8 % and 67 %. As mentioned before, stones which contain 55 to 70 wt. % silica are chemically classified as intermediate igneous rocks (Howe 2001). Thus, the studied samples can be classified as intermediate igneous rocks.

With the results of XRF analysis, a total alkali-silica diagram, which depends on $\text{Na}_2\text{O}+\text{K}_2\text{O}/\text{SiO}_2$ ratio (Le Bas et al 1986), of the stones were prepared and the results were plotted on the diagram. The diagram shows that all the studied samples are in the andesite region (Figure 3.29).

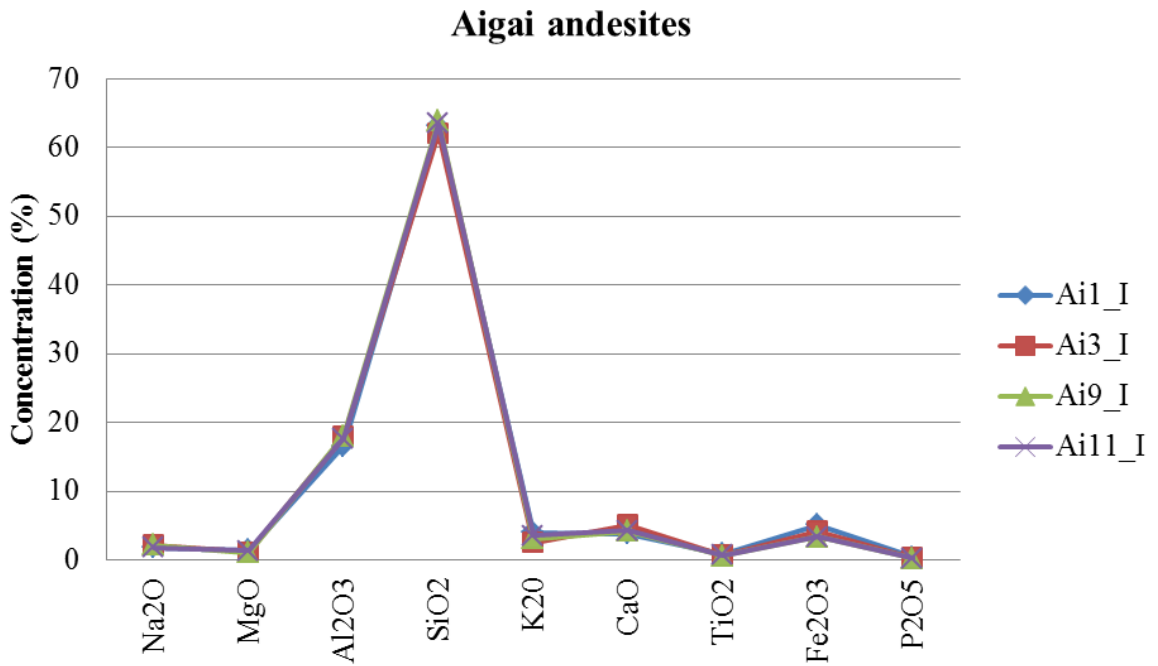


Figure 3.27. XRF results showing the elemental composition of Aigai andesites

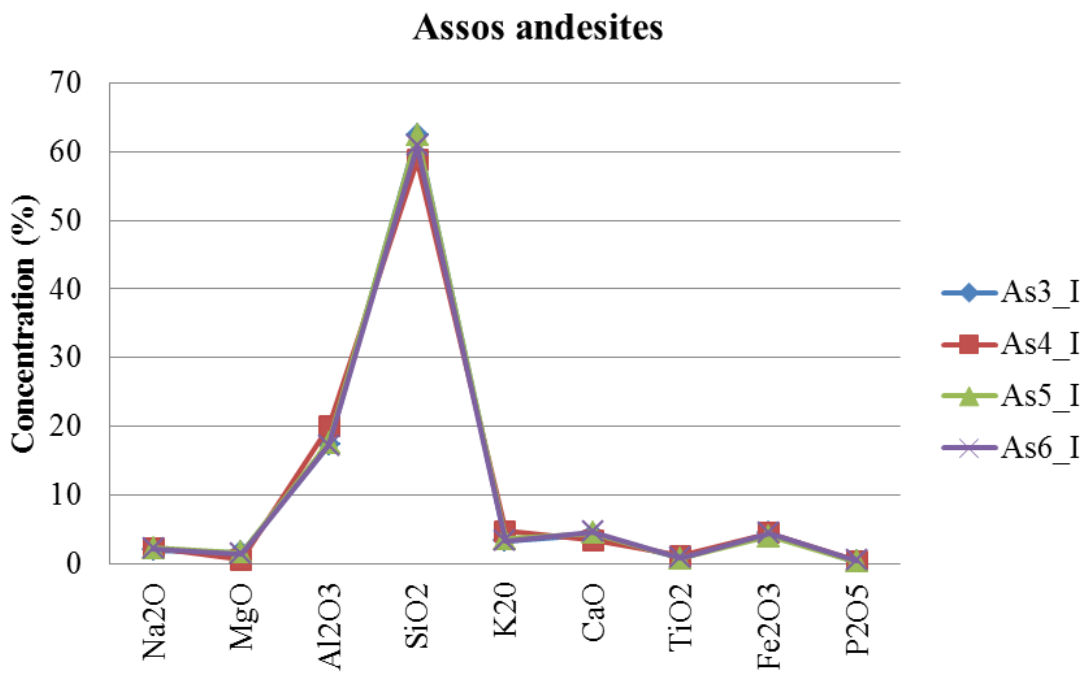


Figure 3.28. XRF results showing the elemental composition of Assos andesites

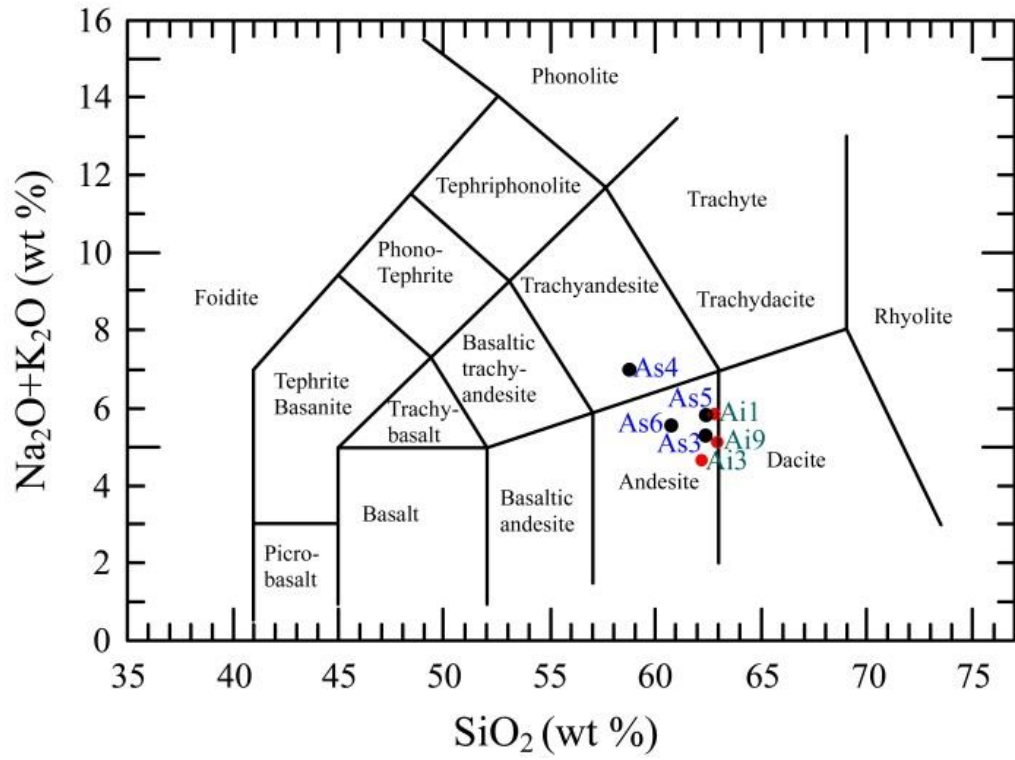


Figure 3.29. Total alkali-silica diagram of the stone samples (Le Bas et al 1986)

Table 3.7. SEM/EDS and *XRF* Results (Elemental Compositions) of Interior Parts of Aigai and Assos Andesites

		Elemental Composition																	
	Sample	SiO ₂		Na ₂ O		MgO		Al ₂ O ₃		K ₂ O		CaO		TiO ₂		FeO		P ₂ O ₅	
Aigai Andesites	Ai1_I	65.7	<i>63.2</i> ± 0.05	3.1	<i>2.8</i> ± 0.059	1.2	<i>1.4</i> ± 0.027	16.6	<i>14.6</i> ± 0.03	4.9	<i>4.0</i> ± 0.014	3.0	<i>4.8</i> ± 0.011	0.7	<i>0.9</i> ± 0.003	4.7	<i>5.1</i> ± 0.008	0.1	<i>0.4</i> ± 0.0021
	Ai2_I	63.7	–	3.4	–	1.9	–	16.7	–	4.1	–	4.3	–	0.8	–	5.1	–	0.0	–
	Ai3_I	63.7	<i>62.1</i> ± 0.05	3.4	<i>2.2</i> ± 0.061	1.9	<i>1.2</i> ± 0.026	16.7	<i>14.0</i> ± 0.03	4.1	<i>3.5</i> ± 0.012	4.3	<i>5.1</i> ± 0.013	0.8	<i>0.7</i> ± 0.0034	5.1	<i>5.2</i> ± 0.007	0.1	<i>0.4</i> ± 0.002
	Ai4_I	63.7	–	3.4	–	1.9	–	16.7	–	4.1	–	4.3	–	0.8	–	5.1	–	0.1	–
	Ai5_I	63.8	–	3.1	–	0.9	–	18.5	–	5.2	–	2.9	–	0.9	–	4.6	–	0.2	–
	Ai6_I	66.6	–	3.3	–	1.1	–	16.5	–	5.2	–	2.4	–	0.5	–	4.3	–	0.1	–
	Ai7_I	64.7	–	3.2	–	1.3	–	16.7	–	4.9	–	3.3	–	0.7	–	5.3	–	0.0	–
	Ai8_I	66.5	–	3.4	–	1.2	–	16.4	–	4.8	–	3.3	–	0.6	–	3.5	–	0.4	–
	Ai9_I	66.7	<i>63.9</i> ± 0.05	3.7	<i>2.8</i> ± 0.062	0.9	<i>1.4</i> ± 0.026	17.1	<i>14.1</i> ± 0.03	3.8	<i>4.1</i> ± 0.013	3.7	<i>4.1</i> ± 0.012	0.4	<i>0.6</i> ± 0.0032	3.4	<i>3.4</i> ± 0.007	0.2	<i>0.3</i> ± 0.0017
	Ai10_I	66.0	–	3.3	–	1.5	–	15.5	–	5.5	–	3.2	–	0.6	–	4.2	–	0.3	–
	Ai11_I	66.7	<i>63.5</i> ± 0.05	3.2	<i>2.8</i> ± 0.061	0.7	<i>1.3</i> ± 0.028	17.5	<i>14.7</i> ± 0.03	4.6	<i>3.6</i> ± 0.014	3.8	<i>5.3</i> ± 0.012	0.5	<i>0.7</i> ± 0.0034	2.9	<i>4.3</i> ± 0.007	0.1	<i>0.3</i> ± 0.0018
Assos Andesites	As1_I	64.8	–	3.9	–	1.5	–	16.9	–	4.6	–	3.6	–	0.8	–	3.1	–	0.1	–
	As2_I	65.4	–	3.7	–	1.1	–	17.2	–	4.6	–	3.3	–	0.6	–	3.1	–	0.1	–
	As3_I	65.7	<i>62.4</i> ± 0.05	4.4	<i>2.8</i> ± 0.059	0.8	<i>1.6</i> ± 0.028	18.4	<i>14.4</i> ± 0.03	4.6	<i>4.6</i> ± 0.013	2.9	<i>4.3</i> ± 0.012	0.3	<i>0.8</i> ± 0.0037	2.5	<i>4.4</i> ± 0.008	0.2	<i>0.3</i> ± 0.0018
	As4_I	62.6	<i>58.8</i> ± 0.05	3.8	<i>2.3</i> ± 0.061	0.7	<i>0.6</i> ± 0.022	20.7	<i>20.0</i> ± 0.03	5.1	<i>4.7</i> ± 0.015	2.9	<i>3.4</i> ± 0.011	0.2	<i>1.2</i> ± 0.004	3.5	<i>4.5</i> ± 0.008	0.3	<i>0.3</i> ± 0.0018
	As5_I	65.1	<i>62.4</i> ± 0.05	3.9	<i>2.5</i> ± 0.065	0.9	<i>1.6</i> ± 0.029	17.8	<i>14.6</i> ± 0.03	4.8	<i>4.6</i> ± 0.015	4.0	<i>4.4</i> ± 0.013	0.4	<i>0.8</i> ± 0.0039	2.9	<i>3.9</i> ± 0.008	0.3	<i>0.3</i> ± 0.0019
	As6_I	63.8	<i>60.8</i> ± 0.05	4.1	<i>2.2</i> ± 0.06	1.2	<i>1.4</i> ± 0.027	17.6	<i>14.3</i> ± 0.03	3.9	<i>4.4</i> ± 0.014	4.4	<i>4.7</i> ± 0.012	0.7	<i>0.8</i> ± 0.0037	3.7	<i>4.5</i> ± 0.008	0.5	<i>0.5</i> ± 0.0023
	As7_I	65.3	–	3.4	–	0.9	–	18.5	–	4.3	–	3.3	–	0.5	–	3.6	–	0.1	–
	As8_I	64.8	–	4.2	–	1.1	–	17.9	–	3.8	–	4.2	–	0.5	–	3.5	–	0.1	–

For further characterization of the chemical characteristics and the possible differences of the studied samples, different chemical diagrams were used with the results of elemental analyses. First, they were separated considering their total alkali contents. As many igneous rocks, total alkali-silica diagram of the samples reveal that all the studied andesites are in the area of sub-alkaline (Figure 3.30) (Irvine and Baragar 1971).

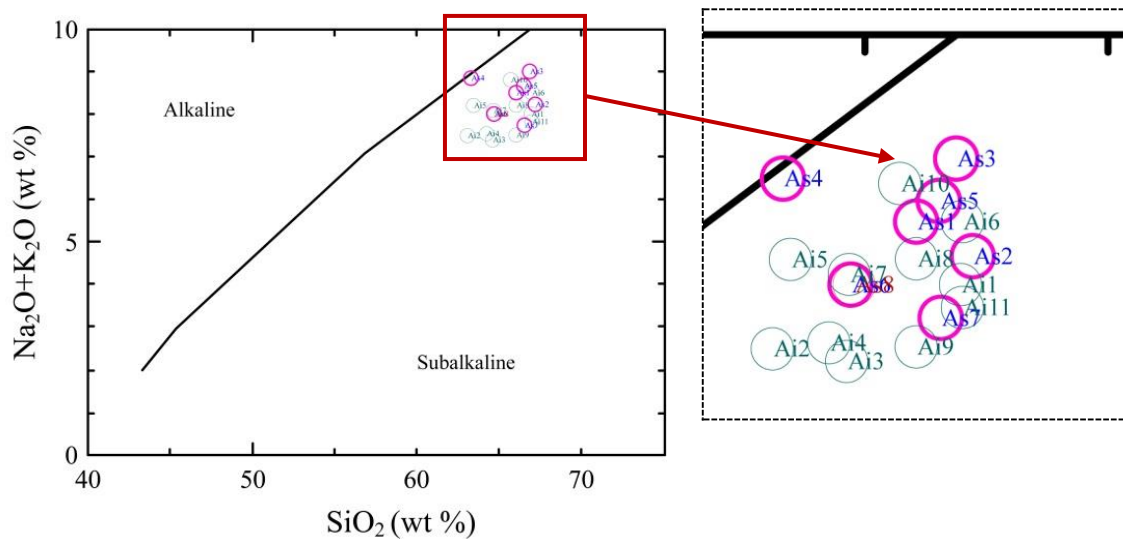


Figure 3.30. Total alkali-silica diagram of the stone samples (Source: Irvine and Baragar 1971)

Sub-alkaline rocks chemically have two main series as tholeiitic (iron rich) and calc-alkaline (calcium rich) rocks (Miyashiro 1974, Le Maitre 1989). With the results of SEM/EDS analysis and based on their SiO_2 vs FeO^*/MgO ratio, andesite samples were separated as tholeiitic and calc-alkaline ones. The results of this classification reveal that all the samples taken from Aigai and Assos contain both tholeiitic and calc-alkaline stones. As1, As2, As3, As5, As7, Ai1, Ai2, Ai3, Ai7, Ai8, Ai9, Ai10 and Ai11 are in the area of calc-alkaline and As4, As6, As8, Ai4, Ai5 and Ai6 are in the area of tholeiitic area (Miyashiro 1974, Le Maitre 1989) (Figure 3.31).

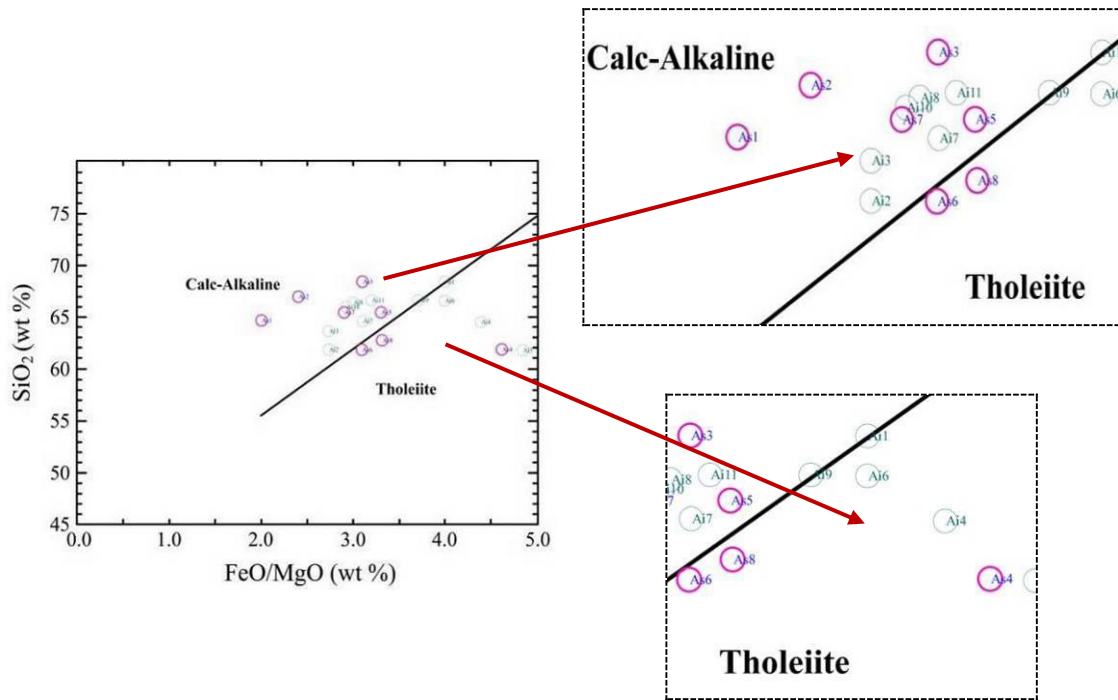


Figure 3.31. SiO_2 - FeO^*/MgO diagram of the stone samples
(Source: Miyashiro 1974, Le Maitre 1989)

The previous studies about the geological characteristics of the study areas were mentioned before (Borsi et al. 1972, Öngür 1973, Akyürek ve Sosyal 1983, Ercan et al. 1995, Genç 1998, Akay and Erdoğan 2004, Özkaymak et al. 2013, Seghedi et al. 2015). In these studies, chemical and petrographic characteristics of the local stones were stated and chemical diagrams, which were also used in this study, were used.

Besides geological mapping of the regions where the studied archaeological sites are located, elemental characteristics of the Yuntdağ andesites were studied by Akay and Erdoğan (2004) and Behram andesites by Ercan et al. 1995 with the stone samples taken from the regions. Then the results were plotted in the chemical diagrams (Table 3.8, Table 3.9).

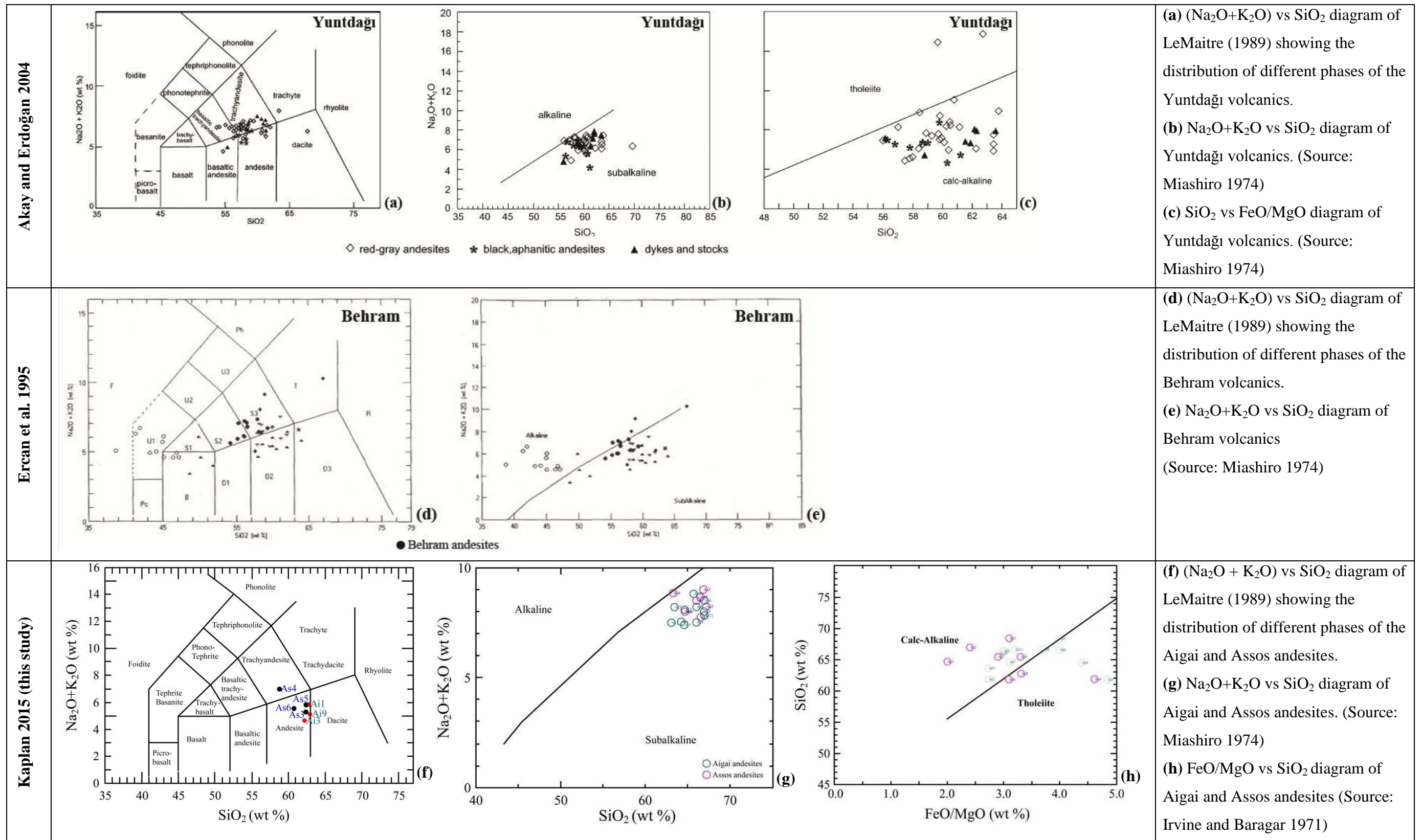
When the chemical characteristics of the Yuntdağ andesites, studied by Akay and Erdoğan (2004) and Behram andesites, studied by Ercan et al. (1995), are compared with the XRF results of this study, similar results with the Aigai and Assos andesites can be seen (Table 3.8). Small differences in the results can be resulted from the location of the samples, because the samples used in the studies of Akay and Erdoğan (2004) and Ercan et al. (1995) were collected from different parts of the whole volcanic units.

As having similar elemental composition results, the chemical diagrams prepared by Akay and Erdoğan (2004) for Yuntdağ andesites and Ercan et al. (1995) for Behram andesites show similarities with the diagrams which are prepared by the XRF and SEM/EDS for Aigai and Assos andesites (Table 3.9). In the diagrams, all the samples are in andesite region and sub-alkaline region and Aigai and Yuntdağ andesites have both calc-alkaline and tholeiitic characteristics (Table 3.9). Further comparison of the results of the chemical characteristics of Behram and Assos andesites could not be done because of the lack of SiO₂ vs FeO/MgO diagram in the study of Ercan et al. (1995).

Table 3.8. Major element contents of Yuntdağ (Source: Akay and Erdoğan 2004), Behram (Source: Ercan et al. 1995), Aigai and Assos andesites (XRF results of the study)

Yuntdağ Andesites	Elemental Composition								
Samples	SiO₂	Na₂O	MgO	Al₂O₃	K₂O	CaO	TiO₂	FeO	P₂O₅
1	63.4	3.5	2.4	15.9	3.0	4.8	0.6	4.5	0.1
2	59.7	3.4	2.8	16.8	2.7	5.8	0.8	5.3	0.2
3	62.7	3.7	1.0	17.4	2.5	5.2	0.6	4.3	0.2
4	62.2	3.3	2.7	15.5	2.8	4.9	0.7	4.1	0.2
5	63.4	3.1	2.4	16.0	3.6	3.7	0.6	4.0	0.2
6	63.4	3.1	2.9	15.2	2.8	5.2	0.6	4.3	0.1
7	60.4	3.3	3.2	16.6	2.2	6.3	0.6	4.8	0.1
8	60.3	3.5	2.3	18.1	2.4	6.0	0.7	4.7	0.2
9	61.2	3.1	4.0	15.0	2.6	5.8	0.5	5.4	0.2
10	60.3	2.8	4.8	14.3	2.8	6.0	0.6	5.7	0.2
11	61.6	3.2	2.4	16.0	3.1	4.1	0.6	4.1	0.2
<i>Aigai Andesites</i>									
<i>Ai1_I</i>	<i>63.2</i>	<i>2.8</i>	<i>1.4</i>	<i>14.6</i>	<i>4.0</i>	<i>4.8</i>	<i>0.9</i>	<i>5.1</i>	<i>0.4</i>
<i>Ai3_I</i>	<i>62.1</i>	<i>2.2</i>	<i>1.2</i>	<i>14.0</i>	<i>3.5</i>	<i>5.1</i>	<i>0.7</i>	<i>5.2</i>	<i>0.4</i>
<i>Ai9_I</i>	<i>63.9</i>	<i>2.8</i>	<i>1.4</i>	<i>14.1</i>	<i>4.1</i>	<i>4.1</i>	<i>0.6</i>	<i>3.4</i>	<i>0.3</i>
<i>Ai11_I</i>	<i>63.5</i>	<i>2.8</i>	<i>1.3</i>	<i>14.7</i>	<i>3.6</i>	<i>4.3</i>	<i>0.7</i>	<i>4.3</i>	<i>0.3</i>
Behram Andesites	Elemental Composition								
Samples	SiO₂	Na₂O	MgO	Al₂O₃	K₂O	CaO	TiO₂	FeO	P₂O₅
1	56.0	2.8	3.0	16.0	3.3	6.6	1.1	7.7	0.3
2	56.5	3.4	2.2	17.2	3.3	6.3	1.0	7.3	0.3
3	58.1	3.0	1.8	17.1	3.4	6.0	1.1	7.9	0.4
<i>Assos Andesites</i>									
<i>As3_I</i>	<i>62.4</i>	<i>2.8</i>	<i>1.6</i>	<i>14.4</i>	<i>4.6</i>	<i>4.3</i>	<i>0.8</i>	<i>4.4</i>	<i>0.3</i>
<i>As4_I</i>	<i>58.8</i>	<i>2.3</i>	<i>0.6</i>	<i>20.0</i>	<i>4.7</i>	<i>3.4</i>	<i>1.2</i>	<i>4.5</i>	<i>0.3</i>
<i>As5_I</i>	<i>62.4</i>	<i>2.5</i>	<i>1.6</i>	<i>14.6</i>	<i>4.6</i>	<i>4.4</i>	<i>0.8</i>	<i>3.9</i>	<i>0.3</i>
<i>As6_I</i>	<i>60.8</i>	<i>2.2</i>	<i>1.4</i>	<i>14.3</i>	<i>4.4</i>	<i>4.7</i>	<i>0.8</i>	<i>4.5</i>	<i>0.5</i>

Table 3.9. Chemical Diagrams of Yuntdağ volcanics (Source: Akay and Erdoğan 2004), Behram volcanics (Source: Ercan et al. 1995) and Aigai and Assos andesites



3.3.4.2. Chemical Weathering Indices

Chemical deterioration of the andesites was determined by using chemical weathering indices with SEM/EDS and XRF results of interior and exterior parts of the andesites and comparison of the results (Table 3.5, Table 3.8). Two weathering indices of Chemical Index of Alteration (CIA) (Nesbitt and Young 1982) and the Weathering Index of Parker (WIP) (Parker 1970, Hamdan and Burnham 1996) were used and the results were compared.

In CIA analysis;

$$CIA = \left(\frac{Al_2O_3}{Al_2O_3 + Na_2O + K_2O + CaO} \right) \times 100$$

and in WIP analysis;

$$WIP = ((2Na_2O/0.35) + (MgO/0.9) + (2K_2O/0.25) + (CaO/0.7)) \times 100$$

formulas were used (Table 3.11).

When the results of SEM/EDS and XRF analyses are compared for both interior and exterior parts of the andesites, less amounts of silicon dioxide (SiO₂), aluminum oxide (Al₂O₃) and sodium oxide (Na₂O) contents and more amounts of iron oxide (Fe₂O₃), potassium oxide (K₂O), magnesium oxide (MgO), calcium oxide (CaO), titanium oxide (TiO₂) and phosphorus pentoxide (P₂O₅) contents were determined in XRF analyzes apart from some exceptional elements in the exterior parts (Table 3.7, Table 3.10).

When the average results of WIP and CIA analyses are compared for interior and exterior parts of the andesites, decrease in WIP values and increase in CIA values in the exterior parts of the stones can be seen (Table 3.11). However, there are only small differences between the interior and exterior results of both WIP and CIA analyses. Although decrease in WIP values and increase in CIA values in the exterior parts of the andesites can be seen in both analyzes, the differences between the values for interior and exterior parts of the andesites acquired with SEM/EDS values are less than the ones acquired with XRF values.

As mentioned before, smaller WIP and higher CIA values indicate higher chemical deterioration (Parker 1970, Nesbitt and Young 1982, Fedo et al. 1995, Hamdan and Burnham 1996, Bahlburg and Dobrzinski 2009) and for CIA values, fresh igneous rocks have the values between 30 and 55 according to their chemical characteristics (Table 1.4) (Nesbitt and Young 1982, Fedo et al. 1995, Bahlburg and Dobrzinski 2009). As a result, as the other experimental methods which were explained before, the results of WIP and CIA analyses of the andesites also show the chemical deterioration of exterior parts of the andesites although the differences between the values are small. Small differences of the results of the analyses between the interior parts and exterior surfaces of the andesites also show slight degree of chemical deterioration of the andesites.

Table 3.10. SEM/EDS and *XRF* Results (Elemental Compositions) of Exterior Parts of Aigai and Assos Andesites

		Elemental Composition																	
	Sample	SiO ₂		Na ₂ O		MgO		Al ₂ O ₃		K ₂ O		CaO		TiO ₂		FeO		P ₂ O ₅	
Aigai Andesites and Soils	Ai1_E	62.3	<i>63.0</i> ± 0.06	2.5	<i>2.4</i> ± 0.11	1.4	<i>1.0</i> ± 0.038	17.5	<i>16.0</i> ± 0.04	4.3	<i>4.2</i> ± 0.022	3.2	<i>3.3</i> ± 0.015	0.8	<i>0.7</i> ± 0.0045	7.2	<i>4.3</i> ± 0.01	0.6	<i>0.3</i> ± 0.0027
	Ai2_E	61.0	<i>59.3</i> ± 0.06	2.7	<i>2.9</i> ± 0.11	2.0	<i>1.7</i> ± 0.043	14.5	<i>15.0</i> ± 0.04	5.0	<i>3.7</i> ± 0.019	5.8	<i>4.9</i> ± 0.017	1.0	<i>0.8</i> ± 0.0048	7.3	<i>4.8</i> ± 0.01	0.6	<i>0.6</i> ± 0.0034
	Ai3_E	64.7	–	3.8	–	1.1	–	17.3	–	3.5	–	4.5	–	0.4	–	4.2	–	0.5	–
	Ai4_E	62.7	–	3.3	–	1.3	–	16.4	–	3.3	–	7.0	–	0.7	–	4.9	–	0.5	–
	Ai5_E	65.3	<i>62.0</i> ± 0.06	3.0	<i>3.0</i> ± 0.13	1.4	<i>1.1</i> ± 0.042	17.3	<i>16.6</i> ± 0.05	4.7	<i>4.2</i> ± 0.023	3.7	<i>3.1</i> ± 0.015	0.7	<i>0.8</i> ± 0.0053	4.0	<i>5.0</i> ± 0.011	0.6	<i>0.4</i> ± 0.0031
	Ai6_E	65.8	–	3.2	–	1.6	–	16.3	–	4.4	–	2.9	–	0.7	–	4.6	–	0.4	–
	Ai7_E	64.2	–	2.9	–	1.2	–	16.6	–	5.2	–	3.2	–	0.7	–	5.4	–	0.7	–
	Ai8_E	64.9	–	2.8	–	1.3	–	16.2	–	5.6	–	3.2	–	0.8	–	4.7	–	0.5	–
	Ai9_E	63.4	–	3.2	–	2.3	–	15.7	–	3.9	–	6.4	–	0.4	–	3.5	–	0.9	–
	Ai10_E	65.2	–	2.8	–	1.7	–	15.9	–	5.1	–	3.1	–	0.7	–	5.0	–	0.3	–
	Ai11_E	64.3	–	3.2	–	1.1	–	17.8	–	3.7	–	5.2	–	0.6	–	3.5	–	0.5	–
Assos Andesites and Soil	As1_E	63.9	–	3.4	–	1.8	–	16.7	–	4.7	–	4.6	–	0.7	–	3.6	–	0.5	–
	As2_E	64.5	–	3.3	–	1.8	–	17.1	–	4.3	–	3.4	–	0.6	–	4.3	–	0.6	–
	As3_E	64.0	<i>61.1</i> ± 0.06	3.6	<i>2.8</i> ± 0.11	1.8	<i>1.7</i> ± 0.044	17.3	<i>16.9</i> ± 0.04	3.9	<i>3.2</i> ± 0.019	3.6	<i>4.0</i> ± 0.015	0.5	<i>0.8</i> ± 0.0049	2.9	<i>4.6</i> ± 0.010	0.2	<i>0.4</i> ± 0.0028
	As4_E	63.0	<i>58.7</i> ± 0.05	4.0	<i>2.7</i> ± 0.099	1.1	<i>1.1</i> ± 0.036	19.6	<i>18.4</i> ± 0.04	4.4	<i>4.0</i> ± 0.019	3.0	<i>3.2</i> ± 0.013	0.3	<i>1.0</i> ± 0.0049	3.8	<i>4.1</i> ± 0.009	0.4	<i>0.3</i> ± 0.0023
	As5_E	63.5	<i>61.1</i> ± 0.06	3.3	<i>2.9</i> ± 0.11	1.7	<i>1.8</i> ± 0.044	16.9	<i>16.9</i> ± 0.04	4.5	<i>3.3</i> ± 0.019	3.8	<i>4.0</i> ± 0.015	0.4	<i>0.8</i> ± 0.0048	4.9	<i>4.2</i> ± 0.01	0.6	<i>0.4</i> ± 0.0029
	As6_E	64.6	<i>54.1</i> ± 0.1	3.6	<i>6.9</i> ± 0.36	1.9	<i>2.2</i> ± 0.095	16.7	<i>16.4</i> ± 0.08	4.0	<i>2.4</i> ± 0.046	3.7	<i>4.4</i> ± 0.03	0.8	<i>0.8</i> ± 0.0093	4.7	<i>4.8</i> ± 0.02	0.2	<i>0.3</i> ± 0.006
	As7_E	64.1	–	3.1	–	1.2	–	18.0	–	4.5	–	3.7	–	0.4	–	4.4	–	0.2	–
	As8_E	65.5	–	4.1	–	1.8	–	17.0	–	3.7	–	3.3	–	0.5	–	3.9	–	0.3	–

Table 3.11. CIA and WIP Results for Aigai and Assos Andesites based on XRF Results

		Interior Parts			Exterior Surfaces	
		Sample	CIA	WIP	CIA	WIP
According to XRF Results	Aigai Andesites	Ai1_I	55.50	56.67	61.61	53.28
		Ai3_I	56.55	55.16	56.58	48.89
		Ai9_I	55.95	56.41	61.76	56.27
		Ai11_I	55.65	53.66	–	–
		Average	55.91	55.47	59.98	52.81
	Assos Andesites	As3_I	55.08	60.75	62.71	49.42
		As4_I	65.16	56.60	65.66	52.66
		As5_I	55.98	58.84	62.30	51.02
		As6_I	56.01	55.64	54.68	66.71
		Average	58.05	57.95	61.33	54.95
According to SEM/EDS Results	Aigai Andesites	Ai1_I	60.1	62.8	63.6	55.1
		Ai2_I	58.5	60.5	56.9	65.4
		Ai3_I	58.5	60.5	59.7	56.7
		Ai4_I	58.5	60.5	54.8	56.3
		Ai5_I	62.1	64.6	61.8	60.5
		Ai6_I	60.2	65.4	60.9	59.2
		Ai7_I	56.4	63.5	59.7	63.6
		Ai8_I	58.8	64.1	58.2	66.8
		Ai9_I	59.3	58.1	55.8	61.0
		Ai10_I	56.3	69.2	59.1	63.0
		Ai11_I	60.3	61.2	59.3	57.0
		Average	59.00	62.76	59.07	60.42
	Assos Andesites	As1_I	58.4	65.9	56.7	65.6
		As2_I	59.7	64.1	60.8	60.0
		As3_I	60.8	66.9	60.9	58.9
		As4_I	63.2	68.0	63.6	63.6
		As5_I	58.4	67.2	59.3	62.2
		As6_I	58.7	62.0	59.6	60.0
		As7_I	62.6	59.7	61.4	60.3
		As8_EI	59.6	61.3	60.5	59.7
Average	60.18	64.39	60.35	61.29		

3.3.4.3. TGA Analyses

Thermal analyses of the andesite samples were carried out by TG/DTA and furnace analyses. As previously mentioned, in the thermal analyses of the samples, weight loss at 103°C is due to the loss of adsorbed water and weight loss at 103 to 550°C is mainly due to the loss of organic materials and dihydroxylation of some types of clays (Tylecote 1979). The weight losses of the interior parts and exterior surfaces and clay fractions of the andesites are given in Figure 3.32 and Figure 3.33. When the weight losses of interior and exterior parts of the andesites and clay fractions are compared, more weight losses at 103°C and between the 103-550°C heat intervals in the exterior parts of the andesites and clay fractions of the andesites can be seen. Results of the thermal analyses show that although the weight losses of interior parts of the andesites between 103°C to 550°C heat intervals are between 0.642-1.750 % (Figure 3.32, Appendix C), they increase to 6.542 % for the exterior surfaces of the andesites and 7.590 % for the clay fractions of the andesites (Figure 3.33, Appendix C). This is resulted from presence of clays in exterior parts and in the cracks of the andesites and water holding capacity of the clays.

As the presence of clays, the presence of organic materials in the stone structure is one of the most important factors in the deterioration of the stones and generally originates from biological sources (Doehne and Price 2010). The amount of organic materials and carbonate content in the stone structures may also be useful in the evaluation of the deterioration of the andesites during burial. Thus, their presence in the andesite structures and soil samples was analyzed.

The analysis for the average values of the organic material proportions shows low amounts of organic material values for both Aigai and Assos andesites. Organic material content is lower than 2.62 % and 2.24 % for Aigai and Assos andesites respectively (Figure 3.34, Appendix C). TGA curves of the stone samples show similar weight losses on the whole. The weight losses of the first and second period samples within a temperature range from 25°C to 550°C are 3.27, 1.71 and 2.74 % respectively for the exterior parts of Aigai andesites and 3.51, 3.1 and 4.8 % for the exterior parts of Assos andesites (Figure 3.35, Figure 3.36, Appendix C).

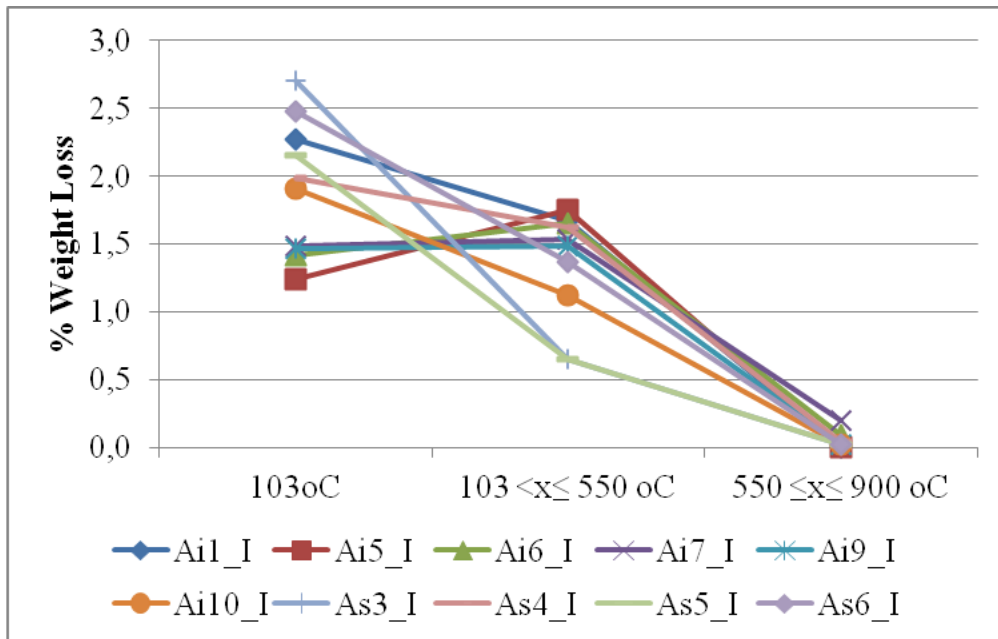


Figure 3.32. TGA results of interior parts of the andesite samples

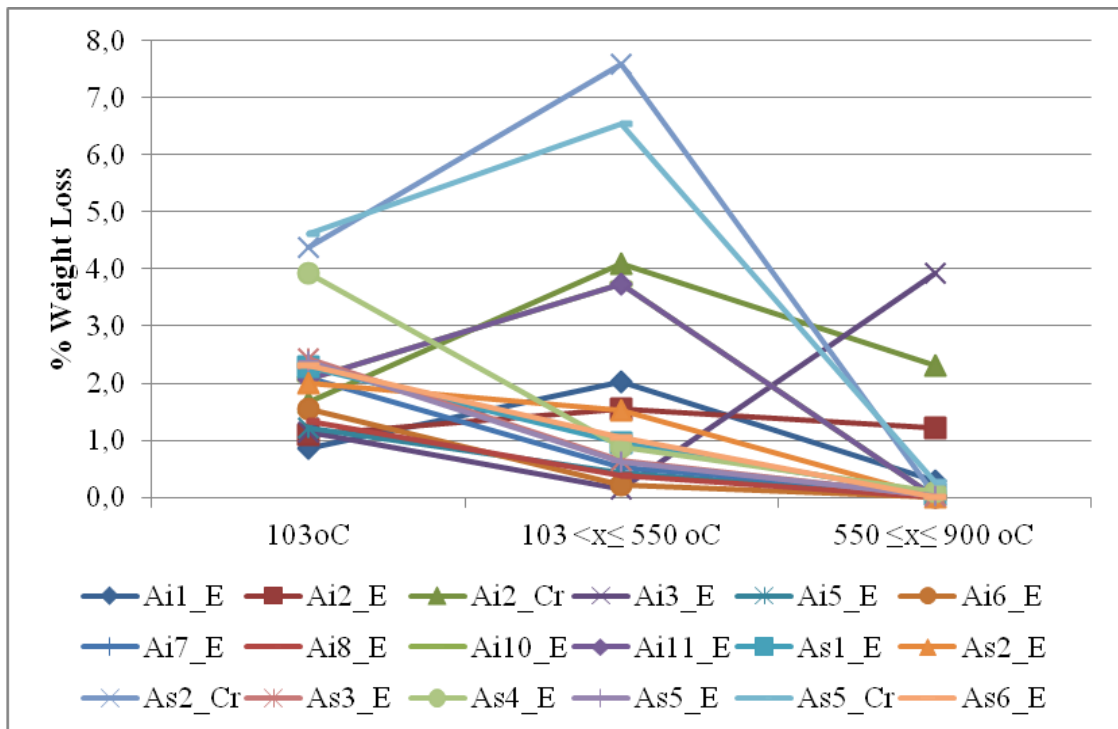


Figure 3.33. TGA results of exterior parts and clay fractions of the andesite samples

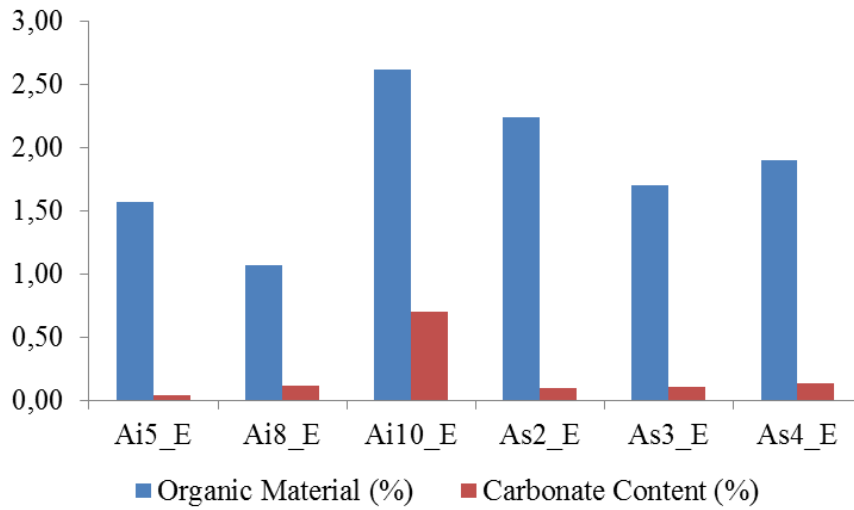


Figure 3.34. % Organic material and carbonate contents of andesite samples of Aigai and Assos

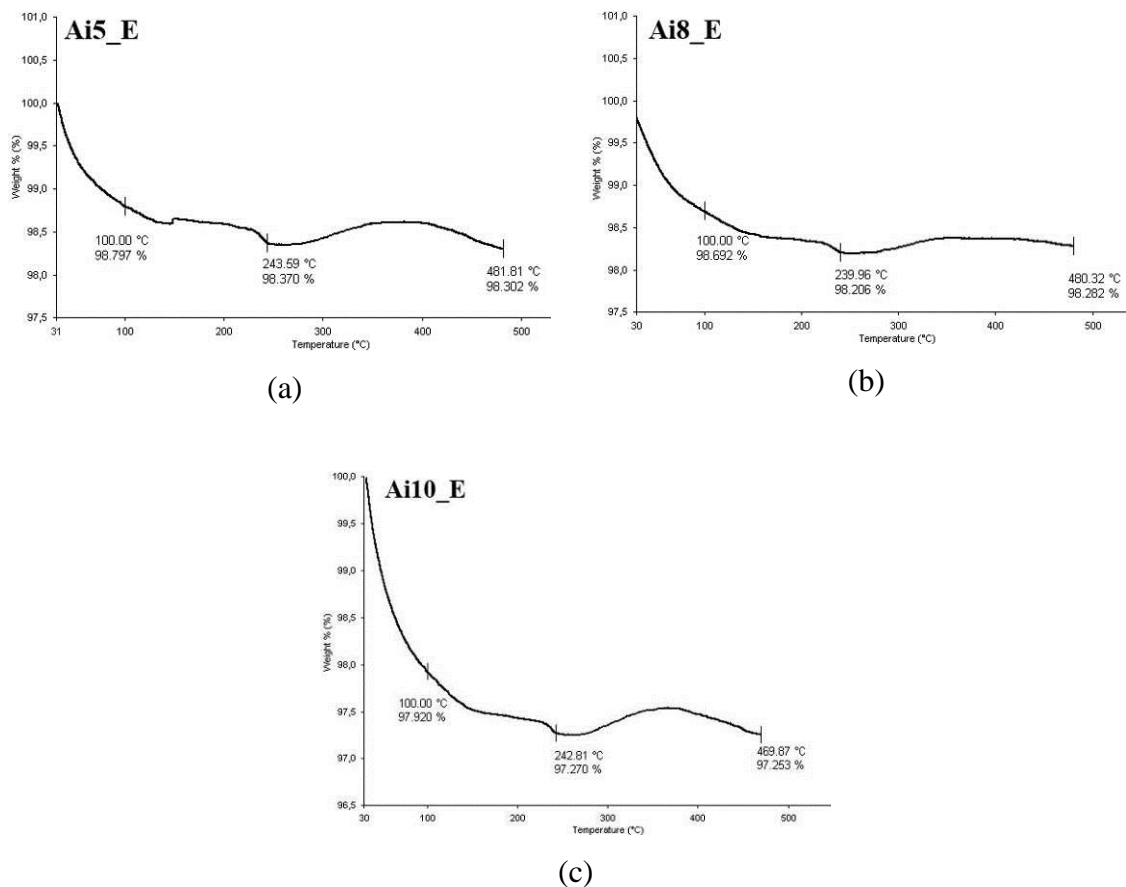


Figure 3.35. TGA graphs of exterior surfaces of Ai5 (a), Ai8 (b) and Ai10

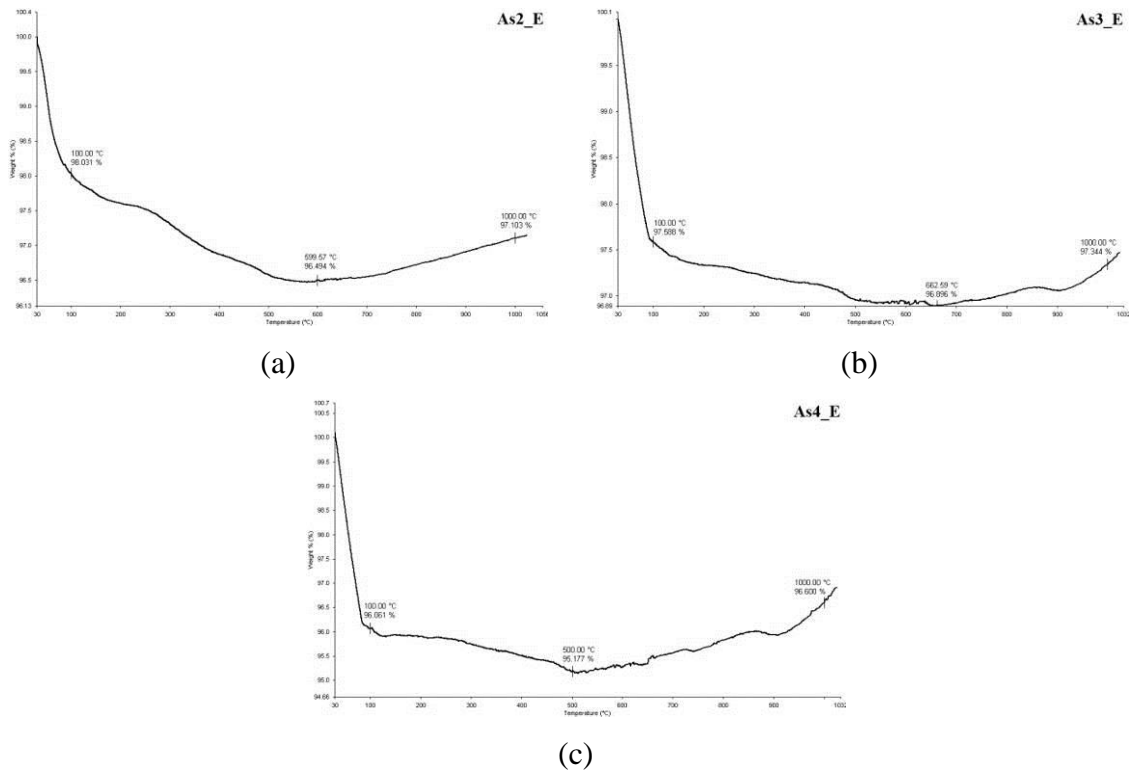


Figure 3.36. TGA graphs of exterior surfaces of As2 (a), As3 (b) and As4 (c)

The presence of organic materials was observed on the andesite surfaces by SEM analysis (Figure 3.37, Figure 3.38). Thus, although the amounts of organic materials in both Aigai and Assos andesites are low, their presence may have affected the deterioration of the andesites. Because they promote chemical deterioration by increasing acidity on the andesite surfaces and also physical deterioration by hyphae penetration through the voids of the stones (Chen et al. 1999, Cronyn 2002, Mortatti and Probst 2003)

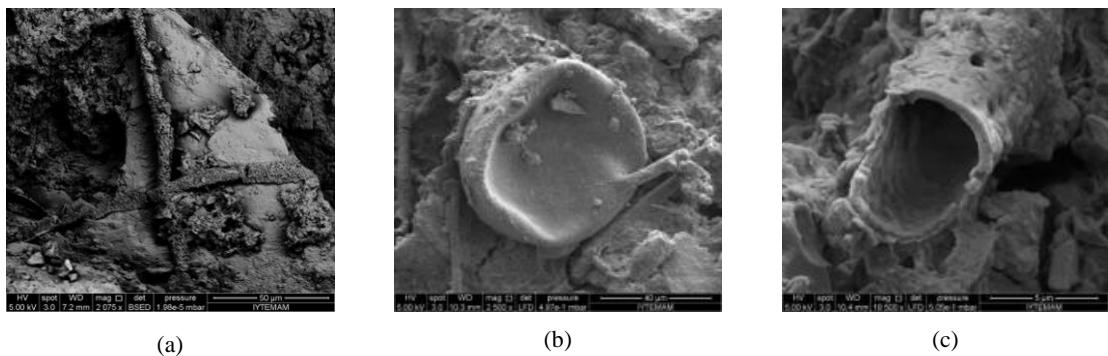


Figure 3.37. SEM images of organic materials on the surface of Ai2 (a) and Ai5 (b) (c)

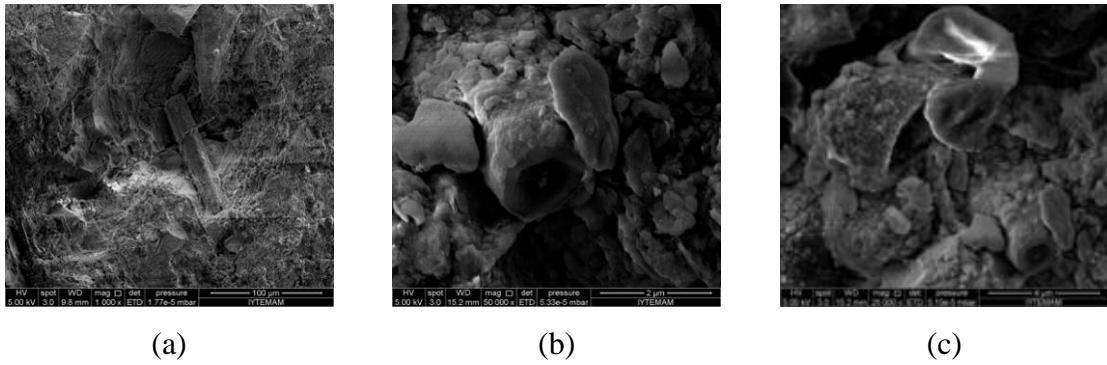


Figure 3.38. SEM images of organic materials on the surface of As7 (a) and As8 (b) (c)

As the presence of organic materials, carbonate contents of the andesites and soils were also analyzed by carbonate content analysis and TGA analysis. As mentioned above, final stage observed in the range of 550-1000 °C in TGA curves of the samples is expected for the decomposition of carbonate.

Both carbonate content and TGA analysis of the andesites which do not have white deposits show trace amounts of carbonate content, ranging between 0.04-0.7 % (Figure 3.35, Figure 3.36). However, exterior parts of the andesites those have white depositions, show higher amounts of carbonate content, which will be explained in the following parts.

3.3.5. Soluble Salt Contents

Percent soluble salts in soil and andesite samples were determined by ion chromatography (IC) in order to evaluate the possible deterioration problems of andesites and possible effects of being near seashore in Assos archaeological site (Doehne and Price 2010).

As mentioned before, soil samples of Aigai and Assos contain trace amounts of soluble salts (Figure 3.6, Appendix A). The results of the IC analyses for andesite samples from Aigai and Assos archaeological sites also contain trace amounts of soluble salts (Figure 3.39, Appendix D). When the results are compared for soil and stone samples, soil samples contain more nitrate and phosphate than the andesites as expected (Figure 3.6, Figure 3.39). Because they are generally produced by the organic decomposition of the materials and by animal excrements (ICCROM 2015). Although

Assos is a coastal archaeological site, soil samples collected from Assos contain trace amounts of soluble salts either. Thus, the results of the analyses show that the soluble salts are less effective in the deterioration of buried Aigai and Assos andesites.

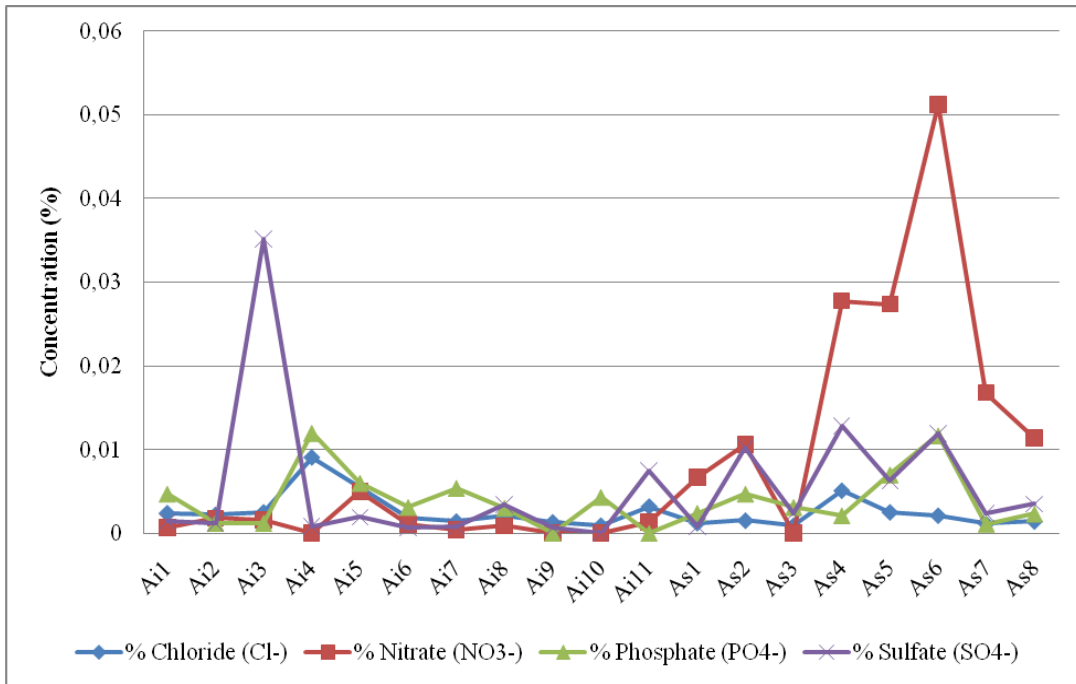


Figure 3.39. % Soluble salt contents of the andesite samples

3.4. Characteristics of Deposits Observed on the Andesites

In the following parts, mineralogical, microstructural, and chemical characteristics of the white and orange deposits observed on the andesite surfaces are described.

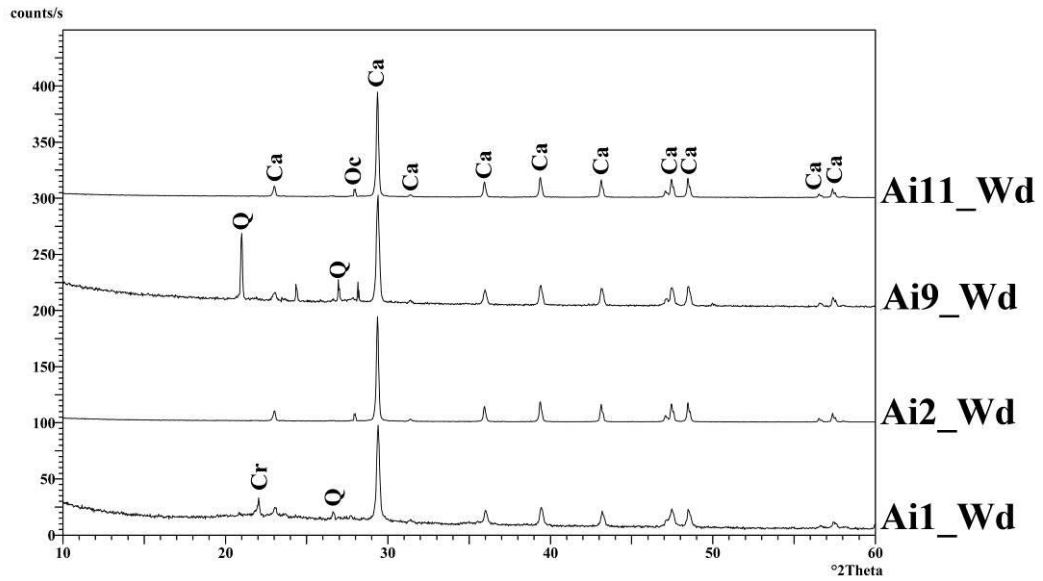
3.4.1. Characteristics of White Deposits

White depositions, which can not be seen on exposed standing stone surfaces, was observed on some newly excavated andesites (Ai1, 2, 9, 11, As1, 2, 7). In the following parts, mineralogical, chemical and microstructural characteristics of the white deposits are explained and their formation is discussed. In addition to characteristics of white deposits, the presence of the fresh-water diatoms observed in the white deposits of Aigai andesites are mentioned.

3.4.1.1. Mineralogical Characteristics

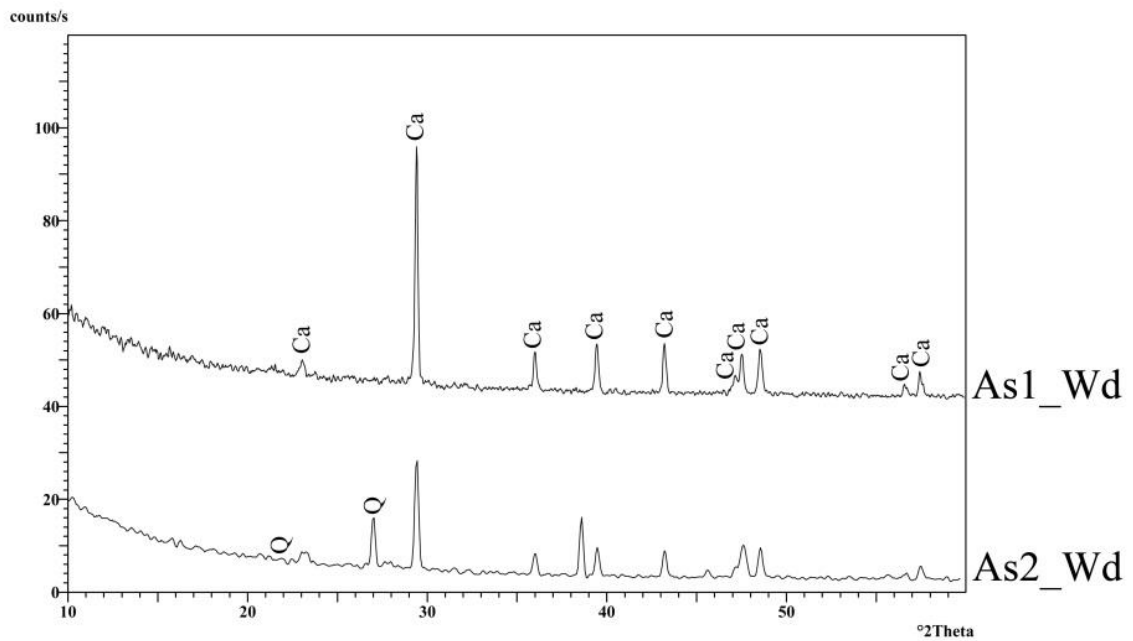
Mineralogical compositions of the white depositions were determined by XRD and FT-IR analyzes. XRD analysis of the white deposits show that they are mostly composed of calcium carbonate (CaCO_3) (Figure 3.40, Figure 3.41). Supporting the results of XRD analyses, C-O stretching and bending bands around 1435 cm^{-1} and 873 cm^{-1} in FT-IR spectra of the deposits also show that the deposits are composed of calcium carbonate (Figure 3.42, Figure 3.43).

Besides the presence of calcium carbonate, Si-O stretching and bending bands around 470 cm^{-1} , 1102 cm^{-1} and 1102 cm^{-1} and O-H stretching bands around 3440 cm^{-1} show the presence of silica minerals (Figure 3.42, Figure 3.43).



Ca: Calcite (72-1937), Cr: Cristoballite (82-1403), Q: Quartz (83-2468)

Figure 3.40. XRD pattern of white deposits of Aigai



Ca: Calcite (72-1937), Q: Quartz (83-2468)

Figure 3.41. XRD pattern of white deposits of Assos

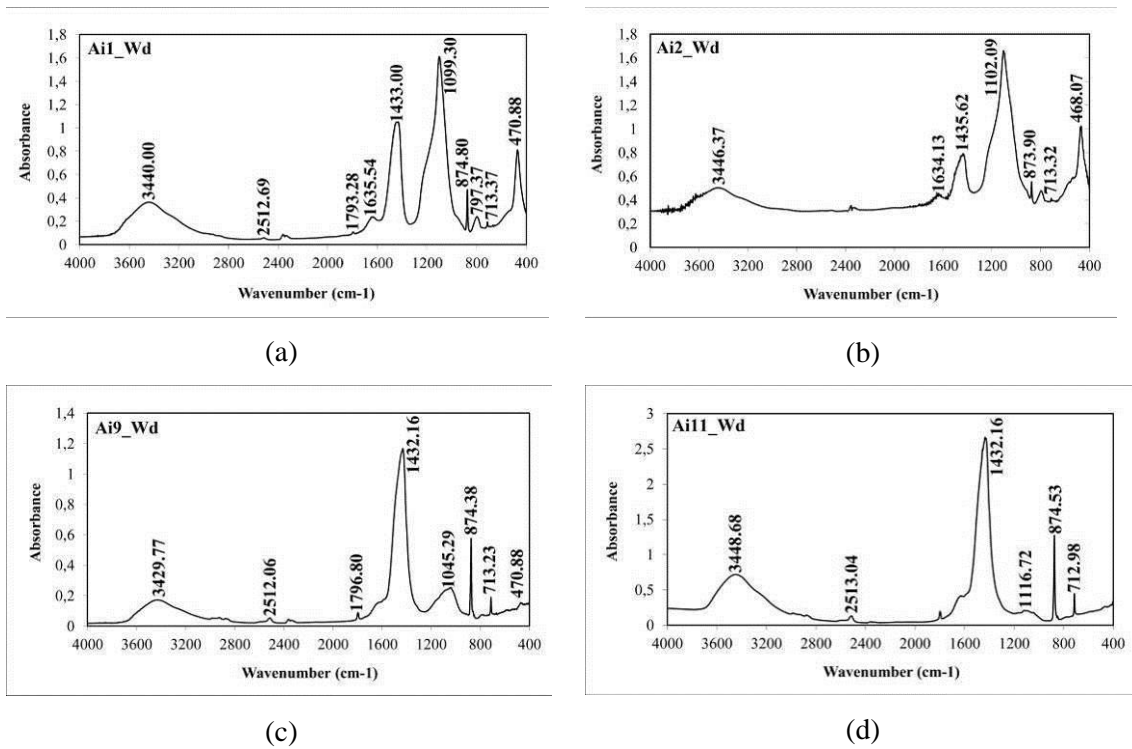


Figure 3.42. FT-IR spectra of white deposits of Aigai: 1 (a), 2 (b), 7 (c) and 11 (d)

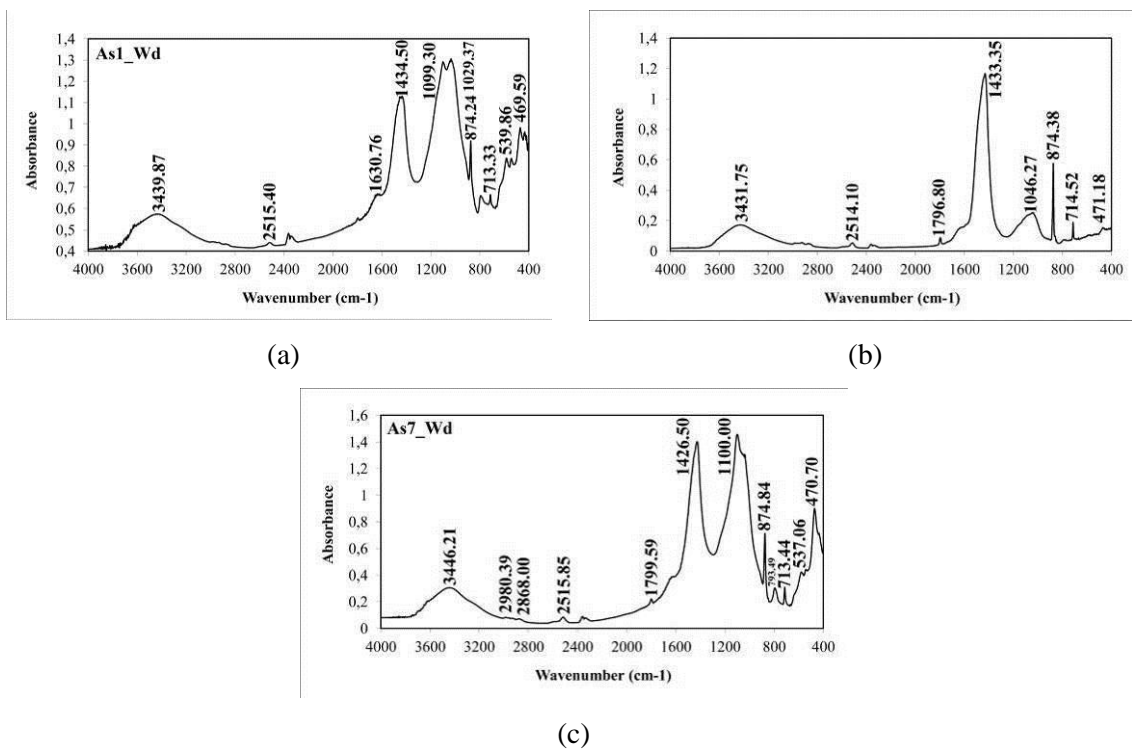


Figure 3.43. FT-IR spectra of white deposits of Assos: 1 (a), 2(b) and 7 (c)

3.4.1.2. Microstructural Characteristics

Microstructural analyses of insoluble white deposits were carried out by SEM analysis of andesite sections and surfaces. SEM analyses of the sections show that the deposition is formed only on the surface of the andesites. The formation could not be observed interior parts of the studied andesites (Ai1, 2, 9, 11 and As1, 2 and 7) (Figure 3.44). This may be because of the movement of the calcium bicarbonate ions to the surface of the andesites and precipitation of the CaCO_3 layer on the andesite surfaces, which will be explained in more detail in the following parts. Thickness of the deposition is between 15 μm (Ai9) and 300 μm (Ai11) for Aigai andesites and 10 μm (As2) and 50 μm (As1) for Assos andesites.

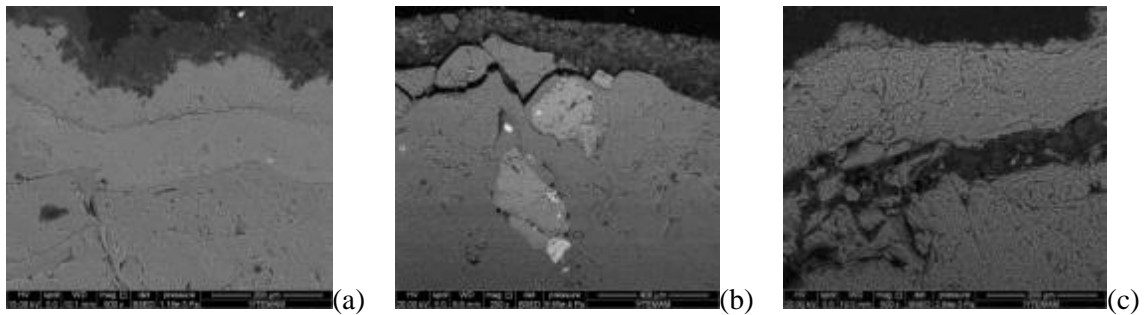


Figure 3.44. SEM images of white deposits of stone sections: Ai2 (a), Ai11 (b) and As1 (c)

Crystal structures of the deposits determined by SEM show that the deposits are mostly composed of rhombohedral crystals and they were formed as a result of precipitation (Figure 3.45, Figure 3.46) (Tiano et al. 1999). Surface analysis of the Ai9 by SEM also shows the presence of calcite crystals with organic materials and needle-shaped calcite crystals (Figure 3.45 (b), Figure 3.47 (c)). Needle-shaped calcite crystals show the re-crystallization of the CaCO_3 in more humid conditions (Figure 3.45, Figure 3.47) (Kuznetsova and Khoklova 2012).

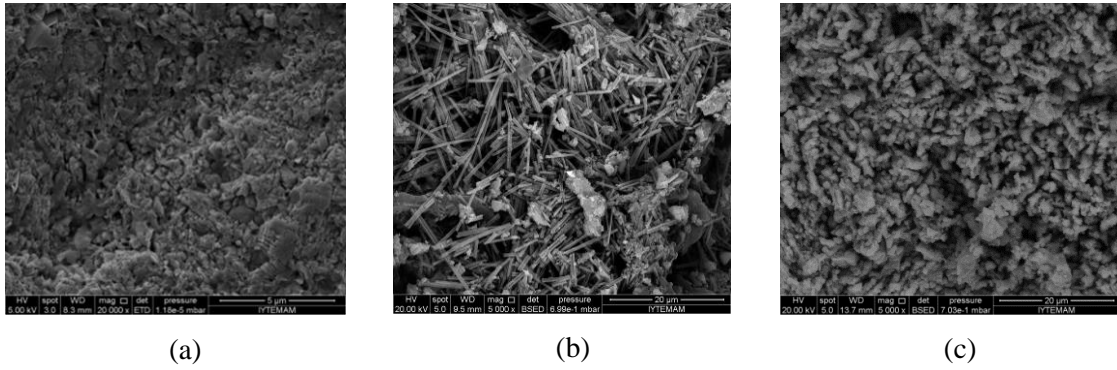


Figure 3.45. SEM images of white deposits of Ai2 (a), Ai9 (b) and Ai11(c)

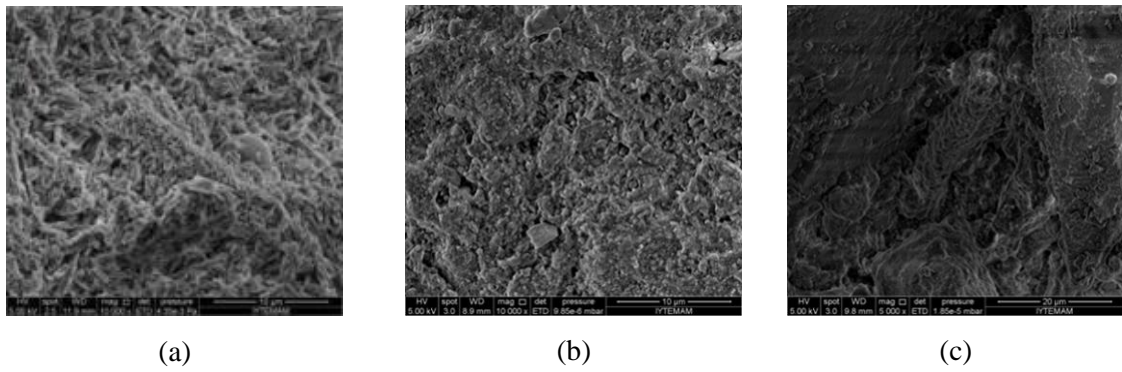


Figure 3.46. SEM images of white deposits of As1 (a), As2 (b) and As7 (c)

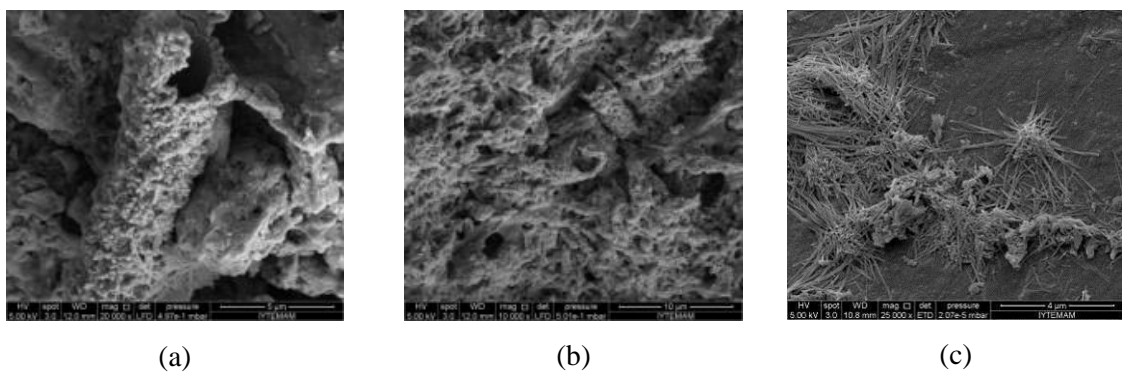


Figure 3.47. SEM images of organic materials and calcite crystals on the surface of Ai9

3.4.1.3. Chemical Characteristics

Chemical analyses of the white deposits were carried out by SEM/EDS analysis of andesite sections. In the analysis, mapping of the andesite sections based on their chemical compositions gathered. The analyses show that these deposits are composed of high amounts of calcium and oxygen and less amounts of aluminum and silica (Figure 3.48, Figure 3.49, Figure 3.50).

Higher CaO content of white deposits can also be seen when the chemical composition of these parts are compared with the interior parts of the andesites and the exterior surfaces which do not have white deposits (Table 3.7, Table 3.10). While the average CaO contents of interior parts of the andesites are 3.5 and 3.6 % and exterior surfaces are 4.3 and 3.7 % for the Aigai and Assos andesites respectively, it increase to more than 80 % for the surfaces which have white deposits. As mentioned before, this may because of the movement of the calcium bicarbonate ions to the surface of the andesites as a result of chemical deterioration and precipitation of the CaCO_3 layer on the andesite surfaces, which will be explained in more detail in the following parts. As can be seen in the chemical maps of the andesite sections, high amounts of calcium and oxygen results from calcium carbonate formation and less amounts of aluminum and silica results from the presence of clay minerals in these parts.

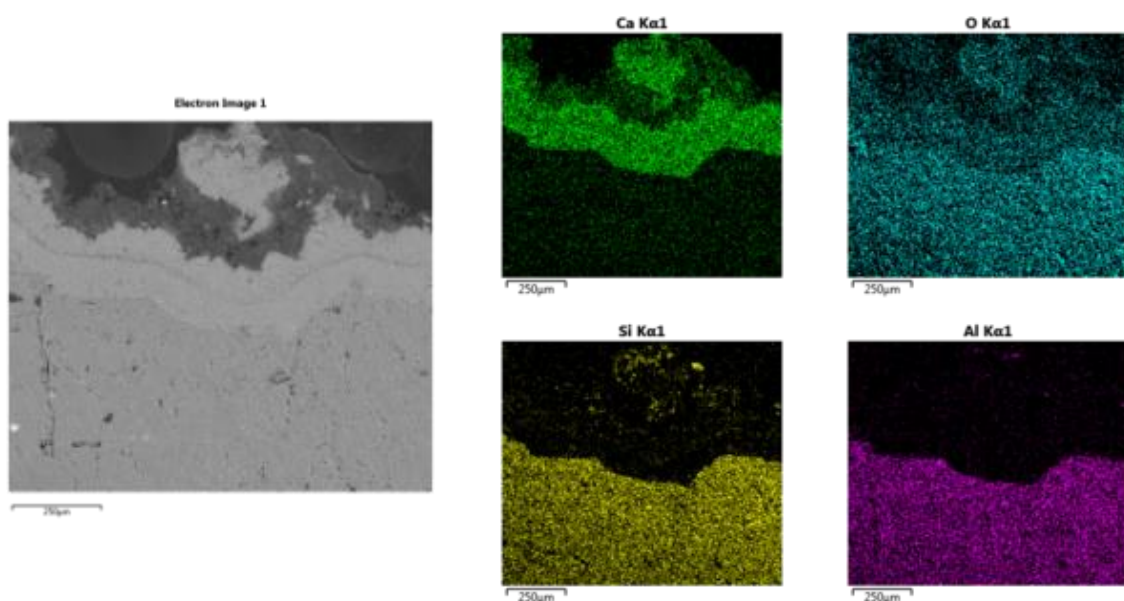


Figure 3.48. Mapping of Ai2 based on chemical composition

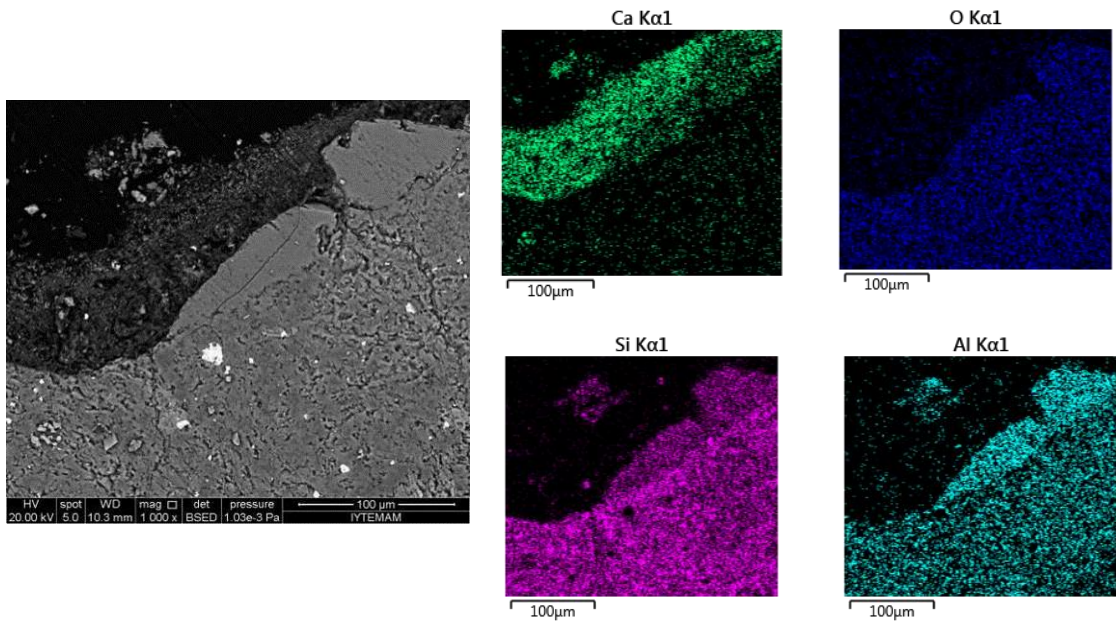


Figure 3.49. Mapping of Ai9 based on chemical composition

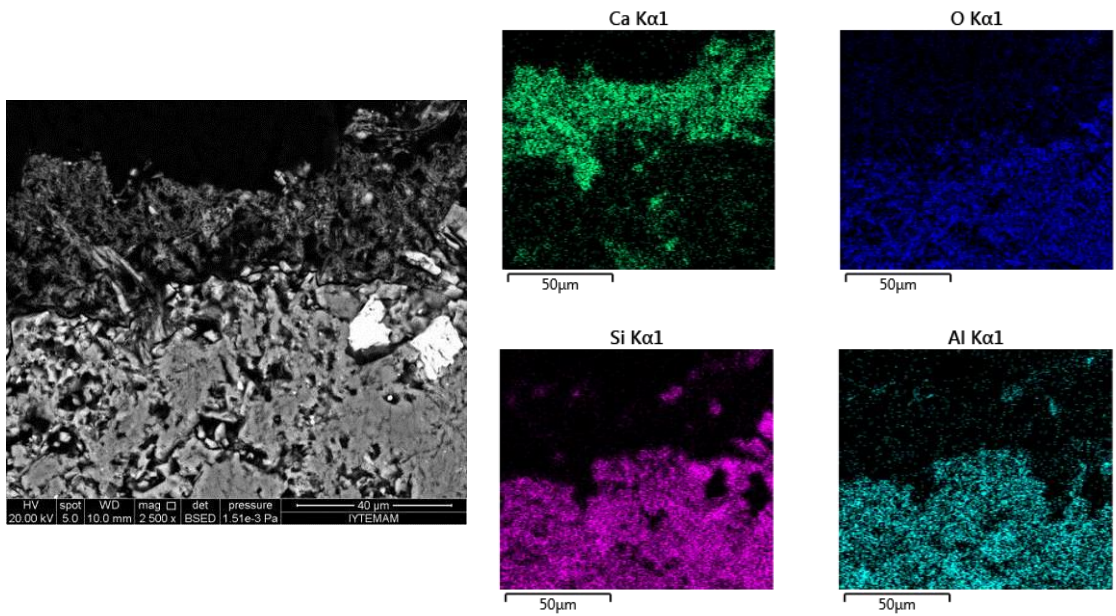


Figure 3.50. Mapping of As2 based on chemical composition

Thermogravimetric analyses of the deposits also support the results of chemical and mineralogical analyses. In TGA curves, high amounts of weight losses of the deposits between 550-900°C, which is due to decomposition of carbonate content, show that they are mostly composed of CaCO₃ (Tylecote 1979). For the ones of Aigai (Ai1, 2, 9 and 11), carbonate contents were 12.7, 6.1, 32.4 and 37.7 % respectively (Figure 3.51). For Assos andesites (As1 and 2), carbonate contents are 23.6 and 31.0 % respectively (Figure 3.52).

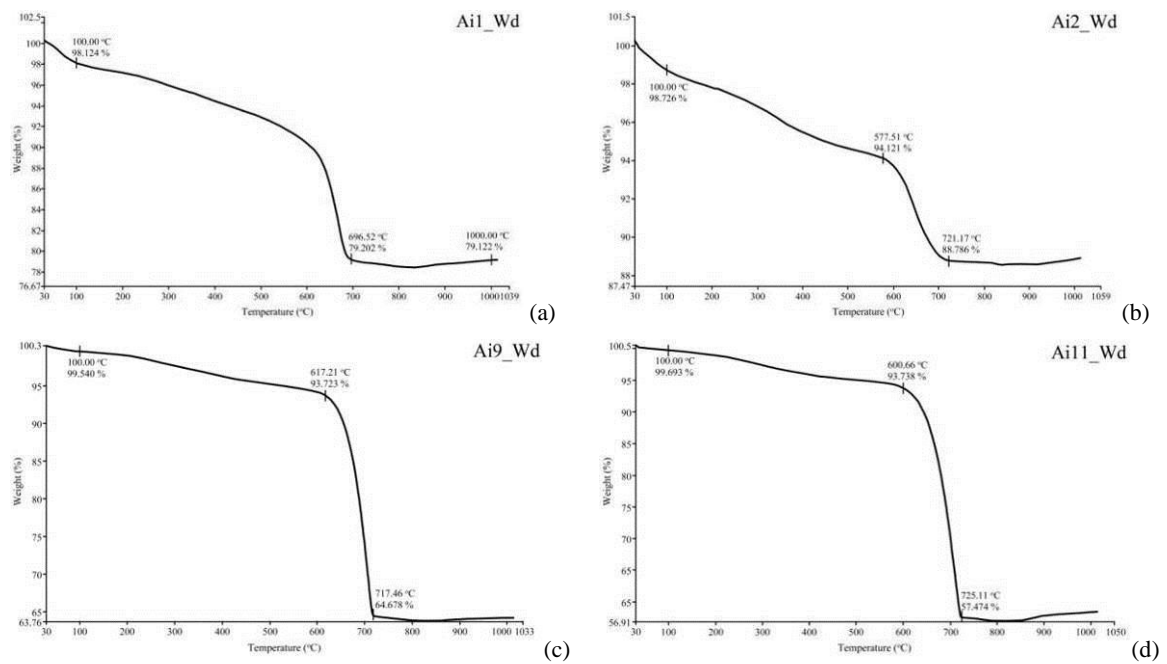


Figure 3.51. TGA graphs of white deposits of Ai1, Ai2 (b), Ai9 (c) and As11 (d)

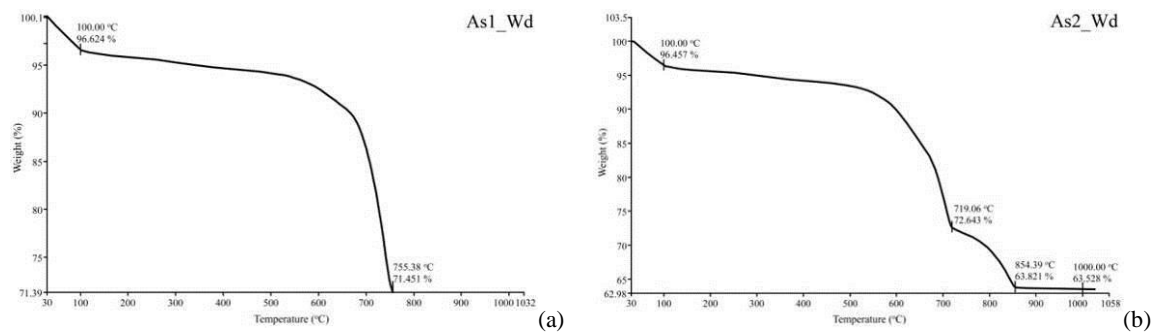


Figure 3.52. TGA graphs of white deposits of As1 and As2 (b)

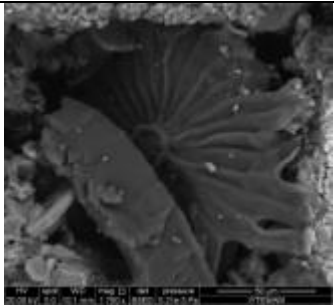


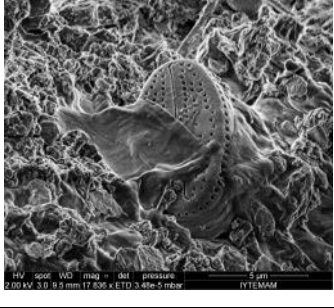
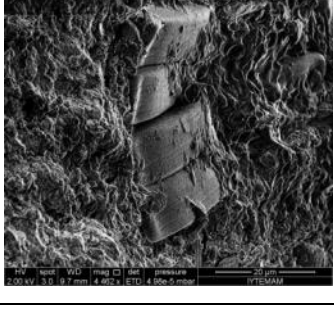
3.4.1.4. Presence of Freshwater Diatoms

The freshwater diatom species on some of the CaCO₃ layer (Ai1, Ai2, Ai9 and Ai11) was observed. They could not be observed on the surfaces of andesite samples of Aigai archaeological site which do not have CaCO₃ layer, the andesite and soil samples of Assos and soil samples and exposed standing andesites of Aigai archaeological site.

Diatoms are siliceous organisms which are abundant in all climates and waters (Breese 1994, Gurel and Yıldız 2007, Lane et al. 2009 and Elmas and Bentli 2012). They have siliceous cell walls (frustules) and dissolved volcanic glass (silica) is the bodybuilding material of them (Gurel and Yıldız 2007, Elmas and Bentli 2012). The classification of the diatoms is made according to the shape of their cell walls. Although there are many sub-groups, they are split up into two groups in general. First one is centric diatoms (centrales) which are radially symmetrical and the second is pennate diatoms (pennales) which are bilaterally symmetrical (Round, Crawford and Mann 2007).

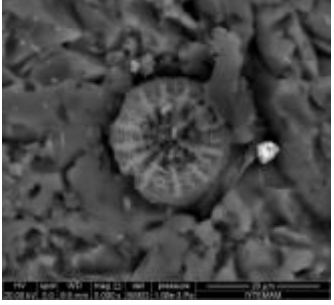
The siliceous cell walls of the diatoms in studied samples were observed in mapping of the samples based on their chemical compositions by SEM/EDS analyses (Figure 3.53, Figure 3.54). In the SEM analyzes of these layers, six types of freshwater diatom species were determined (Table 3.12). According to the classification based on the shape of their cell walls, two of these diatoms are classified as centric and three of them are as pennate diatom. The diatom observed on Ai1 could not found in literature survey. According to their shapes, other five diatoms were also separated to sub-groups as cylotella, naviculoid and eunotia diatoms (Table 3.12). However, their exact names could not found because their all sides and sections could not be analyzed.

Table 3.12. Classification of freshwater diatom species observed on andesite samples

Sample	Diatom	Group	Sub-group	Definition
Ai1		–	–	Diatom type could not found in literature survey.
Ai2		Centric	Cylotella	Deteriorated diatom sample.
Ai9		Pennate	Naviculoid	–
Ai9		Pennate	Naviculoid	–
Ai9		Pennate	Eunotia	–

(cont. on next page)

Table 3.12 (cont.).

<p>Ai11</p>		<p>Centric</p>	<p>Cylotella</p>	<p>Deteriorated diatom sample. Grows in shallow coastal freshwaters (Round, Crawford and Mann 2007)</p>
--------------------	---	----------------	------------------	---

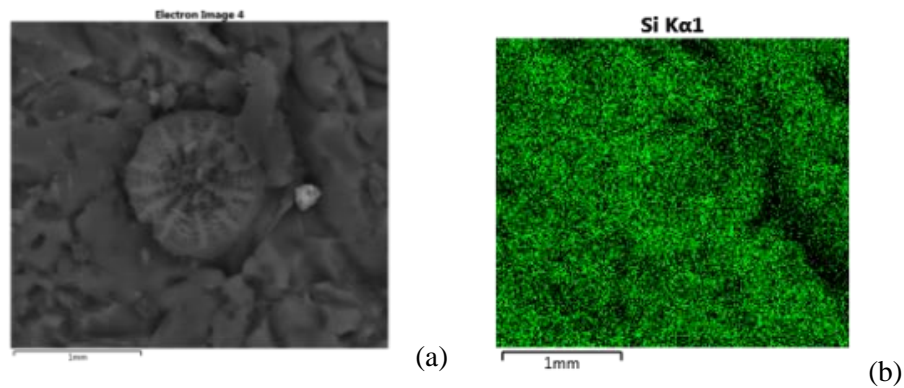


Figure 3.53. Diatom specie observed in Ai11 (a) and mapping of the diatom based on chemical composition (b)

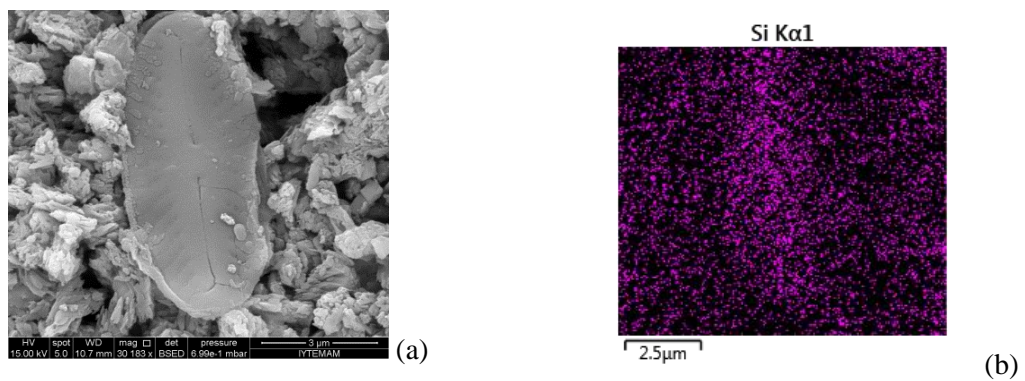


Figure 3.54. Diatom specie observed in Ai2 (a) and mapping of the diatom based on chemical composition (b)

The diatoms observed on andesites can not be formed during formation of the andesites and other volcanic rocks. Because they are all freshwater diatoms (Round, Crawford and Mann 2007) and they can not be formed between 1400-600 °C heat intervals at which the volcanic rocks are formed (Press and Siever 2002). Indeed, they could not be observed on other andesites of both excavated (the ones which do not have white deposits) and exposed standing ones. As mentioned above, they only observed on the andesites of Aigai archaeological site which have white deposits. Hence, the diatoms probably may have formed on the andesite surfaces during burial of the andesites.

The formation of the diatoms during burial of the andesites shows, or requires the presence of water for a long time in subsoil environment (Round, Crawford and Mann 2007). The penetration of the diatoms to calc-alkaline andesites can be explained by the resistance of these andesites to chemical deterioration. As mentioned before, calc-feldspars in the andesite structure are the less resistant minerals to chemical deterioration (Press and Siever 2002). Hence, the dissolution of the minerals and volcanic glass was probably started earlier in these andesites and the diatoms were penetrated to their structure from the soil, which was used to combine the andesites, to reach their bodybuilding material. Thus, such as the formation of white deposits, the presence of diatoms on the stone surfaces may be another sign of deterioration of andesites during burial. In other words, presence of the diatoms on the andesite surfaces which have white deposits in Aigai archaeological site has the sign of poor drainage of the site. It shows the presence of water for a long time in the subsoil environment of Bouleuterion, Stoa and Public Bath buildings and subsequent chemical deterioration of the volcanic glass in the andesite structures during burial.

3.4.2. Characteristics of Orange-Brown Deposits

Orange-brown deposits were observed on some recently excavated andesite surfaces of Aigai archaeological site and two of the samples (Ai1 and Ai6) were taken from these parts (Figure 3.55). In the following parts, mineralogical and chemical characteristics of orange-brown deposits are explained.

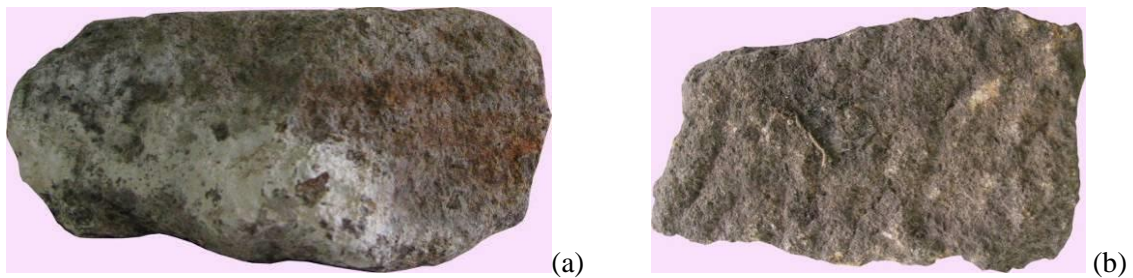
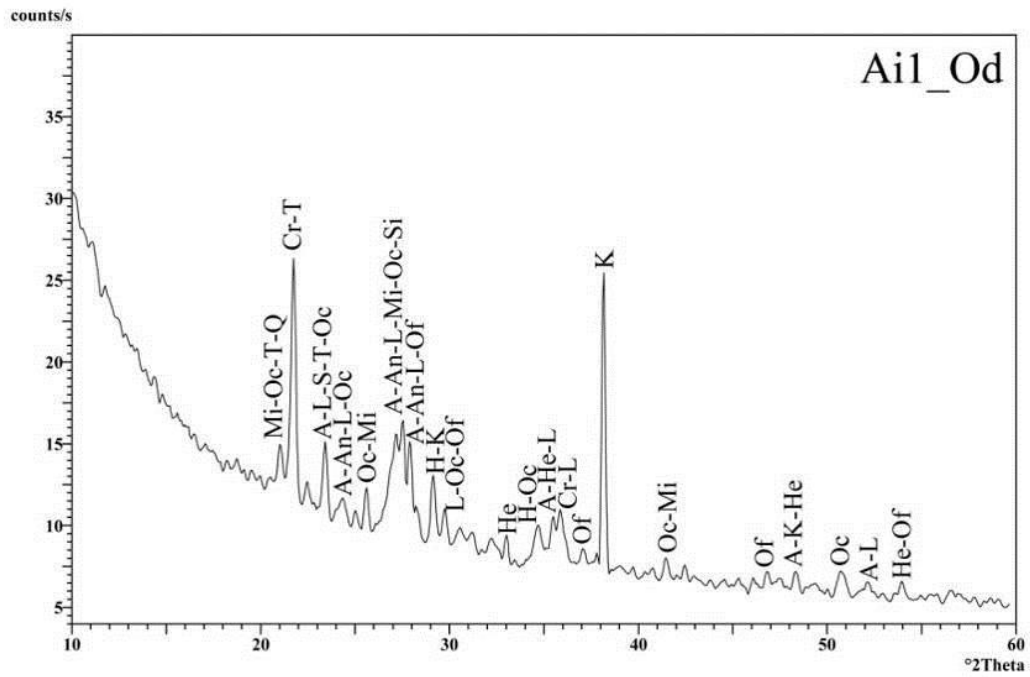


Figure 3.55. Orange-brown deposits on Ai1 (a) and Ai6 (b)

3.4.2.1. Mineralogical and Chemical Characteristics

Mineralogical composition of the orange-brown deposits was determined by XRD analysis. XRD pattern of the exterior surface of the Ai1 shows the presence of iron oxide (hematite) with the other andesite-forming minerals in these parts (Figure 3.56).

Chemical analyses of the orange-brown deposits were carried out by SEM/EDS analysis of andesite sections. In the analysis, mapping of the andesite sections based on their chemical compositions gathered. Supporting the XRD analysis, the mapping of the section of Ai6 based on its chemical composition by SEM/EDS analysis also show the presence of iron oxide (Fe_2O_3) on the surface of Ai6 (Figure 3.57).



A: Andesine (79-1148), Al: Albite high (83-1608), An: Anorthite (70-0287), C: Cristobalite (82-1403), H: Halloysite (03-0184), He: Hematite (87-1165), I: Illite (15-0603), K: Kyanite (72-1441), L: Labradorite (83-1368), Mi: Microcline (76-1238), Mu: Mullite (02-1160), Oc: Orthoclase (75-1190), Of: Orthoferrosilite (83-0668), Q: Quartz (83-2468), S: Sanidine (19-1227), T: Tridymite (42-1401)

Figure 3.56. XRD pattern of surface of Ai1

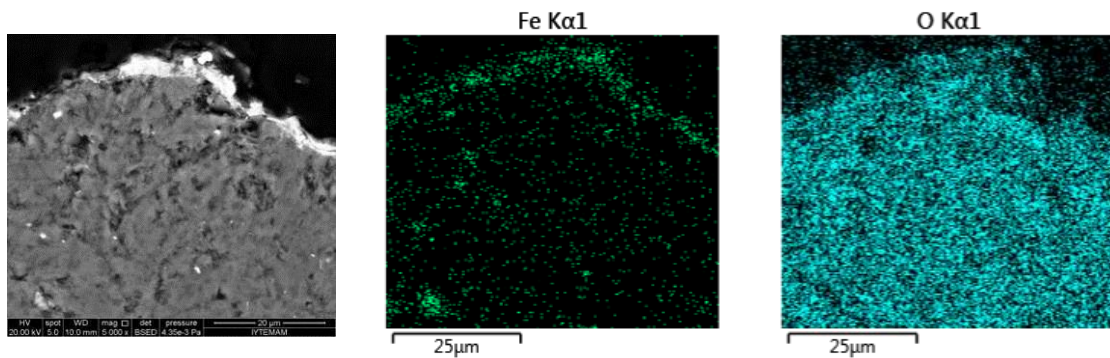
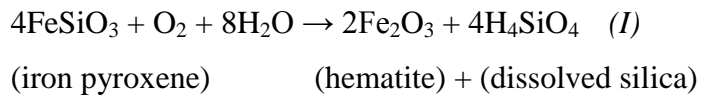


Figure 3.57. Mapping of Ai6 based on chemical composition

Iron oxide (hematite) formation in the andesites is a result of deterioration of the iron silicates such as pyroxenes to iron oxides as a secondary mineral (Press and Siever 2002). The reaction of an iron-rich mineral such as pyroxene with water, its silicate structure dissolves and silica and ferrous iron are released to solution. Then, ferrous iron is oxidized and hematite is formed (Reaction I). Finally it is moved to the stone surface during evaporation of the water and deposited on the surface (Press and Siever 2002).



As previously mentioned, Ai6 was grouped in tholeiitic (iron-rich) stone according to its chemical composition (Figure 3.31). Although Ai1 was grouped in calc-alkaline (calcium rich) stone chemically, its diagram shows that it is very close to the tholeiitic area (Figure 3.31). In other words, it is not as poor as other calc-alkaline andesites according to its iron content. Ai1 has also white deposition on its surface (Figure 3.55). Both white and orange-brown depositions on the stone surfaces show the chemical deterioration of the stones.

CHAPTER 4

CONCLUSIONS

In this study, deterioration problems of buried and excavated andesites were investigated with several excavated andesite monuments in Aigai and Assos archaeological sites to form a basis for the excavation decisions and necessary conservation measures for the purpose of conservation. In order to find out the deterioration problems of excavated andesites, the factors which may affect the deterioration of the buried and exposed standing andesites were also investigated as their importance in the excavated deterioration process.

Aigai was selected as an inland site and Assos was selected as a coastal archaeological site to find out the possible effects of being near the seashore in the deterioration processes of both buried and excavated andesites. All the monuments in the sites were constructed with andesites in the same period and the excavation works in the sites are still ongoing.

Visual analysis of the andesite deteriorations was carried out with the in-situ observations in 2010 and 2014 and documented with the photos. The analyses of the recently excavated and exposed standing parts of the partially excavated andesites resulted less deterioration of the buried parts of the andesites. Exposed standing parts of the andesites have more biological formations than the recently excavated surfaces due to presence of clays, water and sun in the open air conditions. The comparison of completely exposed standing and excavated andesites and partially excavated andesites show slightly deterioration of the stones, which is visible by naked eye, in four years period. Deteriorations observed on the andesites are discoloration, biological forms, pitting and moisture on the andesite surfaces, progress of the cracks and loss of stone materials and they generally determined in the recently excavated parts. The possible sources of the deteriorations were investigated with the laboratory analyses.

In the laboratory analysis, basic physical properties, mineralogical, elemental and chemical compositions, petrographic and microstructural properties of interior parts and exterior surfaces of the andesites, CO₂, organic material and soluble salt contents of andesite and soil samples were determined and compared. The chemical weathering indices of CIA and WIP were used to find out the chemical deterioration of the andesites.

Aigai and Assos andesites are dominated by the minerals of plagioclase feldspars, biotite, hornblende, orthoferrosilite and volcanic glass with lower amounts of quartz. They are mainly composed of SiO₂, Al₂O₃, Fe₂O₃, Na₂O, K₂O, MgO, CaO and trace amounts of TiO₂ and P₂O₅. Based on the amounts of the elements, andesites can be classified as intermediate igneous rocks and contain both tholeiitic and calc-alkaline stones.

Microstructural and petrographic analyses of the andesites indicated that the studied andesites are aphanitic. The mineral grains averages up to 1.5 mm in size for Aigai andesites and up to 2.5 mm in size for Assos andesites. Bigger minerals observed in the Assos andesites indicated that the cooling process of these andesites proceeded slower than the Aigai andesites during their formation.

The comparison of the basic physical properties and microstructural characteristics of interior parts and exterior surfaces of the andesites indicated small variations in density (between 2.2-2.3 g/cm³) and porosity (between 10.1-13.2 %) values. In the exterior surfaces of the andesites, density values decrease approximately 0.1 g/cm³ and porosity values increase approximately 3 %. The results are negligible and indicated slight physical deterioration of the andesites.

The presence of clay minerals in the andesite structures were observed by elemental, chemical and mineralogical analyses of the stones. The clay minerals and the presence of water are the main reasons of andesite deteriorations both during burial and after excavations. Their presence in the andesite structure promotes physical, chemical and biological deterioration of the stones.

Chemical compositions of the interior parts and exterior surfaces of the andesites were used to estimate the degree of chemical deterioration by WIP and CIA analyses. The analyses indicated slight chemical deterioration of excavated andesite surfaces as the differences between the interior parts and exterior surfaces are very small.

Studied andesites contain low amounts of organic material and trace amounts of carbonate and soluble salt contents. The results indicated that they are less effective in the deterioration of excavated Aigai and Assos andesites.

The soils where the andesites were excavated contain low amounts of organic material and carbonate contents and trace amounts of soluble salts. This was indicated that soluble salts are less effective in the deterioration of buried Aigai and Assos andesites. Similar characteristics of the soil samples of Aigai and Assos also indicated to be resulted from their collection from shallow burial parts of the burial environments before the excavations.

White deposits observed on excavated calc-alkaline andesite surfaces are mostly composed of calcium carbonate formed as a result of chemical deterioration of calcium feldspars during burial in the presence of water. They may be evaluated as the protective calcium carbonate layers which show the burial history of the andesites. Thus, they should be conserved as the history of the monuments.

The orange-brown deposits determined on the excavated and exposed standing andesites are hematite resulted from the chemical deterioration of iron silicates to iron oxides.

Freshwater diatoms found on the andesite surfaces of Aigai archaeological site indicated the presence of water for a long time in the burial environment of Bouleuterion, Stoa and Public Bath buildings and subsequent chemical deterioration of the volcanic glass in the andesite structures. The presence of freshwater diatoms could not be found on the andesite surfaces of Assos archaeological site.

Based on the results of visual analysis and experimental studies, which indicated slight deterioration of excavated andesites, it was proposed that the excavations can be carried out and the studied excavated stones do not require active conservation interventions at the sites. However, preventive conservation measures must be carried out to prevent further stone deteriorations in open air conditions.

In order to reduce the effects of clay minerals and water to the studied andesite monuments, preventive conservation measures of controlled drying processes of the andesites during their excavations have to be supplied. After the excavations, the clays on the stone surfaces have to be cleaned and biocides have to be implemented to the stones to prevent the growth of biological forms. In the environmental scale, site planning for the monuments and findings such as drainage to keep the water away from the stones have to be supplied.

REFERENCES

- Aigai Kazısı Resmi Web Sitesi. "Topografik Kent Haritası." Accessed May 25 2015.
http://aigai.info/kazilar_ve_antik_yapilar/aigai_plan.jpg
- Akay, E. and Erdoğan, B. 2004. Evolution of Neogene calc-alkaline to alkaline volcanism in the Aliğa-Foça region (Western Anatolia, Turkey). *Journal of Asian Earth Sciences* 24: 367-387.
- Akyürek, B. and Soysal, Y. 1983. Biga yarımadası güneyinin (Savaştepe-Kırkağaç-Bergama-Ayvalık) temel jeoloji özellikleri. *MTA Dergisi* 95/96 1-12.
- Amundson, R. 2003. *Surface and Ground Water, Weathering, and Soils*, ed. Drever, J. I., vol. 5, Oxford: Elsevier-Perгамon.
- April, R., and Keller, D. 1990. Mineralogy of the rhizosphere in forest soils of the eastern United States. *Biochemistry* 9: 1-18.
- Arıkan, F., Ulusay, R. and Aydın, N., 2007. Characterization of weathered acidic volcanic rocks and a weathering classification based on a rating system. *Springer-Verlag* 66 (4) 415-430.
- Arslan, N. and Böhlendorf-Arslan, B. 2014. *Assos: Taşın Hayat Verdiği Kent*. Homer Kitabevi ve Yayıncılık Ltd. Şti., İstanbul.
- Ascaso, C., Sancho, L.G. and Rodriguez-Pascual, C. 1990. The weathering action of saxicolous lichens in maritime Antarctica. *Polar Biology* 11 33-39.
- Assos Kazısı Resmi Web Sitesi. "Assos Kent Planı." Accessed May 25 2015.
http://assosarchproject.com/bilgilendirme/assos_kent_plani.jpg
- Australia ICOMOS. "The Burra Charter (1979)." Accessed May 25 2015.
http://australia.icomos.org/wp-content/uploads/BURRA_CHARTER.pdf
- Bahlburg, H. and Dobrzinski, N. 2009. A review of the Chemical index of Alteration (CIA) and its application to the study of Neoproterozoic glacial deposits and climate transitions. In *The Geological Record of Neoproterozoic Glaciations*. Arnaud, E., Halverson, G.P. and Shields, G.A. (Ed), Geological Society, London.
- Baer, N.S. and Snickars, F. 2001. *Rational Decision-Making in the Preservation of Cultural Property*. Dahlem Workshop Reports 86. Berlin: Dahlem University Press.

- Bernabe, E., Bromblet, P. and Robert, M. 1995. Role de la cristallisation du natron dans la desagregation sableuse d'un monument granitique en Bretagne -Role of natron crystallization on granular disintegration of a granitic monument in Brittany. *Comptes Rendus Academie des Sciences: Serie IIA, Sciences de la Terre et des Planetes* 320 (7) 571-578.
- Berner, A.R., Lasaga, A.C. and Garrels, R.M. 1983. The carbonate–silicate geochemical cycle and its effect on atmospheric carbon dioxide over the past 100 million years, *American Journal of Science* 283 641-683.
- Bohn, R., and Schuchhardt, C. 1889. *Altertümer von Aigai*, trans. Serttürk, O.K., and Kan, M.H., Berlin: Georg Reimer.
- Borrelli, E. 1999. *Salts* in ARC Laboratory Handbook. ICCROM, Rome, Italy.
- Borsi, S., Ferrara, C., Innocenti, F. and Mazzuoli, R., 1972. Geochronology and etrology of recent volcanics of Eastern Aegean Sea: *Bull. Voic.* 36 473-496.
- Brady, B.H.G. and Brown, E.T. 2004. *Rock Mechanics for underground mining*. Third edition. Springer, P.O. Box 17, 3300 AA Dordrecht, The Netherlands.
- Breese, R. 1994. *Diatomite, industrial minerals and rocks*. Carr (Ed), SMME, Colorado, USA.
- Camuffo D. 1995. Physical weathering of stones. *The Science of the Total Environment* 167 1-14.
- Ceryan, Ş. 2008. New Chemical Weathering Indices for Estimating the Mechanical Properties of Rocks: A Case Study from the Kürtün Granodiorite, NE Turkey. *Turkish Journal of Earth Sciences (Turkish J. Earth Sci.)* 17 187-207.
- Chen, J., Blume, H.P., and Beyer, L. 1999. Weathering of rocks induced by lichen colonization – a review. *Catena* 39: 121-146.
- Choiseul, G. 1809. *Voyage Pittoresque de La Grece*, Paris.
- Colin, F., Brimhall, G.H., Nahon, D., Lewis, C.J., Baronnet, A., and Danti, K., 1992. Equatorial rain forest lateritic mantle: a geomembrane filter. *Geology* 20: 523-526.
- Colman, S.M. 1982. *Chemical Weathering of Basalts and Andesites: Evidence from Weathering Rinds*. United States Government Printing Office, Washington.

- Council of Europe. "European Convention on the Protection of the Archaeological Heritage (1992)." Accessed May 25 2015.
<http://conventions.coe.int/Treaty/en/Treaties/html/143.htm>
- Cronyn, J.M. 2002. *The elements of archaeological conservation*. Routledge, Taylor & Francis Group, London and New York.
- Crow, P. 2008. Mineral weathering in forest soils and its relevance to the preservation of the buried archaeological resource. *Journal of Archaeological Science* 35 2262-2273.
- Curran, J., Smith, B., and Warke, P. 2002. Weathering of igneous rocks during shallow burial in an upland peat environment: observations from the Bronze Age Copney Stone Circle Complex, Northern Ireland. *Catena* 49 139-155.
- Davidson, D.A. and Wilson, C.A. 2006. *Final Report: An assessment of potential soil indicators for the preservation of Cultural Heritage*. School of Biological and Environmental Science, University of Stirling, Stirling.
- Demas, M. 2004. Site unseen: The case for reburial of archaeological sites. *Conservation and Management of Archaeological Sites* 6 (3-4) 137-54.
- Doehne, E. and Price, C.A. 2010. *Stone conservation—An overview of current research*. Getty Publications, Los Angeles, California.
- Doğer, E. 2004. Aigai 2004 Yılı Bouleuterion Çalışmaları. In *Report Archives of the Aigai Excavations*. December 2004.
- Doğer, E. 2007. Aigai 2004-2006 Yılı Kazıları. In *29. Kazı Sonuçları Toplantısı I*. 28 May- 01 June 2007.
- Drever, J.I. 1994. The effect of land plants on weathering rates of silicate minerals. *Geochimica et Cosmochimica Acta* 58 (10): 2325-2332.
- Düzgören-Aydın N.S., Aydın, A., Malpas, J. 2002. Re-assesment of chemical weathering indices: case study on pyroclastic of Hong Kong. *Engineering Geology* 63 99-119.
- Eggleton, R.A. 1986. The relation between crystal structure and silicate weathering rates. In *Rates of Chemical Weathering of Rocks and Minerals*. Colman S.M. and Dethier D.P. (Ed) Academic Press, Inc., Orlando, 21-40.
- Eith, C., Kolb, M., Seubert, A. and Viehweger, H. (Ed.) 2001. *Practical Ion Chromatography: An Introduction*. Metrohm Ltd., CH-9101 Herisau, Switzerland.

- Elmas, N. and Bentli, İ. 2012. Environmental and depositional characteristics of diatomite deposit, Alayunt Neogene Basin (Kutahya), West Anatolia, Turkey. *Environmental Earth Sciences, Springer-Verlag*.
- Ercan, T., Satır, M., Steinitz, G., Dora, A., Sarıfakıoğlu, E., Adis, C., Walter, H.J. and Yıldırım, T. 1995. Biga Yarımadası ile Gökçeada, Bozcaada ve Tavşan Adalarındaki (KB Anadolu) Tersiyer Volkanizmasının Özellikleri. *MTA Dergisi* 117 55-86.
- Ergun, H. 2009. *Afyonkarahisar Bölgesi Andezitlerinin Seramik Çamur Ve Sır Bünyelerinde Değerlendirilmesi*. Unpublished MSc. thesis, Afyon Kocatepe University, 117 p.
- Fedo, C.M., Nesbitt, H.W. and Young, G.M. 1995. Unravelling the effects of potassium metasomatism in sedimentary rocks and paleosols, with implications for paleoweathering conditions and provenance. *Geology* 23 921-924.
- Fichter, L.S., Farmer, G.T. Jr. 1975. *Earth Materials and Earth Process: An Introduction, 2nd Edition*. Minnesota: Burgess Publishing Company.
- Gadsden, J.A. 1975. *Infrared Spectra of Minerals and Related Inorganic Compounds*. London: Butterworths.
- Garcia-Valles, M., Aulinas, M., Lopez-Melcion, J.B. and Moya-Garra, A. 2010. Patinas developed in environmental burial conditions: the Neolithic steles of Reguers de Sero (Lledia, Spain). *Environ Sci Pollut Res* 17 1287-1299.
- Gjelstrup Björdal, C. 2000. *Waterlogged Archaeological Wood-Biodegradation and its Implications for Conservation*. Dissertation. Swedish University of Agricultural Sciences.
- Gökten, E. and Floyd, P.A. 1987. Geochemistry and tectonic environment of the Şarkışla area volcanic rocks in central Anatolia, Turkey. *Mineralogical Magazine* 51 553-559.
- Guggenheim, S. and Martin, R.T., 1995. *Definition of clay and clay mineral*. Joint report of the AIPEA nomenclature and CMS nomenclature committees. *Clays Clay Miner* 43 255-256.
- Gupta, A.S. and Rao, K.S. 2001. Weathering indices and their applicability for crystalline rocks. *Bulletin of Engineering Geology and the Environment*, 60 201-221

- Gurel, A. and Yildiz, A. 2007. Diatom communities, lithofacies characteristics and paleoenvironmental interpretation of Pliocene diatomite deposits in the Ihlara-Selime plain (Aksaray, Central Anatolia, Turkey). *J Asian Earth Sci* 30 (1) 170-180.
- Hamblin W.K. and Christiansen, E.H. 2003. *Earth's dynamic systems*. Prentice Hall, New Jersey, USA.
- Hamdan, J. and Burnham, C.P. 1996. The contribution of nutrients from parent material in three deeply weathering soils of Peninsular Malaysia. *Sedimentary Geology* 55 319-322.
- Hanfmann, G.M.A. 1948. The Journal of Hellenic Studies. Archaeology in Homeric Asia Minor 52 (1).
- Herodotos, 1991. *Herodot Tarihi*. I 149. Trans. M. Ökmen, İstanbul: Remzi Kitabevi.
- Homer, 1962. *Iliada*. Trans. Azra Erhat, İş Bankası.
- Howe, J.E. 2001. *The Geology of Building Stones*. USA: Donhead Publishing Ltd.
- ICCROM. "Conservation of Architectural Heritage, Historic Structures and Materials: ARC Laboratory Handbook." Accessed May 25 2015. http://www.iccrom.org/ifrcdn/pdf/ICCROM_14_ARCLabHandbook01_en.pdf
- ICOMOS. "The Athens Charter for the Restoration of Historic Monuments (1931)." Accessed May 25 2015. <http://www.icomos.org/en/charters-and-texts/179-articles-en-francais/ressources/charters-and-standards/167-the-athens-charter-for-the-restoration-of-historic-monuments>
- ICOMOS. "The Venice Charter (1964)." Accessed May 25 2015. http://www.icomos.org/charters/venice_e.pdf
- ICOMOS. Charter for the Protection and Management of the Archaeological Heritage (1990)." Accessed May 25 2015. http://www.international.icomos.org/charters/arch_e.pdf
- ICOMOS. "The Nara Document on Authenticity (1994)." Accessed May 25 2015. <http://www.icomos.org/charters/nara-e.pdf>
- Iijima, K., Jimenez-Espejo, F. J., and Sakamoto, T. 2005. Filtration Method for -Quantitative Powder X-ray Diffraction Analysis of Clay Minerals in Marine Sediments. *Frontier Research on Earth Evolution* 2 1-3.

- Ilani, S., Rosenfeld, A. and Dvorachek, M. 2002. Archaeometry of a stone tablet with Hebrew inscription referring to repair of the House. *Isr Geol Surv Curr Res* 13 109-116.
- Ilani, S., Rosenfeld, A., Feldman, H.R., Krumbein, W.E. and Kronfeld, J. 2008. Archaeometric analysis of the Jehoash Inscription tablet. *Journal of Archaeological Science* 35 2966-2972.
- Irfan, T.Y. 1996. Mineralogy, fabric properties and classification of weathered granites in Hong Kong. *Quarterly Journal of Engineering Geology and Hydrogeology* 29 5-35.
- Irvine, T. N. and Baragar, W. R. A. 1971. A guide to the chemical classification of the common volcanic rocks. *Canadian Journal of Earth Sciences* 8 523-548.
- Jaeger, J.C. and Cook, N.G.W. 1979. *Fundamentals of rock mechanics*. Chapman and Hall, London.
- Jamtveit, B., Kobchenko, M., Austrheim, H., Malthe-Sørensen, A., Røyne, A. and Svensen, H. 2011. Porosity evolution and crystallization-driven fragmentation during weathering of andesite. *Journal of Geophysical Research* 116 B12204.
- Jones, D.L. 1998. Organic acids in the rhizosphere-a critical review. *Plant and Soil* 1 25-44.
- Kaplan, Ç.D. 2009. *Evaluation of Stone Weathering of Aigai Bouleuterion After its Excavation*. Unpublished MSc. thesis, İzmir Institute of Technology, 151 p.
- Kaplan, Ç.D., Murtezaoğlu, F., İpekoğlu, B. and Böke, H. 2013. Weathering of andesite monuments in archaeological sites. *Journal of Cultural Heritage* 14 (3) e77-e83.
- Kaputoğlu, S. 2013. *Buca Yeşil Andezitlerinin Jeolojisi Malzeme Özellikleri ve Durabilitesinin Araştırılması*. Unpublished MSc. thesis, Dokuz Eylül University, İzmir Institute of Technology, 91 p.
- Karacık, Z., Yılmaz, Y. and Pearce, J.A. 2007. The Dikili-Çandarlı Volcanics, Western Turkey: Magmatic Interactions as Recorded by Petrographic and Geochemical Features. *Turkish Journal of Earth Sciences* 16 493-522.
- Karpuz, C. 1982. *Rock Mechanics Characteristics of Ankara Andesites in Relation to their Degree of Weathering*. Unpublished Ph.D. Thesis, METU, 157 p.
- Kars, H. 1998. Preserving our in situ archaeological heritage: a challenge to the geochemical engineer. *Journal of Geochemical Exploration* 62 139-147.

- Koca, M.Y. 1999. İzmir Yöresinde Andezitlerin Bozunma Ürünü Killerin Oluşum Şekilleri ve Mühendislik Özellikleri. *TJK Bülteni* 42 2.
- Koca, M.Y., Kıncal, C. Arslan A.T. and Yılmaz, H.R. 2011. Anchor application in Karatepe andesite rock slope, İzmir-Türkiye. *International Journal of Rock Mechanics & Mining Sciences* 48 245-258.
- Komatani, S., Aoyama, T., Nakazawa, T. and Tsuji, K. 2013. Comparison of SEM-EDS, Micro-XRF and Confocal Micro-XRF for Electric Device Analysis. *e-Journal of Surface Science and Nanotechnology* 11 133-137.
- Koralay, T. 2010. Petrographic and geochemical characteristics of upper Miocene Tekkedag volcanics (Central Anatolia-Turkey). *Chemie der Erde* 70 335-351.
- Korkanç, M. 2013. Deterioration of different stones used in historical buildings within Niğde province, Cappadocia. *Construction and Building Materials* 48 789-803.
- KUMID. "Recommendations of the Madrid Conference (1904)" Accessed May 25 2015. <http://www.kumid.net/euproject/admin/userfiles/dokumanlar/K-Madrid-Konferansi,1904.pdf>
- Kuznetsova, A.M. and Khokhlova, O.S. 2012. Submicromorphology of pedogenic carbonate accumulations as a proxy of modern and paleoenvironmental conditions. *Boletín de la Sociedad Geológica Mexicana* 64 (2) 199-205.
- Lane, C.R., Reiss, K.C., DeCelles, S. and Brown, M.T. 2009. Benthic diatom composition in isolated forested wetlands subject to drying: implications for monitoring and assessment. *Ecol Ind* 9 1121-1128.
- Le Bas, M. J., Le Maitre, R. W., Streckeisen, A. and Zanettin, B. 1986. A chemical classification of volcanic rocks based on the total alkali-silica diagram. *Journal of Petrology* 27 745-750.
- Lee, C.H. and Yi, J.E. 2007. Weathering damage evaluation of rock properties in the Bunhwangsa temple stone pagoda, Gyeongju, Republic of Korea. *Engineering Geology* 52:1193-1205.
- Le Maitre, R.W. 1989. *A classification of igneous rocks and glossary of terms*. Oxford: Blackwell, 193p.
- Majedova, J. 2002. FTIR techniques in clay mineral studies. *Vibrational Spectroscopy* 31 1-10.

- Margolis, S.V. and Showers, W. 1988. Weathering characteristics, age, and provenance determinations on ancient Greek and Roman marble artifacts. In: Herz N, Waelkens M (eds) *Classical marble: geochemistry, technology, trade*. E-153. NATO ASI Series, 233-242.
- Matsukura, Y. and Hirose, T. 1999. Five year measurements of rock tablet weathering on a forested hillslope in a humid temperate region. *Engineering Geology* 55 69-76.
- Matthiesen, H. 2004. In situ measurement of soil pH. *Journal of Archaeological Science* 31 1373-1381.
- Miyashiro, A. 1974. Volcanic rock series in island arcs and active continental margins. *American Journal of Science* 274 321-355.
- Moropoulou, A., Polikreti, K., Ruf, V. and Deodatis, G. 2003. San Francisco Monastery, Quito, Equador: characterisation of building materials, damage assessment and conservation considerations. *Journal of Cultural Heritage* 4 101-108.
- Mortatti, J. and Probst, J.L. 2003. Silicate rock weathering and atmospheric/soil CO₂ uptake in the Amazon basin estimated from river water geochemistry: seasonal and spatial variations. *Chemical Geology* 197 (1-4) 177-196.
- Mulyanto, B., Stoops, G., and Van Ranst, E. 1999. Precipitation and dissolution of gibbsite during weathering of andesitic boulders in humid tropical West Java, Indonesia. *Geoderma* 89 287-305.
- Mulyanto, B. and Stoops, G. 2003. Mineral neoformation in pore spaces during alteration and weathering of andesitic rocks in humid tropical Indonesia. *Catena* 54 385-391.
- Murtezaoğlu, F. 2009. *Examination of Deterioration Problems of Andesite Used in Aigai Agora*. Unpublished MSc. thesis, İzmir Institute of Technology, 87 p.
- Naumann, R. 2007. *Eski Anadolu Mimarlığı (translation: M. Ökmen)*. Atatürk Kültür, Dil ve Tarih Yüksek Kurumu, Türk Tarih Kurumu Yayınları, Ankara, Turkey.
- Nesbitt, H.W. and Young, G.M. 1982. Early Proterozoic climates and plate motions inferred from major element chemistry of lutites. *Nature* 199 715-717.
- Nord, A.G., Tronner, K., Mattson, E., Borg, G.Ch. and Ullen, I. 2005. Environmental Threats to Buried Archaeological Remains. *Royal Swedish Academy of Sciences* 34 (3) 256-262.

- Oguchi, C. T. and Matsukura, Y. 1999. The effect of porosity on the increase in weathering-rind thickness of andesite gravels. *Engineering Geology* 55 (1-2) 77-89.
- Oguchi C.T. 2001. Formation of Weathering Rinds on andesite. *Earth Surface Processes and Landforms* 26 847-858.
- Orhan, M., Işık, N.S., Topal, T. and Özer, M. 2006. Effect of weathering on the geomechanical properties of andesite, Ankara- Turkey. *Environmental Geology* 50 85-100.
- Öngür, T. 1973. Çanakkale-Tuzla yöresinin volkanolojisi ve jeotermal enerji olanakları. *Unpublished MTA Report*.
- Özkaymak, Ç., Sözbilir, H. and Uzel, B. 2013. Neogene–Quaternary evolution of the Manisa Basin: evidence for variation in the stress pattern of the İzmir–Balıkesir Transfer Zone, western Anatolia. *Journal of Geodynamics* 65 117-135.
- Panoramio. “Agora - Kazı Sonrası.” Accessed May 25 2015.
<http://www.panoramio.com/photo/23455689>
- Parker, A. 1970. An index of weathering for silicate rocks. *Geological Magazine* 107 501-504.
- Peccerillo, A. and Taylor, S.R. 1976. Geochemistry of Eocene calc-alkaline volcanic rocks from the Kastamonu area, northern Turkey. *Contributions to Mineralogy and Petrology* 58: 63-81
- Polikreti, K. 2007. Detection of ancient marble forgery: techniques and limitations. *Archaeometry* 49(4) 603-619.
- Polikreti, K. and Christofides, C. 2009. The role of humic substances in the formation of marble patinas under soil burial conditions. *Phys Chem Minerals* 36 271-279.
- Pope, G.A., Meierding, T.C. and Paradise, T.R. 2002. Geomorphology’s role in the study of weathering of cultural stone. *Geomorphology* 47 211-225.
- Power, E.T. 1989. *Subsurface weathering of granitoid rocks in different climates*. Ph.D. thesis, Queen’s University, Belfast, Northern Ireland.
- Press, F., and Siever, R. 2002. *Understanding Earth*, 3rd Ed., New York: W.H. Freeman and Company.
- Ramsay, W.M. 1881. Contributions to the History of Aeolis. *The Journal of Hellenic Studies* 2.

- Ray, D., Rajan, S., Ravindra, R. and Jana, A. 2011. Microtextural and mineral chemical analyses of andesite–dacite from Barren and Narcondam islands: Evidences for magma mixing and petrological implications. *Journal of Earth System Science* 120 (1): 145-155.
- Reiche, P. 1943. Graphics representation of chemical weathering. *Journal of Sediment Petrology* 13 58-68.
- RILEM 1980. Tests Defining the Structure. *Materials and Construction* 13 (73) 179-181.
- Rodriguez-Navarro, C., Sebastian, E., Doehne, E. and Ginell, W.S. 1998. The role of sepiolite-palygorskite in the decay of ancient Egyptian limestone sculptures. *Clays and Clay Minerals* 46 (4) 414-422.
- Round, F.E., Crawford, R.M. and Mann, D.G. 2007. *The Diatoms: Biology and Morphology of the Genera*. Cambridge University Press, New York. USA.
- Sak, P.B, Navarre-Sitchler, A.K., Miller, C.E., Daniel, C.C., Gaillardet, J., Buss, H.L., Lebedeva, M.I. and Brantley, S.L. 2010. Controls on rind thickness on basaltic andesite clasts weathering in Guadeloupe. *Chemical Geology* 276 129-143.
- Sarıışık, A., Sarıışık, G. and Şentürk, A. 2011. Applications of glaze and decor on dimensioned andesites used in construction sector. *Construction and Building Materials* 25 3694-3702.
- Scherer, G.W. 2006. Internal stress and cracking in stone and masonry. in: M.S. Konsta-Gdoutos (Ed.), *Measuring, monitoring and modeling concrete properties*, Springer, Dordrecht, The Netherlands 633-641.
- Seghedi, I., Helvacı, C. and Pecskey, Z. 2015. Composite volcanoes in the south-eastern part of İzmir–Balıkesir Transfer Zone, Western Anatolia, Turkey. *Journal of Volcanology and Geothermal Research* 291 72–85.
- Serdaroğlu, Ü. 1995. *Assos (Behramkale)*. Arkeoloji ve Sanat Yayınları, İstanbul.
- Shao, J., Yang, S. and Li, C. 2012. Chemical indices (CIA and WIP) as proxies for integrated chemical weathering in China: Inferences from analysis of fluvial sediments. *Sedimentary Geology* 265-266 110-120.
- Siegesmund, S., Weiss, T. and Vollbrecht, A. (eds) 2002. *Natural Stone, Weathering Phenomena, Conservation Strategies and Case Studies*. Special Publications, 205, Geological Society, London.

- Snethlage, R. and Wendler, E. 1997. Moisture cycles and sandstone degradation. In *Saving Our Architectural Heritage: The Conservation of Historic Stone Structures; Report of the Dahlem Workshop on Saving Our Architectural Heritage, The Conservation of Historic Stone Structures, Berlin, March 3-8 1996*. Baer, N.S. and Snethlage, R. (Ed), John Wiley & Sons.
- Spock, L.E. 1953. *Guide to the Study of Rocks*. New York: Harper & Row Publishing.
- Strobon, 1969. *Geography*. Trans. H.L. Jones, Loeb classical Lib.
- Tankut, A. 1985. Ankara dolaylarındaki Neojen yaşlı volkaniklerin jeokimyası. *Türkiye Jeoloji Kurumu Bülteni C. 28* 55-66.
- Taqieddin, S.A.I. 1972. *Driliability of Yalıncaözü Limestone Ankara Andesite and their Comparison*. Unpublished M.Sc.Thesis, METU, 98 p.
- Thorn, C.E., Darmody, R.G., Darmody, R.G. and Allen, C.E. 2006. A 10-year record of the weathering rates of surficial pebbles in Kärkevagge, Swedish Lapland. *Catena* 65 272-278.
- Tiano, P., Biagiotti, L., and Mastromei, G., 1999. Bacterial bio-mediated calcite precipitation for monumental stones conservation: methods of evaluation, *Journal of Microbiological Methods* 36: 139-145.
- Tjeerdsma, B.F. and Militz, H. 2005. Chemical changes in hydrothermal treated wood: FTIR analysis of combined hydrothermal and dry heat-treated wood. *European Journal of Wood and Wood Products* 63(2) 102-111.
- Tokmak, M. 2005. *Documentation and Examination of Historic Building Materials for the Purpose of Conservation: Case Study, Part of the Walls at the Citadel of Ankara*. Unpublished MSc. Thesis, METU, 73 p.
- Tül, Ş. 1995. *Aiolis'te Bir Dağ Kenti*. İstanbul: Ege Yayınları.
- Türkmen, F. and Kun, N. 2001. İzmir İli Volkanitlerinin Doğaltaş Sektöründeki Yeri, Afyon: *Türkiye III. Mermer Sempozyumu Bildiriler Kitabı*. Kozan Ofset Matbaacılık San. Ve Ticaret Ltd Şti.
- Tylecote, R.F. 1979. The effect of soil conditions on the long-term corrosion of buried tin-bronzes and copper. *Journal of Archaeological Science* 6 (4) 345-368.
- Umar, B. 2002. *Aiolis*. İstanbul: İnkılâp Kitabevi.

- UNESCO. "Recommendation on International Principles Applicable to Archaeological Excavations (1956)." Accessed May 25 2015. http://portal.unesco.org/en/ev.php-URL_ID=13062&URL_DO=DO_TOPIC&URL_SECTION=201.html
- Uzun, İ. and Terzi, S. 2012. Evaluation of andesite waste as mineral filler in asphaltic concrete mixture. *Construction and Building Materials* 31 284-288.
- Wang, Q., Odlyha, M. and Cohen, N.S. 2000. Thermal Analyses of Selected Soil Samples from the Tombs at the Tianma-Qucun Site, Shanxi, China. Elsevier Science B. V. 189-195.
- Warke, P.A., Curran, J.M., Smith, B.J., Gardiner, M., and Foley, C. 2010. Post-Excavation Deterioration of the Copney Bronze Age Stone Circle Complex: A Geomorphological Perspective. *Geoarchaeology: An International Journal* 25(5) 541-571.
- Williams, A.G., Ternan, L. and Kent, M. 1986. Some observations on the chemical weathering of the Dartmoor Granite. *Earth Surface Processes and Landforms* 11: 557-574.
- World Coin Catalog. "Greek City States of Asia Minor." Accessed May 25 2015 <http://worldcoincatalog.com/AC/C2/Greece/AG/CSofIonia.htm>
- Wüst, R.A.J. and McLane, J. 2000. Rock deterioration in the Royal Tomb of Seti I, Valley of the Kings, Luxor, Egypt. *Engineering Geology* 58: 163-190.
- Wüst, R.A.J. and McLane, J. 2000. Rock deterioration in the Royal Tomb of Seti I, Valley of the Kings, Luxor, Egypt. *Engineering Geology* 58 163-190.
- Velde, B. and Meunier, A. 2008. *The Origin of Clay Minerals in Soils and Weathered Rocks*. Berlin Heidelberg: Springer-Verlag.
- Viñas, S.M., 2005. *Contemporary Theory of Conservation*. Elsevier Butterworth Heinemann.
- Yavuz, A.B. 2006. Deterioration of the volcanic kerb and pavement stones in a humid environment in the city centre of İzmir, Turkey. *Environmental Geology* 51 211-227.
- Yavuz, H. 2011. Effect of freeze–thaw and thermal shock weathering on the physical and mechanical properties of an andesite stone. *Bulletin of Engineering Geology and the Environment* 70 187-192.
- Young, A.R.M. 1987. Salt as an agent in the development of cavernous weathering.

Zedef, V. and Ünal, M. 2003. Effect of Salt Crystallization on the Building Stones Used in Konya, Central Turkey. *International Journal of Economic and Environment Geology* 1 (1) 51-52.

Zedef, V., Ağaçayak, T., Söğüt, A.R. and Koçak, K. 2011. Dimension stones used in Central Anatolia: Some of their geological and mechanical properties. *Scientific Research and Essays* 6 (13) 2655-2659.

APPENDIX A

SOLUBLE SALT CONTENTS OF SOILS

	Sample	Collected Depth (cm)	% Chloride (Cl ⁻)	% Nitrate (NO ₃ ⁻)	% Phosphate (PO ₄ ⁻)	% Sulfate (SO ₄ ⁻)
Aigai Soils	AiSo1	~20	8x10 ⁻⁴	34 x10 ⁻⁴	128 x10 ⁻⁴	25 x10 ⁻⁴
	AiSo2	~50	6 x10 ⁻⁴	8 x10 ⁻⁴	72 x10 ⁻⁴	20 x10 ⁻⁴
	AiSo3	~100	5 x10 ⁻⁴	13 x10 ⁻⁴	136 x10 ⁻⁴	24 x10 ⁻⁴
	AiSo4	~100	4 x10 ⁻⁴	12 x10 ⁻⁴	91 x10 ⁻⁴	16 x10 ⁻⁴
	AiSo5	~180	8 x10 ⁻⁴	539 x10 ⁻⁴	70 x10 ⁻⁴	96 x10 ⁻⁴
Assos Soils	AsSo1	~20	8 x10 ⁻⁴	18 x10 ⁻⁴	54 x10 ⁻⁴	8 x10 ⁻⁴
	AsSo2	~20	4 x10 ⁻⁴	25 x10 ⁻⁴	211 x10 ⁻⁴	12 x10 ⁻⁴
	AsSo3	~30	7 x10 ⁻⁴	18 x10 ⁻⁴	117 x10 ⁻⁴	53 x10 ⁻⁴
	AsSo4	~50	16 x10 ⁻⁴	183 x10 ⁻⁴	150 x10 ⁻⁴	18 x10 ⁻⁴

APPENDIX B

BASIC PHYSICAL PROPERTIES OF INTERIOR AND EXTERIOR PARTS OF ANDESITES

	Interior Parts			Exterior Parts	
	<i>Sample</i>	<i>Average Density (g/cm³)</i>	<i>Average Porosity (%)</i>	<i>Average Density (g/cm³)</i>	<i>Average Porosity (%)</i>
Aigai Andesites	<i>Ai1_I</i>	2.3	9.4	2.2	16.8
	<i>Ai2_I</i>	2.3	10.0	2.2	14.0
	<i>Ai3_I</i>	2.5	4.8	2.5	5.3
	<i>Ai5_I</i>	2.2	15.8	2.1	16.8
	<i>Ai6_I</i>	2.1	18.0	2.0	20.2
	<i>Ai7_I</i>	2.1	15.0	2.1	16.6
	<i>Ai9_I</i>	2.5	4.0	2.4	5.7
	<i>Ai10_I</i>	2.3	11.0	2.2	11.7
	<i>Ai11_I</i>	2.1	2.5	2.4	3.1
	Average	2.3	10.1	2.2	12.2
Assos Andesites	<i>As1_I</i>	2.4	11.0	2.3	11.9
	<i>As2_I</i>	2.3	12.1	2.3	12.6
	<i>As3_I</i>	2.2	14.9	2.2	15.4
	<i>As4_I</i>	2.4	8.6	2.2	13.2
	<i>As5_I</i>	2.3	11.2	2.3	13.0
	<i>As6_I</i>	2.4	8.9	2.4	9.5
	<i>As7_I</i>	2.2	13.1	2.2	12.0
	<i>As8_I</i>	2.4	10.2	2.1	18.1
	Average	2.3	11.3	2.2	13.2

APPENDIX C

TGA RESULTS OF INTERIOR AND EXTERIOR PARTS, CLAY FRACTIONS AND WHITE DEPOSITS OF ANDESITES AND CLAY *FRACTIONS OF SOILS*

INTERIOR PARTS				
	Sample	% Weight Loss		
		103 °C	103 <x≤ 550 °C	550 ≤x≤ 900 °C
Aigai Andesites	Ai1_I	2.275	1.670	0.007
	Ai5_I	1.240	1.750	Error
	Ai6_I	1.412	1.650	0.087
	Ai7_I	1.490	1.553	0.201
	Ai9_I	1.467	1.484	0.026
	Ai10_I	1.911	1.118	0.026
Assos Andesites	As3_I	2.704	0.654	0.022
	As4_I	1.982	1.626	0.037
	As5_I	2.158	0.655	0.018
	As6_I	2.473	1.368	0.019

EXTERIOR PARTS, CLAY FRACTIONS, WTHITE DEPOSITS OF ANDESITES AND CLAY FRACTIONS OF SOILS				
	Sample	% Weight Loss		
		103 °C	103 <x≤ 550 °C	550 ≤x≤ 900 °C
Aigai Andesites and Soils	Ai1_E	0.870	2.024	0.286
	Ai1_Wd	1.760	6.213	12.709
	Ai1_Od	0.602	3.898	0.376
	Ai2_E	1.091	1.561	1.218
	Ai2_Cr	1.670	4.090	2.302
	Ai2_Wd	1.315	4.413	6.102
	Ai3_E	1.156	0.148	3.936
	Ai5_E	1.218	0.424	0.020
	Ai6_E	1.543	0.225	Error
	Ai7_E	2.090	0.535	0.072
	Ai8_E	1.334	0.382	Error
	Ai9_Wd	0.463	4.782	32.490
	Ai10_E	2.080	3.747	Error
	Ai11_Cr	0.147	2.543	0.888
	Ai11_Wd	0.342	5.032	37.716
	<i>AiSo1_Cl</i>	3.830	28.403	7.578
	<i>AiSo2_Cl</i>	3.669	19.006	6.015
<i>AiSo3_Cl</i>	3.803	15.029	3.218	
<i>AiSo4_Cl</i>	2.884	10.540	3.416	
Assos Andesites and Soils	As1_E	2.276	0.955	0.054
	As1_Wd	3.515	2.928	23.664
	As2_E	2.006	1.536	0.010
	As2_Cr	4.373	7.590	0.030
	As2_Wd	3.668	4.123	31.087
	As3_E	2.427	0.658	0.025
	As4_E	3.917	0.884	0.097
	As5_E	2.373	0.622	0.033
	As5_Cr	4.614	6.542	0.275
	As6_E	2.313	1.060	0.0139
	<i>AsSo4_Cl</i>	3.023	42.494	13.689

APPENDIX D

SOLUBLE SALT CONTENTS OF ANDESITES

	Sample	% Chloride (Cl ⁻)	% Nitrate (NO ₃ ⁻)	% Phosphate (PO ₄ ⁻)	% Sulfate (SO ₄ ⁻)
Aigai Andesites	Ai1_I	24 x10 ⁻⁴	7 x10 ⁻⁴	47 x10 ⁻⁴	14 x10 ⁻⁴
	Ai2_I	22 x10 ⁻⁴	18 x10 ⁻⁴	12 x10 ⁻⁴	12 x10 ⁻⁴
	Ai3_I	25 x10 ⁻⁴	16 x10 ⁻⁴	12 x10 ⁻⁴	352 x10 ⁻⁴
	Ai4_I	91 x10 ⁻⁴	---	120 x10 ⁻⁴	8 x10 ⁻⁴
	Ai5_I	55 x10 ⁻⁴	50 x10 ⁻⁴	60 x10 ⁻⁴	19 x10 ⁻⁴
	Ai6_I	18 x10 ⁻⁴	11 x10 ⁻⁴	31 x10 ⁻⁴	7 x10 ⁻⁴
	Ai7_I	14 x10 ⁻⁴	4 x10 ⁻⁴	54 x10 ⁻⁴	8 x10 ⁻⁴
	Ai8_I	21 x10 ⁻⁴	9 x10 ⁻⁴	30 x10 ⁻⁴	34 x10 ⁻⁴
	Ai9_I	13 x10 ⁻⁴	---	---	6 x10 ⁻⁴
	Ai10_I	9 x10 ⁻⁴	---	43 x10 ⁻⁴	---
	Ai11_I	32 x10 ⁻⁴	13 x10 ⁻⁴	---	75 x10 ⁻⁴
Assos Andesites	As1_I	12 x10 ⁻⁴	67 x10 ⁻⁴	24 x10 ⁻⁴	8 x10 ⁻⁴
	As2_I	15 x10 ⁻⁴	106 x10 ⁻⁴	47 x10 ⁻⁴	102 x10 ⁻⁴
	As3_I	9 x10 ⁻⁴	---	31 x10 ⁻⁴	24 x10 ⁻⁴
	As4_I	51 x10 ⁻⁴	278 x10 ⁻⁴	21 x10 ⁻⁴	128 x10 ⁻⁴
	As5_I	25 x10 ⁻⁴	274 x10 ⁻⁴	70 x10 ⁻⁴	63 x10 ⁻⁴
	As6_I	21 x10 ⁻⁴	513 x10 ⁻⁴	117 x10 ⁻⁴	119 x10 ⁻⁴
	As7_I	11 x10 ⁻⁴	168 x10 ⁻⁴	11 x10 ⁻⁴	24 x10 ⁻⁴
	As8_I	14 x10 ⁻⁴	114 x10 ⁻⁴	23 x10 ⁻⁴	35 x10 ⁻⁴

VITA

Çağlayan Deniz KAPLAN

Date of Birth:

20.11.1983

Place of Birth:

Yatağan/MUĞLA

Education:

B.Arch., İzmir Institute of Technology, Department of Architecture (2006)

M.Sc., İzmir Institute of Technology, Department of Architectural Restoration (2009)

Ph.D., İzmir Institute of Technology, Department of Architecture (2015)

Working Experience:

Research Assistant, Department of Architectural Restoration, İzmir Institute of Technology (2006-2014)

Architect, Department of Survey and Project, Directorate of Historical Environment and Cultural Properties, İzmir Metropolitan Municipality (since 2014)